FATIGUE DAMAGE ASSESSMENT OF REINFORCED CONCRETE SLABS USING INTEGRATED DYNAMIC TESTING AND SIMULATION

ADIZA BINTI JAMADIN

FACULTY OF ENGINEERING
UNIVERSITY OF MALAYA
KUALA LUMPUR

2020

FATIGUE DAMAGE ASSESSMENT OF REINFORCED CONCRETE SLABS USING INTEGRATED DYNAMIC TESTING AND SIMULATION

ADIZA BINTI JAMADIN

THESIS SUBMITTED IN FULFILMENT OF THE REQUIREMENTS FOR THE DEGREE OF DOCTOR OF PHILOSOPHY

FACULTY OF ENGINEERING
UNIVERSITY OF MALAYA
KUALA LUMPUR

2020

<div align="center">

UNIVERSITY OF MALAYA

ORIGINAL LITERARY WORK DECLARATION

</div>

Name of Candidate: **ADIZA BINTI JAMADIN**

Matric No: **KHA 120019**

Name of Degree: **PhD**

Title of Project Paper/Research Report/Dissertation/Thesis ("this Work"):

FATIGUE DAMAGE ASSESSMENT OF REINFORCED CONCRETE SLABS

USING INTEGRATED DYNAMIC TESTING AND SIMULATION

Field of Study: **CIVIL ENGINEERING**

I do solemnly and sincerely declare that:

(1) I am the sole author/writer of this Work;
(2) This Work is original;
(3) Any use of any work in which copyright exists was done by way of fair dealing and for permitted purposes and any excerpt or extract from, or reference to or reproduction of any copyright work has been disclosed expressly and sufficiently and the title of the Work and its authorship have been acknowledged in this Work;
(4) I do not have any actual knowledge nor do I ought reasonably to know that the making of this work constitutes an infringement of any copyright work;
(5) I hereby assign all and every rights in the copyright to this Work to the University of Malaya ("UM"), who henceforth shall be owner of the copyright in this Work and that any reproduction or use in any form or by any means whatsoever is prohibited without the written consent of UM having been first had and obtained;
(6) I am fully aware that if in the course of making this Work I have infringed any copyright whether intentionally or otherwise, I may be subject to legal action or any other action as may be determined by UM.

    Candidate's Signature   Date: 13 April 202

Subscribed and solemnly declared before,

    Witness's Signature   Date:

Name:

Designation:

ABSTRACT

Assessment of existing fatigued structures is an important aspect of civil engineering infrastructure. This is critical in most loaded civil engineering structures such as bridges that are constantly subjected to dynamic loading, causing fatigue in the materials over time. Bridge deck slabs are one of the most structural elements susceptible to different cyclic loads, requiring regular checks for damage to fatigue. In order to understand the deterioration, fatigue carrying capacity and residual strength, the serviceability of the slab under the fatigue loads was not fully explored. Therefore, this research is designed to use vibration-based techniques to investigate the integrity of fatigued RC slabs. The objective of the study was to develop an integrated technique to evaluate the serviceability of fatigued RC slab structures including their dynamic characteristics, stiffness reduction, fatigue carrying capacity and residual strength through an integrated dynamic test and finite element (FE) model and update. Static, fatigue and dynamic testing of RC slabs were involved in the experimental program. A series of investigations have been carried out and have been divided into three phases. Phase one identified the dynamic characteristics of RC slabs at different levels of fatigue damage, including natural frequencies, mode shapes and damping ratios. The parameters of the test include the different number of fatigue loads at 1 million, 1.5 million and 2 million; and the different level of damage at undamaged, fatigued and damaged condition. The dynamic characteristics of RC slabs have been studied at different levels of fatigue damage. The natural frequencies show the drop from 38.6 Hz to 36 Hz and to 29.2 Hz due to the increase in the level of fatigue damage. It can be concluded that the dynamic behavior was significantly influenced by the RC slabs experiencing fatigue loads. Phase two of the FE modeling developed to represent the identical behavior of the RC slabs tested. The FE model was then correlated and updated using parametric optimization against experimental data to reflect the actual

condition of RC slabs. It has been shown that, compared to the initial models, the updated FE models have a small error of 0.22 percent for the first mode and thus better improvements in terms of agreement on natural frequencies. It can be seen that the natural frequencies of the updated FE models were close to the experimental data measured with a minimum percentage of 0.26% and a maximum of 2.74% for the first mode. RC slabs ' efficiency would be reduced–making it necessary to evaluate fatigue carrying capacity. Phase three observed the RC slabs ' fatigue carrying capacity through the structural stiffness change. It also concluded that the dynamic behavior was significantly influenced by the RC slabs experiencing a loss in stiffness. The maximum decrease of 70.26 percent in structural stiffness was observed from undamaged to the highest fatigued state in the first mode. The relationship between stiffness, load cycles and natural frequency dynamic response is thus established. The residual strength of the RC slabs was observed in this phase. The decrease in residual strength justifies the loss of the damaged RC slabs ' stiffness, which is accounted for by the Young's modulus and moment of inertia. The strength capacity can be estimated theoretically through the relationship of these parameters. Compared to the updated model, the results are verified and a good agreement with a maximum error is 0.52%. An efficient method of assessing fatigue damage that integrates the dynamic testing and simulation on concrete structure introduced in this thesis provides a comprehensive technique and therefore has a very good potential for predicting future structural performance in service.

Keywords: Reinforced concrete slab, Fatigue testing, Modal testing, Finite element model and updating, and structural stiffness.

ABSTRAK

Penilaian ke atas struktur yang lesu adalah satu aspek penting dalam infrastruktur kejuruteraan awam. Ini adalah kritikal dalam kebanyakan infrastruktur seperti jambatan yang sentiasa dikenakan beban dinamik, menyebabkan bahan menjadi lesu dengan masa. Papak jambatan adalah salah satu elemen struktur yang paling terdedah kepada beban berterusan, maka pemeriksaan rutin untuk memantau tahap kelesuan adalah diperlukan. Kebolehgunaan papak di bawah beban lesu belum diterokai sepenuhnya untuk memahami kemerosotan, kapasiti keletihan dan baki kekuatan. Oleh itu, penyelidikan ini direka untuk menyiasat integriti kepingan papak konrit dengan menggunakan teknik berasaskan getaran. Kajian ini bertujuan untuk membangunkan teknik bersepadu dalam menilai kebolehlaksanaan struktur papak konrit termasuk ciri dinamiknya, pengurangan kekukuhan, kapasiti keupayaan akibat keletihan dan baki kekuatan melalui dinamik bersepadu dan model unsur terhingga (FE) dan pengemaskinian. Program eksperimen ini melibatkan ujian statik, ujian lesu dan ujian dinamik ke atas papak konkrit. Satu siri penyelidikan telah dijalankan dan telah dibahagikan kepada tiga fasa. Fasa pertama mengenal pasti ciri-ciri dinamik papak konkrit termasuk frekuensi semulajadi, bentuk mod dan nisbah redaman pada pelbagai tahap kelesuan. Parameter ujian termasuk jumlah bilangan beban yang berbeza iaitu pada 1 juta, 1.5 juta dan 2 juta; dan tahap kerosakan yang berbeza pada keadaan tidak rosak, lesu atau rosak. Ciri-ciri dinamik papak konkrit pada tahap kerosakan yang berbeza akan dipelajari. Frekuensi semulajadi menunjukkan penurunan yang dikaitkan dengan peningkatan tahap kelesuan. Dapat disimpulkan bahawa papak konkrit mengalami beban lesu yang mempengaruhi perilaku dinamik. Fasa dua dibangunkan dari pemodelan FE untuk mewakili tingkah laku yang sama dari papak konkrit yang diuji. Model FE kemudiannya dikolerasi dan dikemaskini terhadap data eksperimen untuk mencerminkan keadaan sebenar papak konkrit melalui pengoptimuman

parametrik. Telah ditunjukkan bahawa, model FE yang dikemaskini mempunyai perbezaan kecil dengan model awal, dan, dengan itu, peningkatan yang lebih baik dari segi frekuensi semula jadi. Ia dapat dilihat, frekuensi semula jadi model FE yang telah dikemas kini hampir kepada data eksperimen yang diukur. Kecekapan papak konkrit akan berkurangan menyebabkan penaksiran keupayaan keletihan diperlukan. Tahap tiga memerhatikan daya tahan yang ditanggung oleh papak konkrit melalui perubahan kekukuhan struktur. Juga membuat kesimpulan bahawa slab RC mengalami penurunan dalam kekukuhan dengan ketara justeru turut dipengaruhi perilaku dinamik. Oleh itu, hubungan di antara kekukuhan, kitaran beban dan tindak balas dinamik frekuensi semula jadi diterbikan. Dalam fasa empat, baki kekuatan papak konkrit telah diperhatikan. Pengurangan baki kekuatan membenarkan kehilangan kekukuhan papak konkrit yang rosak, yang diambil kira oleh Young modulus dan momen inersia. Melalui hubungan parameter-parameter ini secara teori, kapasiti kekuatan boleh dianggarkan. Hasilnya disahkan dengan membandingkan bersama model yang dikemas kini dan ia menunjukkan persetujuan yang baik. Oleh itu, penyediaan teknik komprehensif mengenai penilaian kerosakan keletihan pada struktur papak konkrit telah dicadangkan, kaedah ini mempunyai potensi yang baik untuk ramalan perkhidmatan prestasi masa depan struktur.

Kata kunci : Papak konkrit bertetulang, Ujian lesu, Ujian modal, Model unsur terhingga dan mengemaskini, dan Kekukuhan struktur.

ACKNOWLEDGEMENTS

All blessings and praises are due to Allah SWT, the Most Gracious and the Most Merciful.

I would like to express my deepest gratitude, respect and appreciation to my distinguished supervisor, Associate Professor Dr. Zainah Ibrahim, for her constant supervision, guidance, invaluable advice and patience throughout my entire study period. I would like to thank Professor Ir. Dr. Mohd Zamin Jumaat, my co-supervisor, for his support throughout the research,

I am very grateful for the help of all the laboratory technicians, especially Mr. Sree, Mr. Tarmizi, Mr. Syafiq, Mr. Rizal, Mr. Shafrizat and Mr. Amir, who provided technical assistance. I would also like to thank Mrs. Ezahtul Shahreen for helping me to carry out a lab test for this research.

I would like to thank my parents, Hj Jamadin Ahmat Marzuki and Hjh Samsien Abd Salam, the in-law of my parents and all the members of my family for their encouragement, their unconditional trust and their endless prayers. Special thanks to my dear husband, Hardisura Mohd Turjah and my daughters, Abid Humayraa, Abid Dhamiyaa and Abid Khaliesah for their endless patience, encouraging me during this challenging period of my life.

I would also like to acknowledge the financial support provided by University of Malaya, Universiti Teknologi Mara and the Malaysian Ministry of Education.

TABLE OF CONTENTS

LIST OF FIGURES

LIST OF SYMBOLS AND ABBREVIATIONS

A	Cross section area
AVT	Ambient vibration testing
C	Damping
b	Width of slab
DOE	Design of experiment
D_K	Stiffness damage under fatigue load
D_{S_R}	Residual strength damage under fatigue load
E	Young's modulus
EFDD	Enhanced frequency domain decomposition
E_c	Concrete Young's modulus
E_s	Steel Young's modulus
E_N	Fatigued Young's modulus
$E_{c,s}$	Static concrete modulus of elasticity
$E_{c,d}$	Dynamic concrete modulus of elasticity
FE	Finite element
f	Natural frequencies
f_v	Frequency band
f_s	Sampling frequency
f_{max}	Maximum frequency
f_{min}	Minimum frequency
f_c	Compressive concrete stress
f_{fem}	Numerical natural frequency
f_{exp}	Experimental natural frequency
$f_{fem,upd}$	Numerical updated natural frequency
f_r	Rupture of concrete

$f_{r,N}$	Fatigued rupture of concrete
HCF	High-cycle fatigue
HA	Highest axle load
HB	Highest body load
h	High of slab
I	Moment of inertia
$I_{E,N}$	Fatigued effective moment of inertia
$I_{cr,N}$	Cracked moment of inertia
K	Stiffness matrices
k	Stiffness
L	Length of slab
LCF	Low-cycle fatigue
M	Mass
$M_{cr,N}$	Fatigued cracked moment
M_u	Ultimate moment
N	Number of load cycles
n	Number of mode shape
OMA	Operational modal analysis
PSD	Power spectral density
P_{ult}	Ultimate load
P_{max}	Maximum load
P_{min}	Minimum load
$P_{analytical}$	Analytical load
$P_{experimental}$	Experimental load
P_{error}	Error (Different) load
R	Regression

RSM	Response surface method
RC	Reinforced concrete
SHCF	Super high-cycle fatigue
SS1	Slab subjected to static load only
SF1M	Slab at 1 million fatigue loads
SF1.5M	Slab at 1.5 million fatigue loads
SF2M	Slab at 2 million fatigue loads
SVD	Singular value decomposition
S_{RA}	Residual strength analytical
S_{RE}	Residual strength experimental
T_{tot}	Total time series length
ε_c	Concrete cyclic creep strain
ρ	Concrete density
ω	Eigenvalue
ζ	Damping ratio
$\emptyset$	Eigenvector

LIST OF APPENDIX

CHAPTER 1: INTRODUCTION

1.1 Research Background

An important aspect of civil engineering infrastructure is the assessment of existing fatigued structures. This evaluation is critical in most loaded civil structures such as bridges that are constantly subjected to dynamic loading, causing the materials to fatigue over time (Benmokrane et al., 2006; Liu et al., 2012; Oh, Sim, & Meyer, 2005; Suthiwarapirak & Matsumoto, 2006). As these structures are constantly subjected to cyclic loading, there is a need for frequent structural monitoring to assess structural health levels in order to avoid any catastrophic failures that are not only exorbitant to restore but can also result in injuries. Bridge structure is categorized under high-cycle fatigue load, characterized by applying large load cycle numbers at low stress levels, according to Hsu (1981). Because of population and economic growth, traffic intensity has increased dramatically and, in response, accelerates the rate of structural fatigue leading to the cracking and deterioration of the structure's stiffness and load-bearing capacity.

Moving loads from vehicles acting on bridge decks of reinforced concrete (RC) causes the super structure consisting of beams and slabs to shift relatively quickly from their position of balance. The structure's mass and inherent elasticity tends to restore the bridge deck back to its position of equilibrium, but in the meantime causes a series of vibrations due to vehicle movement on the deck. The structure's dynamic characteristics can be determined through a non-destructive vibration test technique. This experimental technique is used under various environmental and loading conditions to monitor the health condition of a structure and can also be used to verify analytical models. To this end, the use of Non-Destructive Test (NDT) and Non-Destructive Evaluation (NDE) is highly advantageous and effective as the existing structures do not sustain any damage throughout the process with no disruption to normal use of the structure (Bayraktar,

Altunişik, & Türker, 2016; Bayraktar et al., 2010; Ko & Ni, 2003; Sevim et al., 2016). These methods are also more accurate than conventional structural visual inspection, which is highly subjective and does not provide structural health that can be quantified. Vibration testing method, also known as modal testing and modal analysis, is one of the commonly used NDTs for measuring structural health (Kashif et al., 2016; Kutanis, Boru, & Işık, 2017; Yoon et al., 2009).

It can be seen that substantial research has indeed been carried out to investigate the mechanical behavior of fatigued concrete structures under incremental statically applied load under various damaged conditions (Al-Rousan & Issa, 2011; Aljazaeri & Myers, 2015; Carvelli, Pisani, & Poggi, 2010; Cho et al., 2011; Katakalos & Papakonstantinou, 2009; Liu et al., 2012; Oh et al., 2005). Nevertheless, the open literature still lacks suitable dynamic behavior of concrete structures undergoing fatigue analysis and modal analysis (Plachy & Polak, 2007; Prasad & Seshu, 2010). This is essential in actual applications of civil engineering, where structures such as bridges, roads, airfields, dams, offshore structures, etc. are susceptible to cyclical loading that causes fatigue. This research therefore introduces high-cycle fatigue loading on RC slabs in order to simulate the effects of fatigue loading as in the RC deck of the actual bridge. The capacity of the residual load carrying fatigued RC slabs is then determined by static testing. To determine the dynamic characteristics of fatigued RC slabs, modal testing method was applied on all RC slabs. More importantly, the relevance of using this method to determine the relationship between fatigue cycles and load carrying capacity was demonstrated, which shows that NDT can be used for effective monitoring of structural health.

1.2   Problem Statement

Most of Malaysia's bridges have been built over the past 80 years using reinforced concrete. With the aging of existing bridges and the accumulated stress cycles under traffic loads, it has become more important than ever to evaluate service life for continuous service. Due to fatigue loads, structures are subject to changes and it is desirable to evaluate their structural health conditions in an optimized manner to mitigate risks, prevent disasters and plan maintenance activities. Structural health monitoring of fatigued structures based on non-destructive dynamic techniques is currently being applied more widely in infrastructure as they are more practical and more efficient. This is essential in actual civil engineering applications where structures such as bridges, roads, airfields, dams, offshore structures, etc. are susceptible to fatigue-induced cyclic loading. The efficiency and precision method for evaluating the serviceability performance of fatigued structures for safe continuing service is a more difficult problem. Currently, structural condition assessment is largely based on visual observation which is can only be simply classified as safe or not safe. Therefore, there is an urgent need to develop methodology for efficient and reliable assessment of existing structure for continuing service which is not only being able to qualify but also to quantify the structural performance on current and future conditions. By propose an integrated dynamic testing and simulation in this research, it is possible to quantify and predict future performance of a fatigued structure. Furthermore, this investigation technique could be apply to monitor the dynamic characteristics of existing structures by using only non-destructive field tests as opposed to having a destructive test of the real structures with so many restrictions on the risk of damaged structures, disrupting normal operations and taking longer as well.

1.3   Research Objectives

The general aim of this research project is to present an efficient method for assessment of fatigue damaged RC slabs using an integrated dynamic testing and FE model updating. It will also develop a capable model of assessing the serviceability and the residual strength of the fatigued RC slabs. To achieve the stated aim, the specific objectives of this study are:

1. To experimentally determine the influence of dynamic fatigue loads of RC slabs on the change of its modal characteristics under three different damage levels; undamaged, fatigued and damaged structures.

2. To develop and update the FE model of the RC slabs to correlate with the experimental modal analysis.

3. To propose a prediction model for assessing the serviceability of fatigued RC slabs.

4. To determine the residual strength of the RC slabs due to varying levels of fatigue damage.

1.4   Scope and Limitation of Study

Damage assessment of fatigued RC slabs will be analytically and experimentally investigated using an integrated vibration measurement technique for dynamic testing and simulation. A capable model will be developed to evaluate the serviceability of fatigued RC slabs. Consequently, this study's scope and limitations are described as:

1.   To investigate the dynamic characteristics of fatigued RC slabs, three different loading cycles (1, 1.5 and 2 million) were used.

2.   Using vibration measurement technique through modal testing, dynamic characterization of the RC slab is carried out. Modal testing was performed in the condition of the specimen being undamaged, fatigued and damaged. Fatigue load testing

was performed to make the specimen in fatigue condition according to specific different cyclic load number. The modal parameter will be identified after each cycle by means of modal testing. By incremental static load test, the damaged structure is presented, the RC slabs are loaded in four-point bending until failure. Modal testing will then be performed to identify the damaged modal parameter structure.

3.   The dynamic characteristics of RC slabs are modelled using commercial FE software through modal analysis to simulate the vibration behavior of RC slabs. Experimental modal testing on RC slabs will validate the model later. One of these techniques of validation is updating the model. By adjusting the parameters in an FE model, model updating will match the results of the FE model with the experimental ones. FE model will be updated to simulate the fatigued and damaged structures' current conditions. The approach is based on modal analysis where the nonlinearity of the damaged structure is not considered. Finally, a new predictive model is being proposed to estimate the serviceability of fatigued RC slabs.

4.   A static load test on the fatigued RC slabs will determine the quantification of the residual strength capacity of fatigued RC slabs.

1.5   Research Significance

An important aspect of the entire civil engineering infrastructure is the assessment of existing fatigued structures. This is critical in most loaded civil structures such as bridges that are constantly subjected to dynamic loading, causing fatigue in the materials over time. Bridge deck slabs are one of the most structural elements susceptible to different cyclic loads-requiring regular checks for damage to fatigue. In order to understand the deterioration, fatigue carrying capacity and residual strength, the serviceability of the slab under the fatigue loads was not fully explored. Therefore, this research is designed to use vibration-based techniques to investigate the integrity of

fatigued RC slabs. An efficient method of assessing fatigue damage that integrates the dynamic testing and simulation on concrete structure introduced in this thesis provides a comprehensive technique and therefore has a very good potential for predicting future structural performance in service. The predictive model from this study should be sufficiently reliable to demonstrate the expected findings that could be beneficial to the authority or structural owner to ensure safe operation of their civil structures and present no risk to the public for use.

1.6   Thesis outline

There are five chapters in this thesis. The following is a brief description of the work included in the following chapters.

Chapter 1 provides general study information including an overview of the current state of structural assessment technique on civil structures. Problem statements, objectives, scope of study and research significance are also described.

Chapter 2 provides knowledge of fatigue structures. A discussion of the factors affecting the performance under continuous moving load conditions of existing bridge deck slab structures is presented. Previous research is reviewed on the dynamic performance of various types of bridge structural assessment techniques. Also, this chapter summarizes the previous research on FE modeling and updating bridge structure technique on modal analysis.

The details of the experimental work and finite element modelling performed in this research are presented in Chapter 3. It describes the specification, size and manufacture of the RC deck slabs tested and the properties of the materials used. Detailing of the instruments and devices used in the experimental was presented here. The test setup, loading system and testing procedure are described in the details of the experimental

program. Also discussed and summarized in this chapter are the effects of fatigue damage of RC slabs on dynamic response. In this chapter also present a method of FE modeling, correlation and updating of RC slabs at different structural conditions; undamaged, fatigued and damaged. This chapter begins with a section discussing a model and analysis methodology adopted on FE. A detailed description of the correlation and updating process used on undamaged, fatigued and damaged RC slabs is followed. Also introduced is a parametric study using the optimization method to investigate the effect of different levels of damage on the dynamic behavior of RC slabs.

Chapter 4 deals with the results and discussion on experimental work, FE modeling and updating and also the findings on effect of fatigue damage on the performance of RC slabs in serviceability. New prediction model to estimate the serviceability of fatigued RC slabs is proposed based on the experimental results and updated FE modeling. This chapter includes an analytical method for determining the residual strength capacity of fatigued RC slabs and then comparing it with the predictive model developed for reliability in this chapter.

Chapter 5 contains a summary and the conclusions drawn from this study's findings. Some suggestions and recommendations are also presented for future work.

CHAPTER 2: LITERATURE REVIEW

2.1 Introduction

This chapter reviews the details of the mechanism of fatigue, in general and especially in the application of civil engineering on concrete literature structures. The vibration-based method of structural health monitoring (SHM) was reviewed through an integrated modal testing, modal analysis, finite element (FE) model and model updating. Finally, qualitatively and quantitatively the methods of structural condition assessment were explained.

2.1.1 Phenomena of Fatigue Load

Hanson et al. (1997) defined fatigue terminology as a process of gradual permanent internal structural change in a material under repeated stress. Material fatigue was first observed for iron and documented. On the other hand, the fatigue phenomenon was observed rather late for concrete.

Fatigue loading is a repetitive loading phenomenon that can cause fatigue failure when sufficient load cycles reach the fatigue limit. Low-cycle fatigue (LCF) and high-cycle fatigue (HCF) can be categorized as fatigue loading. LCF is approximately up to 103 load cycles for low load cycles. It is called HCF if the test is longer than this limit. There is also a third limit for an unusual fatigue test, about 107 load cycles, called super-high cycle fatigue (SHCF). Many structures are often subject to cyclic loads that are repeated. Some of them come from civil engineering, such as bridges, roads, sleepers on the railway, offshore structures, etc. Hsu (1981) gave some examples of some structures in Figure 2.1 and to which category of fatigue they belong.

BS 5400:Part 10-Code of practice for fatigue (1980) defined fatigue failure as a failure that occurs by gradually cracking a structural part below a material's stress limit

when exposed to repeated loading. Steel and concrete are most widely used in structural applications in civil engineering. Some materials have a limit on fatigue, which means that no fatigue failure will occur below this load. Steel is such a material but no such limit was detected for concrete Hordijk (1991). This fact was also revealed by Hanson et al. (1997), shown in Figure 2.2 evidences that there is no apparent endurance limit for the concrete up to 10 million cycles. The reason for this difference is because steel is a strain-hardening material (in large strains, the strength increases) and concrete is a strain-softening material (in large strains, the strength decreases).
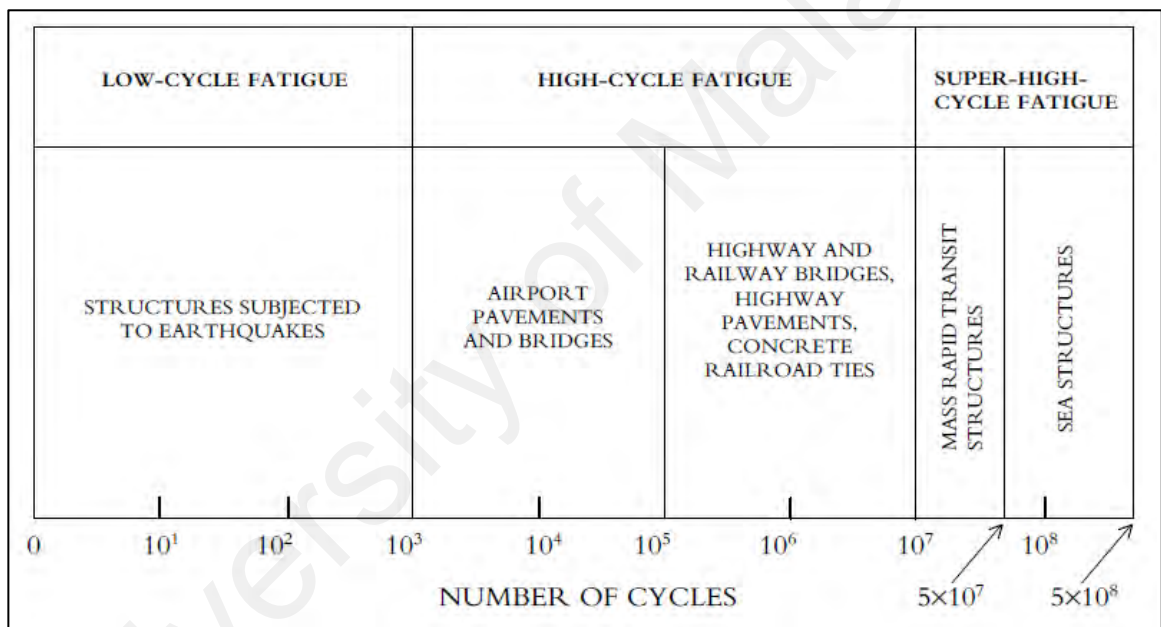
Figure 2.1: Fatigue Load Spectrum (Hsu, 1981)
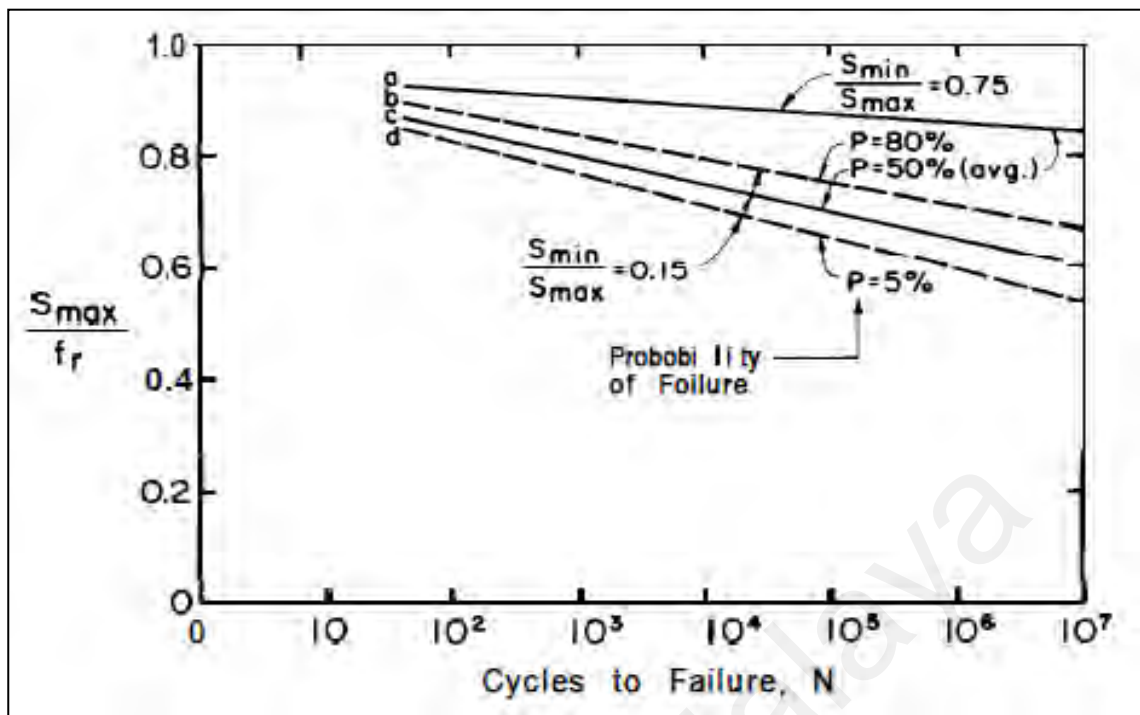
Figure 2.2: Fatigue strength of plain concrete beams (Hanson et al., 1997)

2.1.2   Fatigue Load on Civil Engineering Structures

Today, transport networks are becoming an essential element in developing countries in order to bring together economic demands and communities. It appears that more roads and bridges need to be built and traffic intensity needs to be increased without prejudice to the existing structures that need to be upgraded to ensure continued public safety service. Continuous moving traffic loads can lead to a reduction in strength and stiffness of the bridge deck slab, which is the most fatigued loaded elements.

Hsu (1981) states that subsequently the development of highway systems in the 1920s resulted in further interest in concrete fatigue, as the concrete pavements used for highways are subjected to millions of load cycles from axle loads of cars and trucks. Due to slimmer structures, higher traffic speeds and higher axle loads, the concrete fatigue phenomenon has again gained interest in recent years, especially for railway bridges. The increased axle loads on the existing railway lines caused problems with the

bridges as the conditions for the bridges were changed compared to those when they were built. One of the problems is that when evaluated with the current concrete codes, the bridges are often predicted to fail in the fatigue analysis. For better performance and adequate safety of bridges or other structures that are subject to continuous moving load, bridge designers must consider fatigue limiting status under static and fatigue loading during the design lifetime (Youn & Chang, 1998).

Bridges is one of the essential elements in the transport system known as an enormous structural made of concrete, steel, timber or composite material designated by a safety and aesthetic value bridge engineer. Given the interaction with moving parts, it is categorized under dynamic structure and normal to have vibrations. It is therefore very important to avoid disaster due to the dynamic effects of frequent vibration, which will affect the material strength locally and the structure's load carrying capacity globally. This phenomenon known as fatigue damage and some of the bridges need maintenance, rehabilitation, repair, replacement and improvement due to the material degradation parallel to continuous traffic loads. For example, the collapse of the Point Pleasant Bridge in West Virgina in 1967 and the Yellow Mill Pond Bridge in Connecticut in 1976 may be jeopardized by failure to diagnose the damage and timely arrest of the problem. Therefore, it is necessary to examine the bridge by schedule using an efficient method, especially in order to quantify the current load carrying capacity of the fatigue structure in accordance with established specifications for sustained use. Today, transport networks are becoming an essential element in developing countries in order to bring together economic demands and communities. It appears that more roads and bridges need to be built and traffic intensity needs to be increased without prejudice to the existing structures that need to be upgraded to ensure continued public safety service. Continuous moving traffic loads can lead to a reduction in strength and stiffness of the bridge deck slab, which are the most fatigued loaded elements.

2.2   Structural Health Monitoring of Vibrating Structures

2.2.1   Vibration-based Non-destructive Technique

For its intended daily use, civil structures need to have an effective health monitoring technique. This monitoring technique originated during the Structural Health Monitoring (SHM) term in the early 1990s, before the technologies for structural monitoring were rapidly developed (Brownjohn et al., 2011). In the case of bridges and buildings, the structural integrity of vibrating structures involving interaction with surrounding media such as soil-structure interaction and soil-water-structure interaction in the case of dams and bridges is of crucial concern. The consequences of these are dynamic problems in terms of vibration, noise and fatigue that are constantly present. These conditions would deteriorate over time the capacity of the service and the structural integrity. Therefore, the evaluation of the serviceability of existing vibrating structures mainly due to continuous cyclic loads with different levels of fatigue damage becomes more important without compromising structural safety. Typically, conventional method of assessment relies on visual observation to give subjective results for large and complex structures. Vibration-based non-destructive testing (NDT) has been used as a tool for assessing the serviceability of existing civil structures to address these issues. This technique is a SHM area sub-category. The modernization of the vibration-based method has been extensively explored in monitoring civil structures (Brownjohn et al., 2011; Nanda, Maity, & Maiti, 2014).

Using vibration-based NDT is highly beneficial and effective as the existing structures do not sustain any damage throughout the process without interruption of normal operation (Bayraktar et al., 2010; Ko & Ni, 2003). Vibration testing is the technique most frequently used to monitor structural health as it offers a better ability to detect damage. The technique is based on measurements of vibration taken from the structures to identify the structures' dynamic characteristics. Changing parameters of

dynamic characteristics such as natural frequency, shape of the mode and damping ratio can become an indicator of structural performance. Basically, the idea of vibration-based detection of damage is that when the physical properties (mass, damping, and stiffness) change due to the damage caused, it will cause obvious changes in dynamic characteristics or synonymous with modal parameters (natural frequency, mode shape and damping ratio) (Ewins, 2000). Thus, the structural damage can be identified by analyzing the variations in vibration characteristics. Through modal testing and modal analysis, these modal parameters can be measured.

Many engineering fields, including aerospace, mechanical and civil, use modal testing. The method for determining modal parameters can be divided into two categories of force excitation or forced vibration testing (FVT)–experimental modal analysis (EMA) and ambient excitation or ambient vibration testing (AVT)–operational modal analysis (OMA)–in modal analysis modal analysis. Previously, both force and ambient excitation methods were applied and are capable of determining structural dynamic characteristics. FVT, which uses controlled input force, appears to be more complex and expensive, particularly for large and massive structures. For example, in order to carry out an FVT on bridge structures, the traffic needed to shut down will definitely interrupt the transport network and not be good for economic aspects. While it may disrupt the occupants when FVT was performed on the building and may have to run the test after working hours, so the testing cost increased. Because of their small size of specimens that is easy to handle and tested in laboratories with controlled conditions, the theory FVT is well developed in mechanical system. The main advantage of FVT is the level of excitation force to induce vibration can be carefully controlled. The most common techniques for FVT are impact, shaker and pull back or quick-release tests. Table 2.1 provides a short summary the typical applications of OMA and EMA based on the controlled input in mechanical and civil engineering fields

(Brincker & Ventura, 2015). In FVT, controlled force is a known force to be used in determines the structure's dynamic properties by measuring the structure's response to these known forces. Then it is possible to calculate the frequency response function (FRF) between a measured excitation point and the time history acceleration response. These FRFs can later be used to determine the structures ' modal parameters. In the field of civil engineering there is no such advantage, producing compatible large forces is impractical to excite large civil structures at low frequencies. Table 2.2 shows general characteristics of environmental excitation related structural response (Brincker & Ventura, 2015). This brings challenge in extracting low frequency modes with high capability of sensors, acquisition system, and software analyzer. The evolution of techniques accompanied by tremendous technology in recent years has impressively enhanced the use of AVT to characterize the dynamic properties of large civil engineering structures. The technique makes it easier and more effective for users to perform an OMA.

Table 2.1: Typical applications of OMA and EMA based on the controlled input
(Brincker & Ventura, 2015)

Field	Mechanical Engineering	Civil Engineering
EMA	*Artificial excitation* Impact hammer, shaker, controlled blast, well-defined measured input.	*Artificial excitation* Shaker, drop weight, pull back test, eccentric shaker and exciter, well-defined measured and controlled blast.
OMA	*Artificial excitation* Scratching device, air flow, acoustics emission unknown signal, random in time and space.	*Natural excitation* Wind, wave, traffic, unknown signal, random in time and space, with some spatial correlation.

Table 2.2: General characteristics of structural response (Brincker & Ventura, 2015)

Vibration excitation	Frequency range (Hz)	Displacement range (Hz)	Velocity range (Hz)	Acceleration range (µg)	Suggested measuring quantity
Traffic: road, rail ground-borne	1 - 80	1 - 200	0.2 - 50	2 - 100	Velocity
Blasting vibration ground-borne	1 – 300	100 - 2500	0.2 - 500	2 - 500	Velocity
Pile driving ground-borne	1 – 100	10 - 50	0.2 - 50	2 - 200	Velocity
Machinery outside ground-borne	1 – 300	10 - 1000	0.2 - 50	2 - 100	Velocity/ acceleration
Acoustic: traffic, machinery outside	10 - 250	1 - 1100	0.2 - 30	2 - 100	Velocity/ acceleration
Air over pressure	1 – 40				Velocity
Machinery inside	1 – 1000	1 - 100	0.2 - 30	2 - 100	Velocity/ acceleration
Human activities a) Impact b) Direct	0.1 – 100 0.1 - 12	100 – 500 100 - 5000	0.2 - 20 0.2 - 5.0	2 – 500 2 - 20	Velocity/ acceleration
Earthquakes	0.1 - 30	10 - 10^5	0.2 - 400	2 - 2000	Velocity/ acceleration
Wind	0.1 - 10	10 - 10^5			acceleration
Acoustic inside	5 - 500				

2.2.2 Evolution of Modal Analysis in Civil Engineering Field

Studies of vibrations affecting civil engineering structures were conducted in the early 1930s in the twentieth century, improving the behavior of buildings during earthquakes. In 1935, after the Long Beach earthquake in California in 1933, Carder carried out vibration tests in more than 200 buildings which were then used in the design code to estimate natural frequencies of new building design (Brincker & Ventura, 2015), as shown in Figure 2.3. Ivanovic et al. (2000) states that the experimental vibration of full-scale structures was began in the seventies in order to determine structural dynamic characteristics. Figure 2.3 showed that the publication of vibration test papers on large structures such as buildings, dams, chimneys, silos and

bridges began to be published and quoted in 1964. More frequent publications appear after the 1970s and produce actively year after year.
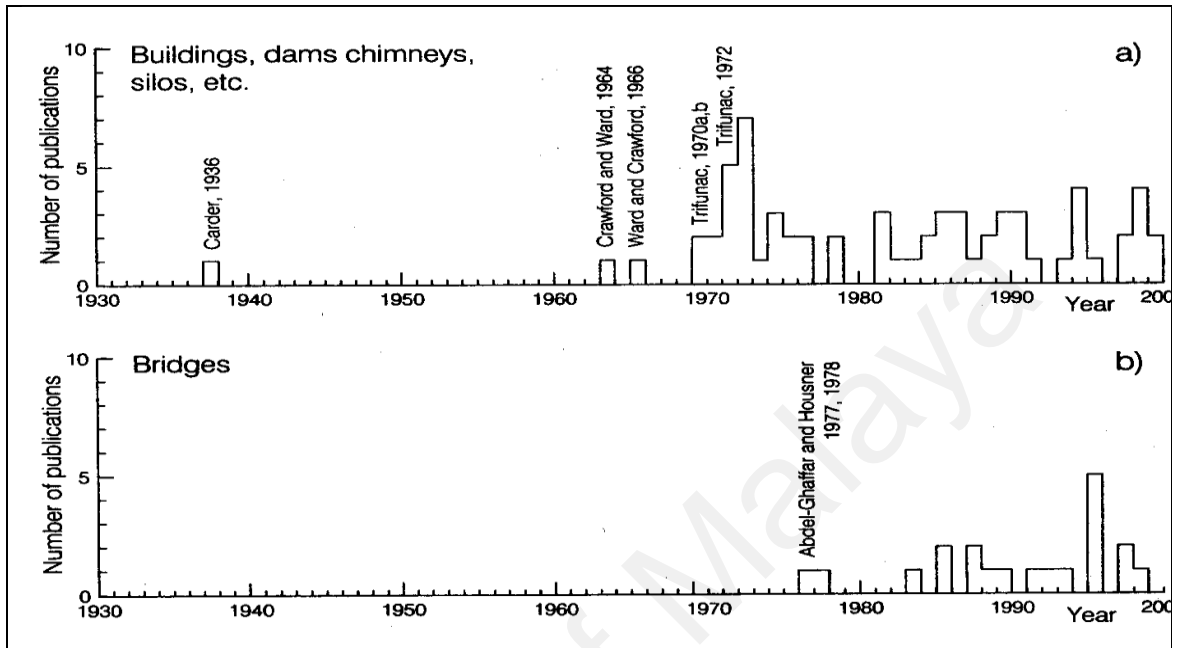
Figure 2.3: Frequency of occurrence of published contributions to the subject of vibration testing of full-scale structures: (a) buildings, dams, chimneys, silos, etc. (b) bridges (Ivanovic et al., 2000)

Nowadays vibration-based technique is widely used in huge real civil engineering SHM. Previously, researchers were well utilized forced vibration techniques to identify the civil structural dynamic properties even though the excitation forces is challenging. Cunha & Caetano (2006) in their review paper reported about the equipment that had been used in that conventional modal tests. Initially, impulse hammer is used in excitation of small and medium-size structures (Figure 2.4(a)). However, some of the relevant modes of vibration were not excited due to the lack of energy and low frequency resolution in spectral estimation. Further, since to this problem, special impulse devices have been designed and built to excite larger structure, such as bridges (Figure 2.4(b)). Another alternative, to reach the excitation at lower frequency range and higher frequency resolution, electrodynamic shaker had been introduced (Figure 2.4(c)). This type of shaker has the capability in applying sinusoidal forces to allow the

structure excited at resonance frequencies. The function of the shaker had been enhanced with variable frequency and amplitude of sinusoidal forces; it is known as eccentric mass vibrator (Figure 2.4(d)). The capability function of the shaker has undergone continuous improvement by having a servo-hydraulic shaker, its wide-band features can excite wide range of frequency for large civil structures such as bridges and dams (Figure 2.4(e)). In the past, FVT had been successfully applied on large civil engineering structures by using heavy excitation devices and accurately identified the vibration modes of Swedish Norsjo dam (Cantieni et al., 1994; Cantieni, 2001; Pietrzko et al., 1996) as shown in Figure 2.5. FVT continues facing difficulty in exciting very large flexible civil structures such as suspension or cable-stayed bridges which requiring extremely heavy and expensive equipment to reach the most significant vibration modes in a low range of frequencies. Fortunately, as structural analysis techniques continually evolve and high technology development in equipment become progressively sophisticated, the very low levels of dynamic response induced by ambient excitations like traffic or wind can be measured, therefore, AVT became a great alternative in civil engineering field. Moreover, AVT does not require traffic shutdown or interruption of normal operation of the structures. The investigated modal parameters of the civil structures using AVT were reported by many teams (Agardh, 1994; Altunişik et al., 2012; Andersen et al., 2007, 2008; Baptista et al., 2004; Bayraktar et al., 2010; Bayraktar et al., 2016, 2010; Brincker et al., 2000; Brownjohn et al., 2010; Capraro et al., 2015; Farrar & James, 1997; Foti et al., 2012; Hashim et al., 2013; Ibrahim & Reynolds, 2008; Ivanovic et al., 2000; Ren et al., 2004; Rent & Zong, 2004; Sevim et al., 2016; Ventura et al., 2002). Figure 2.6 presents a common procedure for the dynamic testing of bridge structures (Bien & Zwolski, 2007).
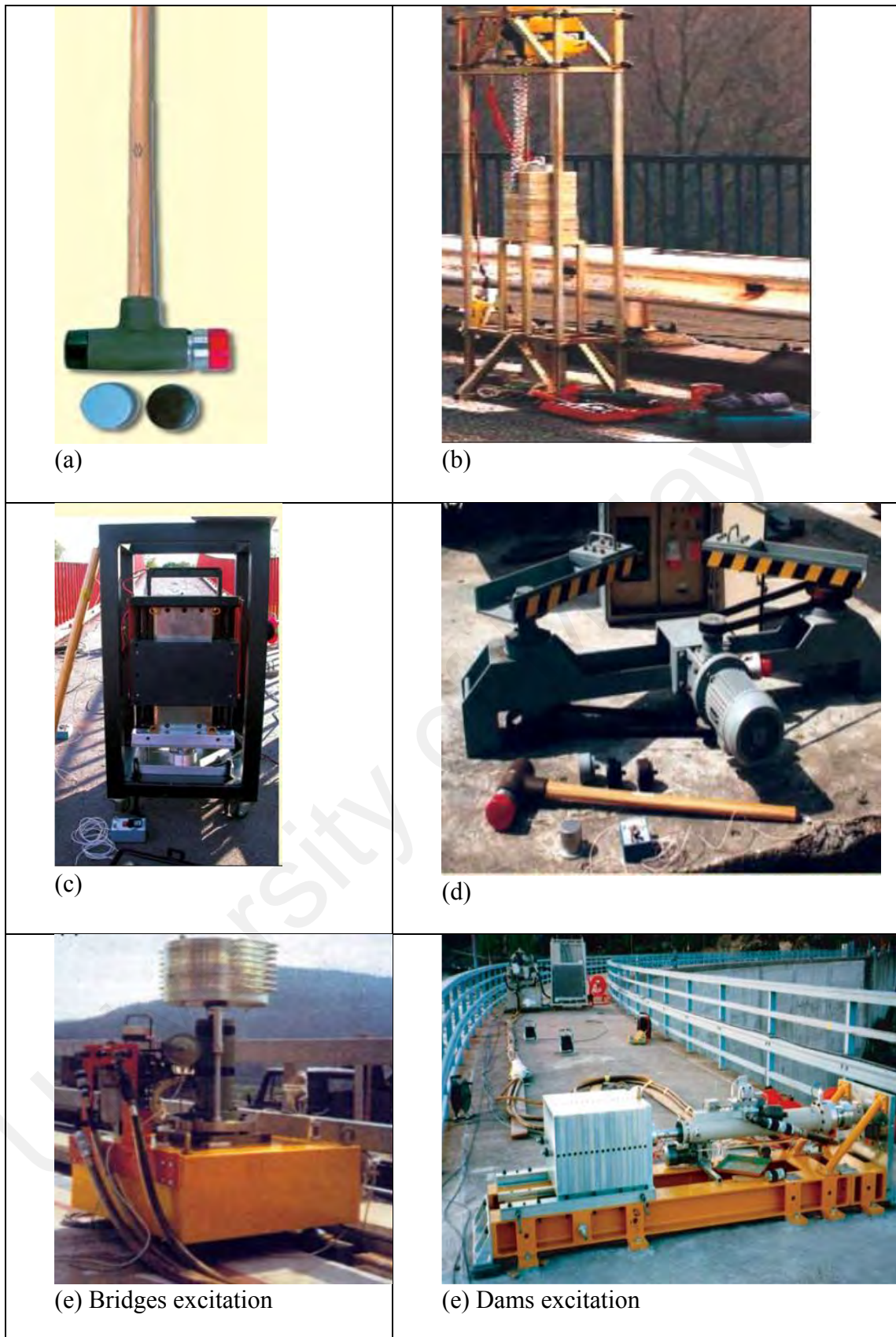
Figure 2.4: (a) Impulse hammer; (b) Impulse excitation device for bridges;
(c) Electrodynamic shaker; d) Eccentric mass vibrator; e) Server-hydraulic shaker.
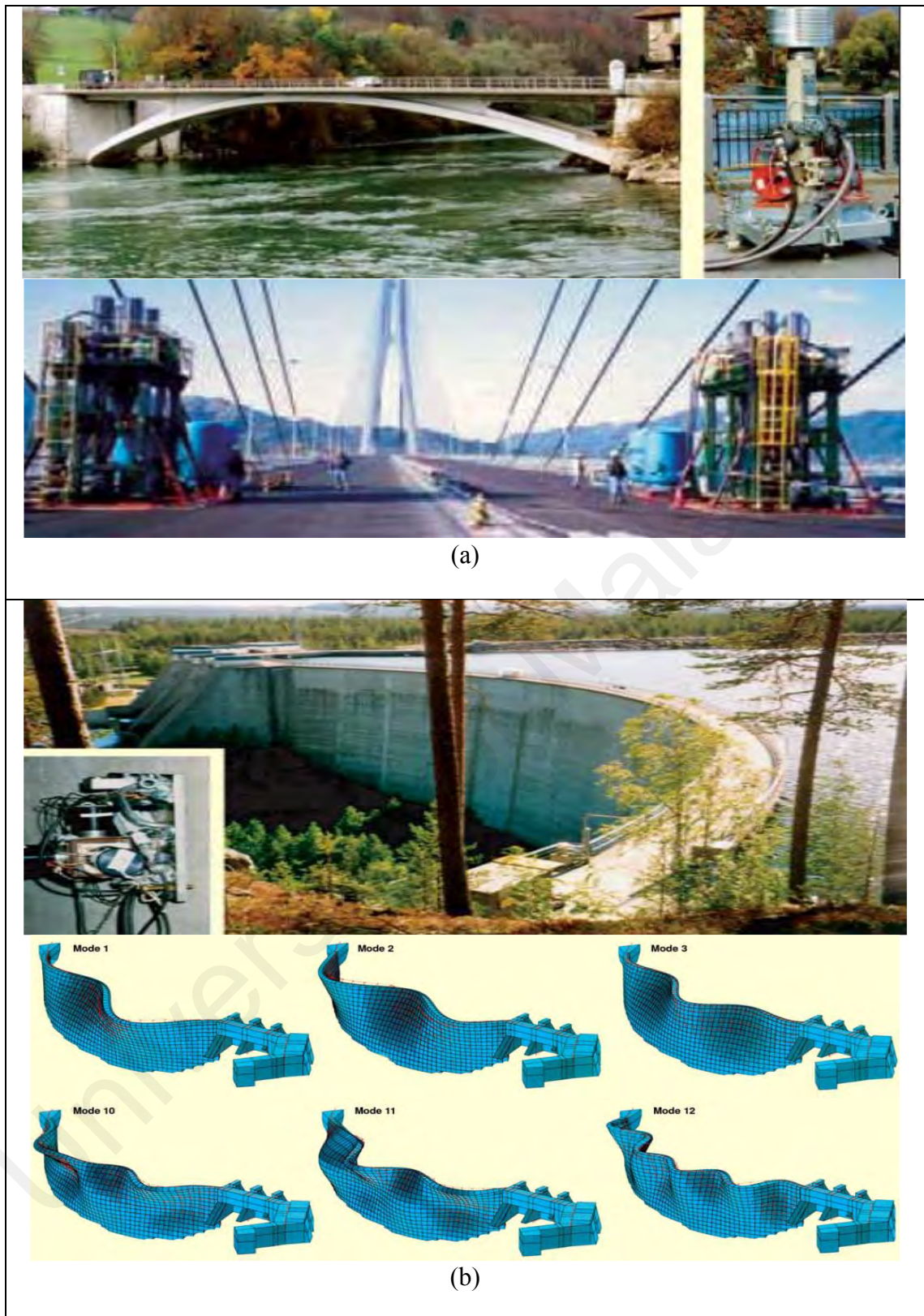
Figure 2.5: FVT on large civil engineering structures; (a) bridge structures; (b) dam structure.
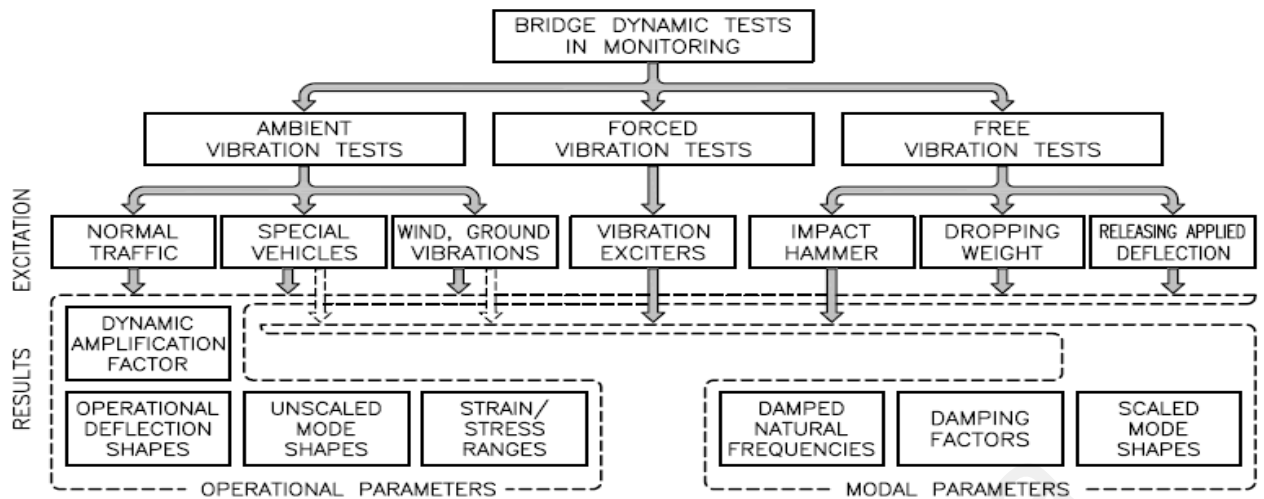
Figure 2.6: Dynamic tests applied in bridge monitoring (Bien & Zwolski, 2007)

To be more efficient and save costs, this AVT technique has been continuously improved. The forces are larger in large structures, and the frequencies are lower. To carry out vibration testing on large civil engineering structures, high sensitivity and a high number of sensors and cables are therefore required. However, a limited number of sensors can be used with the sophisticated vibration measurement technique. To obtain the overall area of the measurement structure, several data sets are required. One reference sensor is stored in the same point in each data set to record all data sets while the remaining sensors are rotated over the structure. High data sets from a single test are normal in many cases. It is therefore very important during the planning stage to excite all interest vibration modes in all data sets in terms of the appropriate number of sensors, their orientation, and the placement of the reference sensor. OMA's use in very large structure, however, remains a challenge in managing all those long sensor cables. But, with today's fast technology, we're heading towards the digital wireless sensors, and cabling issues are disappearing. In addition, FVT can be applied in virtually any type of large structures. Because the potential is there, for further development, the theory for AVT still requires extensive attention from researchers.

In EMA, due to the known forcing function, the measured time signals can be processed in the time domain or frequency domain. Unlike EMA, the assumption that the input does not contain any specific information due to unknown forcing function justifies OMA testing without any controlled excitation. The analysis therefore depends on the operational response's correlation functions and spectral density functions. This is because it is not possible to calculate the frequency response functions between input and output signal. Peak-picking technique (PP) is the fast method widely used to estimate modal parameters in OMA for all types of application. With this concept, Felber (1994) developed this technique, which will have strong responses near its natural frequencies when a structure is subjected to ambient excitation. Then, for the time histories captured by the sensors, these frequencies can be estimated from the peaks in the power spectral densities (PSD). Continuously developed the OMA technique, two other techniques were introduced in the 1990s; stochastic subspace identification (SSI) and frequency-domain decomposition (FDD) techniques by (Overschee et al. (1996) and Brincker et al. (2001), respectively. Guillaume et al. (2003) was introduced to the engineering community after the millennium. The FDD technique was then upgraded to Enhanced Frequency Domain Decomposition (EFDD) by Jacobsen et al. (2007) Jacobsen et al. (2007) based on an automated method. Figure 2.7 shows the various types of numerical techniques used to develop modal identification and visualization software. Rodrigues et al. (2004) implemented, applied and compared these methods.
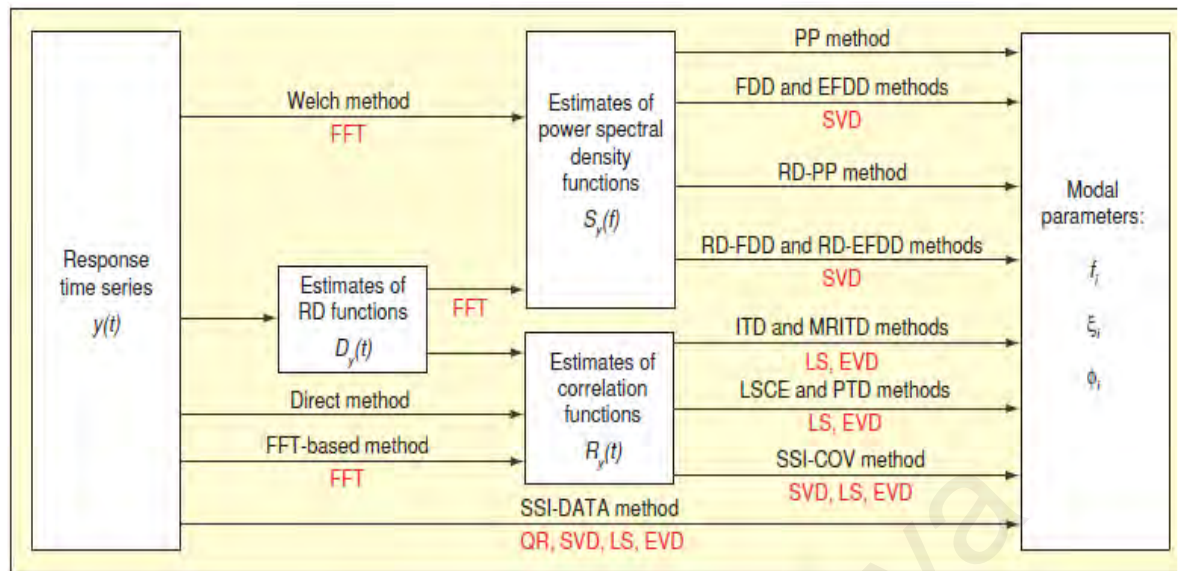
Figure 2.7: Schematic representation of output-only modal identification methods (Rodrigues et al., 2004)

2.3 Finite Element Modeling, Correlation and Updating of Test Structures

2.3.1 Finite Element Method

The finite element (FE) method is a numerical method for solving problems of engineering and mathematical physics include solution such as in structural analysis, fluid flow, heat transfer and mass transport. FE method offers acceptable solution when analytical mathematical solution impossible to obtain especially for problems involving complicated loadings, geometries, and material properties. The unique of this FE method is the equations were formulated for each smaller unit (finite elements) and combine them to obtain the solution of the whole body or system, instead of solving the problem for the entire body in one operation. The basic approach, general principles and the concept of FE method can be found sufficiently in several text books, and one of it, is from Logan (2011). FE analysis is a computerized method for simulating the physical effects of an object due to the any given physical phenomenon such as forces, vibration, heat, fluid flow and etc. The simulation model representing the actual behavior of the object and could be beneficial for future prediction. The output results of FE analysis show the response of an object in the way it was designed. FE model actually has produced detailed visualizations of a problem by understanding the physical behaviors

of a complex object. Engineers usually use FE model to reduce the number of physical prototypes and experiments and optimize components in their design phase to develop better design and also reducing cost and time consumption. There are three main procedures associated with the FE model; pre-processing, processing and post-processing. In first procedure of pre-processing, user need to define several things as the input parameters which are the geometrical properties, element type to be used, material properties, the element connectivity (meshing the model, physical constraints (boundary conditions), and the loadings. Based on these input parameters, the unknown values computed in the solution processing stage and the output parameters will be resulted in the form of values, graphs, tables, graphic figures and animations at the post-processing stage. Hence, the FE method was widely used due to its availability, versatility and convenient of use. However, results produced in output parameters of FE model might have disagreement with actual measured in experimental and may cause the model less reliable and robustness. In this condition, modifications are required to minimize the error by making the modeling and experimental results closer. This is usually done through model correlation and updating process.

2.3.2 Finite Element Model Correlation and Updating

FE model correlation and updating is a process that aims to develop an FE model that simulates the dynamic behavior of the actual structure accurately and reliably. This technique was carried out by adjusting certain parameters of structural modeling, such as material or geometric properties. The inputs are also the initial FE model as a reference data and an updated model is the output. Figure 2.8 shows a model updating study's general scheme (Heylen et al., 1997). It has been widely used by mechanical and aerospace engineers since the 1980s as an important tool (Allemang & Brown, 1982; Berman & Nagy, 1983; Caesar, 1986; Heylen & Sas, 1987; Ibrahim, 1988; Sidhu & Ewins, 1984).

This technique has also been adopted in the field of civil engineering. The civil engineering community continuously studied this research on civil structures at the beginning of the 1990s. In their updated building floor model, Caetano & Cunha (1993) started with the FE model correlation. A high consistency between predicted (FE model) and measured (experimental) modal parameters has been achieved. Subsequently, excellent work was carried out (Gardner & Huston, 1993) on modal testing, FE modeling and manual updating of a pedestrian bridge with 55 m of cable span. Sensitivity analysis was performed to identify the most sensitive parameters that caused significant uncertainty in the FE model. The same manual updating procedure was applied by Pavic and teams to several footbridges and concrete floors (Pavic et al., 1994; Pavic et al., 1999; Pavic et al., 2001; Reynolds et al., 1999).

The FE model correlation and updating is now available in commercial computer software in line with the advancement of computer technology. The advantage is that it has the ability to update automatic model parameters in a more systematic, i.e. presented approach (Brownjohn et al., 2001; Pavic et al., 2002). However, manual updating is presumably used before performing automatic updates for the analyst to have a good starting value of parameters. Poor starting values with unstable iterations and unrealistic results can affect the updating process (Widjaja, 2004).

Stepping further from model correlation and validation, updating the FE model can be used as a much better tool for structural condition assessment and future civil engineering structures damage prognosis. The structure's dynamic properties for various conditions such as undamaged, gradual damage (fatigue) or damage status could be modelled through the automatic model update process and changes in structural parameters could be identified.

```
                    ┌─────────────────────┐
                    │      Structure      │
                    └─────────────────────┘
                  │                           │
                  ▼                           ▼
      ┌──────────────────┐        ┌──────────────────┐
      │    FE analysis   │        │    Experimental  │
      └──────────────────┘        └──────────────────┘
                  │                           │
                  └─────────────┬─────────────┘
                                ▼
                  ┌──────────────────────────┐
                  │   Correlation analysis   │──────────┐
                  └──────────────────────────┘          │
        Bad     │                                       ▼
              Good │                        ┌──────────────────────┐
                ▼                           │   Reliable FE model  │
      ┌──────────────────────────┐         └──────────────────────┘
      │      Model updating      │
      └──────────────────────────┘
                ▼
      ┌──────────────────────────┐
      │    Correction of the FE  │
      └──────────────────────────┘
```
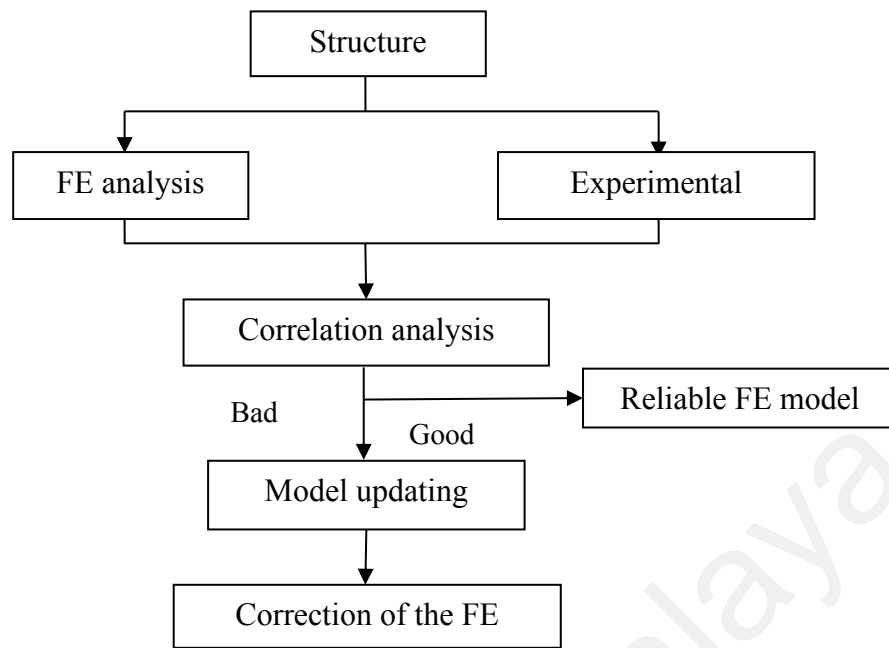
Figure 2.8: General scheme of a model updating study (Heylen et al., 1997)

2.4 Structural Condition Assessment

2.4.1 Vibration-based damage detection

The need to inspect damage in structures based on NDT technique led to the development of SHM. The advances in hardware sensing, signal processing software, and better understanding of structural materials have facilitated vibration-based NDT techniques to become an integral part of SHM and, moreover, the engineering research community has gained great interest. Through modal testing and modal analysis, this technique involves vibration response data to identify modal parameters such as natural frequencies, mode shape and damping ratio. These modal parameters are part of the dynamic characteristics that reflected the physical parameters (mass, stiffness and damping) and structure condition. The concept is any changes in physical properties as the deterioration of the structure may indicate changes in modal parameters. These model parameters are therefore necessary for SHM to be used in the identification and quantification of structural damage. Rytter (1993) initially introduced the classification of methods of damage identification, which had been widely referred by many

researchers. The method was defined under four levels of damage identification; Level 1 — Determining the presence of damage in the structure; Level 2 — Determining the geometric location of the damage; Level 3 — Quantification of the severity of the damage; and Level 4— Prediction of the structure's remaining service life. Kong et al. (2017) described the four damage identification levels in a single flowchart as shown in Figure 2.9. In identifying the presence of damage in the structure, the first step is to extract vibration measurements. In order to prolong the structural life span, damage identification is required at a very early stage for timely maintenance and repair work. After that, a structural model, such as using the FE model, needs to be developed. This model required a validation by updating the structural parameters to reflect similar behavior with the real structure. To minimize the difference between the measured response and the FE model, the sensitivity analysis is performed here. In order to achieve an optimized reasonable result, the procedure could be repeated several times. The severity of the damage has already quantified at this stage. Then the remaining service life can be assessed and predicted for future structural condition based on the information of the quantified damage. Eventually, any structural owner's intervention and decision can be made to ensure continuity of structural safety and reliability during its service life.

In general, damage refers to structural changes such as changes in material and/or geometric properties and boundary conditions that adversely affect current structural integrity and future performance (Nanda et al., 2014). Therefore, the classification of damage identification introduced in SHM; level 3 (quantification of the severity of the damage) and level 4 (prediction of the remaining service life of the structure) become the most important part of the assessment to determine the current structural health condition, quantify the current carrying capacity of the load and predict the remaining service. Damage identification through the initial vibration-based method developed in

the field of automotive and aerospace to improve their products through studies of simulation and design. The concept of structural damage identification in the civil / structural engineering field was adopted since 1970s (Mao et al., 2019). Aktan et al. (1996) and Aktan et al. (1997) explained the definition, terminology and experimental aspects related to identifying structural damage. Since vibration-based method and model updating technique have been used to identify structural damage, comprehensive literature review related to model updating has been presented (Mottershead & Friswell, 1993) and Friswell & Mottershead (1995) has written detailed explanation of FE model updating in structural dynamics.
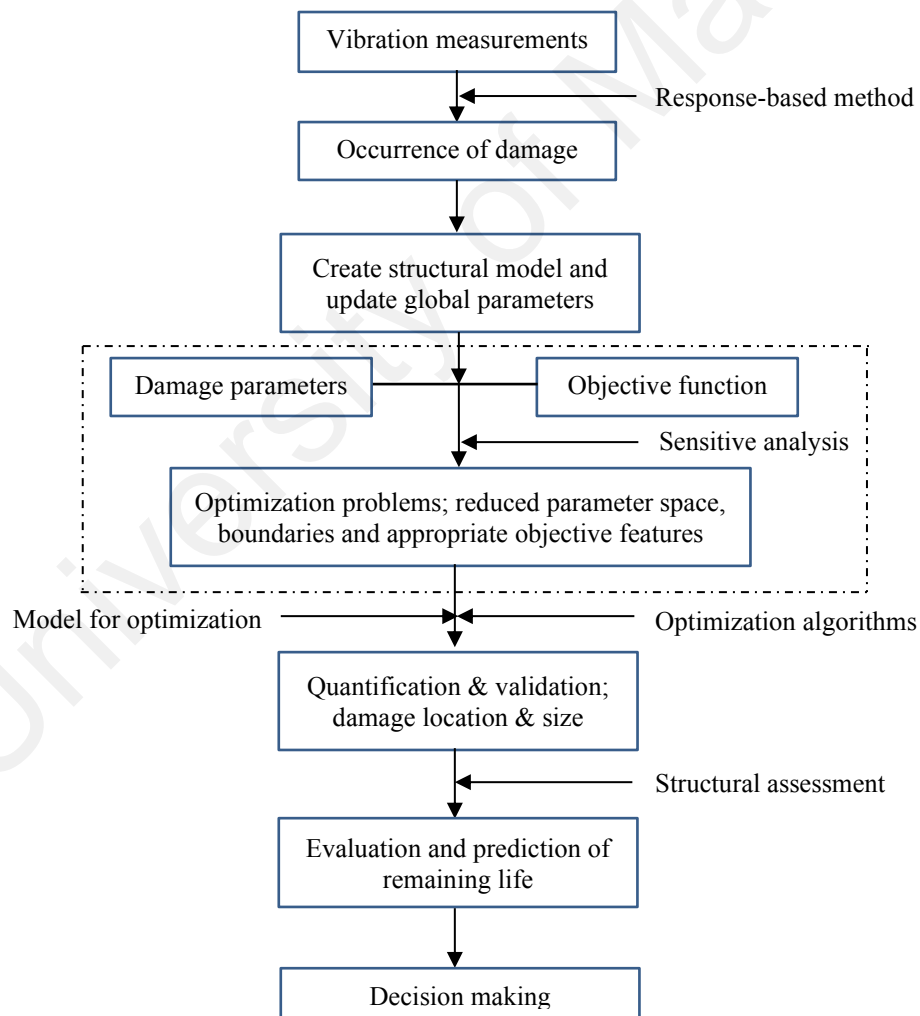
Figure 2.9: Flowchart of damage identification (Kong et al., 2017)

Doebling & Farrar (1998); Doebling et al. (1996); Salawu (1997); Sohn et al. (2004) discussed the use of natural frequency, damping and mode shape as a diagnostic parameter in structural evaluation procedures. Law et al. (1995a, 1995b) presented a method for estimating the load carrying capacity of the RC bridge deck slab from an integrated static test and modal test by making steel percentage and natural frequency as investigative parameters in the application on civil engineering structures.

Brownjohn et al. (2001) and Xia & Brownjohn (2004) then enhanced this study by offering solution through automatic updating techniques of the FE model. Many researchers have examined in the available literature the dynamic behavior of concrete structures in various undamaged conditions (Altunişik et al., 2018; Kutanis et al., 2017) and damaged structures under incremental statically applied load (Carreira et al., 2017; Carvelli et al., 2010; Hsu, 1981; Lenschow, 1980; Liu et al., 2012; Maas et al., 2012; Oh et al., 2005; Xia & Brownjohn, 2004). Nevertheless, the open literature still lacks adequate dynamic behavior of concrete structures subject to cyclic loads and fatigue analysis (Plachy & Polak, 2007; Prasad & Seshu, 2010). This is essential to reflect the actual civil engineering applications that are susceptible to fatigue-causing cyclic loads such as bridges, roads, airfields, dams and offshore structures.

2.4.2   Serviceability of existing structures

Existing RC structures built over decades ago continue to deteriorate and decrease serviceability levels and certainly affect structural security. Thus, the evaluation of structural elements and materials in service life is gaining importance. By identifying the degree of damage, structural safety can be measured through qualitative and quantitative judgment. By evaluating the current strength or load carrying capacity of fatigued or damaged structures, the damage can be quantified and further the structural serviceability can be predicted. There are currently several practical methods that can be

applied or integrated through systematic evaluation to provide quantitative measurement of the performance of structural serviceability. Over the years, high-tech equipment and powerful FE method for load carrying capacity prediction in civil engineering structures through vibration-based methods have been developed and have gained tremendous popularity over the past two decades. The first estimate of the capacity of load carrying through the moment of the parameter of inertia (Law et al., 1995a, 1995b). By introducing a sensitivity-based model updating method, Brownjohn & Xia (2000) enhanced the structural condition assessment procedure. This method was applied to real bridges shortly afterwards (Brownjohn et al., 2001). By using Young's modulus as a sensitive parameter, Teughels et al. (2002) also used sensitivity-based approach to identify bending stiffness reduction. The method was then refined by Xia & Brownjohn (2004) by identifying several parameters (moment of inertia, effective steel ratio and ultimate moment of damaged structure) that led to the estimation of load carrying capacity. Ding et al. (2012) proposed the combination technique of nonlinear FE analysis and the model updating to evaluate the load carrying capacity of the slab-girder bridge taking into account nonlinear material properties with the rapid development of computer capability. Recently, Jamali et al., (2019) enhanced the procedure by having a multi-tier assessment in estimating the capacity of existing bridge structures through an integrated of advanced nonlinear FE analysis, structural health monitoring and probabilistic technique. Most research on load carrying capacity, however, is limited to structural damage before and after. Evaluation of the fatigue condition reflecting the actual condition of civil engineering structures in service is still a challenging and unresolved issue. There is still a lack of study in the open literature on the modal parameters of concrete structures subject to cyclic loads and fatigue analysis (Plachy & Polak, 2007; Prasad & Seshu, 2010). As is known, ageing structures may deteriorate after many years of service due to the fatigue condition, their current capacity may not

be sufficient for continuous service charges. Extensive study of fatigue performance of structures during their service life via vibration-based method is therefore highly required for a better forecast of future accumulation of damage. With increased researchers contributions, advancement in knowledge of materials science and development in computer technology, structure prediction of service life is possible.

Level of fatigue and progressive damage of a RC structure can be characterized and quantified using modal parameters of vibration signal (non-destructive method) and remaining load carrying capacity of the structure (destructive method method). It can be used as an assessment method to evaluate the whole structural integrity. This gradual degradation of structural performance could be presented in service life prediction model. Reviewed by Alexander & Beushausen (2019), service life of a concrete structure was defined as the expected period of a structure or an element of the structure is to be functioned for its intended purposes with scheduled maintenance but not included a major repair. Service life was categorizing under a serviceability limit state condition. Therefore, infrastructure owners require to expect a future operation of the infrastructure by probably having a serviceability predictive model. The concept of structure's service life illustrated in Figure 2.10 explained the mechanism of deterioration progress of two structures A and B. the durability of structure A is adequate to resist deterioration compared to structure B before reaching inappropriate quality at the limit of its expected service life. This is a scenario often encountered by the owner of the infrastructure in ensuring that it is well maintained and may increase the service life expectancy. Thus, they need to have the ability to anticipate their structural durability, hence, the tools to make such prediction as the service life prediction model is very important and necessitate. This model has the ability to identify the level of reliability and quantify the serviceability.
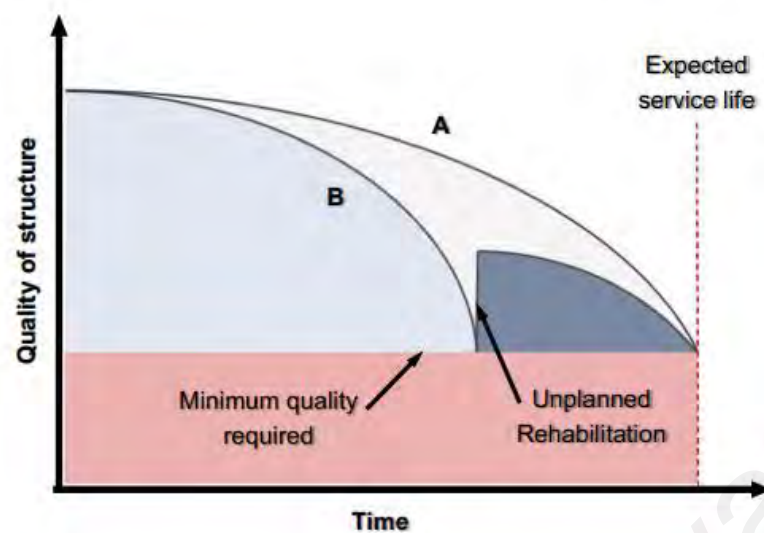
Figure 2.10: Schematic illustration of the concept of service life of a structure (Alexander & Beushausen, 2019)

According to Walraven (2009), the service life assessment involves six elements: (1) limit state criteria; (2) a defined service life; (3) deterioration models; (4) compliance tests; (5) a strategy for maintenance and repair; and (6) quality control systems. The deterioration or service life model should be developed mathematically including parameters that linked to the performance criteria and verified by test methods. This idea is illustrated in

Figure 2.11 have been replicated from Somerville (1997) and extensively presented by Alexander & Thomas (2015). While Dhawan et al., (2019) had developed a remaining service life model of reinforced concrete structures from consideration of wind/seismic natural conditions.
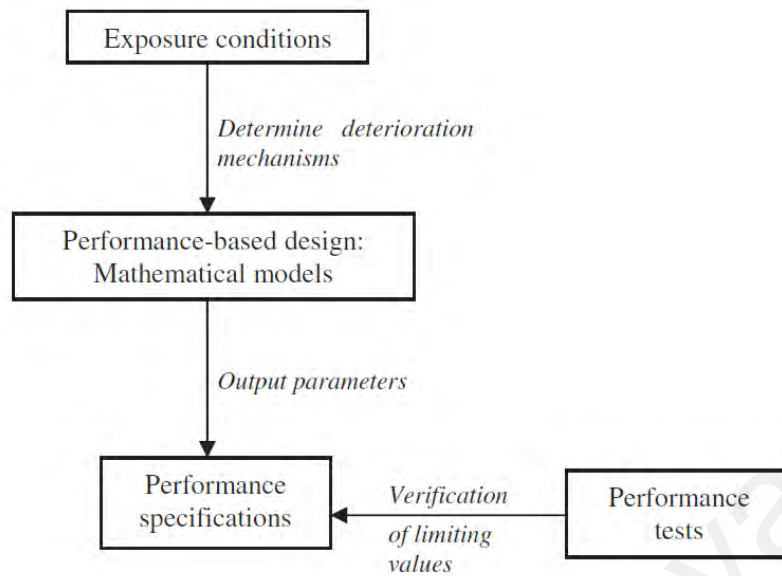
Figure 2.11: Schematic representation of the performance-based approach
(Somerville, 1997)

2.5 Summary

In the vibration-based structural damage identification integrated with FE modeling and updating, there have been many developments from the above review. Only a few researchers have applied these techniques to fatigued concrete structures in terms of civil engineering structures. In this study, therefore, research was conducted on fatigued concrete structures to simulate and evaluate the performance of fatigued structures in serviceability for safe continuing service.

By developing an important model in this research, it is possible to quantify and predict future performance of a fatigued structure and its serviceability. Furthermore, this investigation technique gives the authority the advantage of monitoring its dynamic characteristics of existing structures, such as bridges, buildings and dams, by using only non-destructive field tests, as opposed to a destructive test of real structures, which has so many restrictions on the risk of damaged structures and disrupts traffic operations.

CHAPTER 3: RESEARCH METHODOLOGY

3.1   Introduction

This chapter presents the method of research in experimental works of non-destructive (modal) and destructive (fatigue and static) testing of reinforced concrete (RC) slabs to investigate dynamic characteristics between different structural conditions of undamaged, fatigued and damaged structures. Sections 3.2 and 3.3, respectively, describe the research method and the design of the experimental programme. The remaining sections 3.4 to 3.8 describe, respectively, the materials and specimens, instrumentations, experimental testing, finite element (FE) analysis and response surface based method on FE model updating.

3.2   Research Methodology

The study consisted of three phases. Phase 1 was the study of the dynamic characteristics of RC slabs under constant fatigue loads of amplitude and due to varying levels of fatigue damage. Due to the fatigue load, it was crucial to determine how the fatigue damage could affect the strength of these RC slabs because of the deterioration of these RC slabs. Determining how dynamic structural response parameters including natural frequencies and damping ratios changed with increased load cycles and fatigue damage was also important. Through an integrated static test, fatigue test and modal test these parameters can be measured. It will focus on the dynamic interaction between the fatigue loading structure and how this system affects the structure properties that need to be considered when calculating structural dynamic response. They have thus established their respective characteristic response to load cycles. This could be called a predictive model because it can be used to predict an existing structure's serviceability.

Phase 2 of this study was the development of models of FE based on the initial design under RC slabs' fatigue and damaged condition. Models of the corresponding FE

may not represent the current condition of the RC slabs. Changes in material degradation such as stiffness and Young's modulus should be properly quantified to establish a predictive model that is accurate. The initial FE model must therefore be updated to measured parameters accordingly. For further predictions, the result of an updated FE model is a more reliable model.

Finally, in phase 3, the input parameter of material properties such as moment of inertia, Young's modulus and density were updated in phase 3, based on experimental result and FE model updating. The current conditions of the fatigued and damaged structures reflect these material properties. Then, through the concept of stiffness in the mechanical and dynamic behavior of RC slab structures, it was possible to estimate the current load carrying capacity of fatigued RC slabs from the moment relationship of inertia, steel ratio and the ultimate moment capacity. Figure 3.1 illustrates the research program.

3.3   Experimental programme

In this phase 1, a research program is structured to investigate the change in structural dynamic characteristics of RC slabs due to different levels of fatigue damage through the integrated laboratory method of modal testing, fatigue testing and static testing. The experimental findings then were used in FE model including model updating to develop a capable model to quantify the serviceability of existing structures. However, analyzing the dynamic behavior is not straightforward. Experimental or / and numerical methods have identified modal parameters of a civil structure. This research has therefore been programmed through an integrated dynamic testing and simulation.
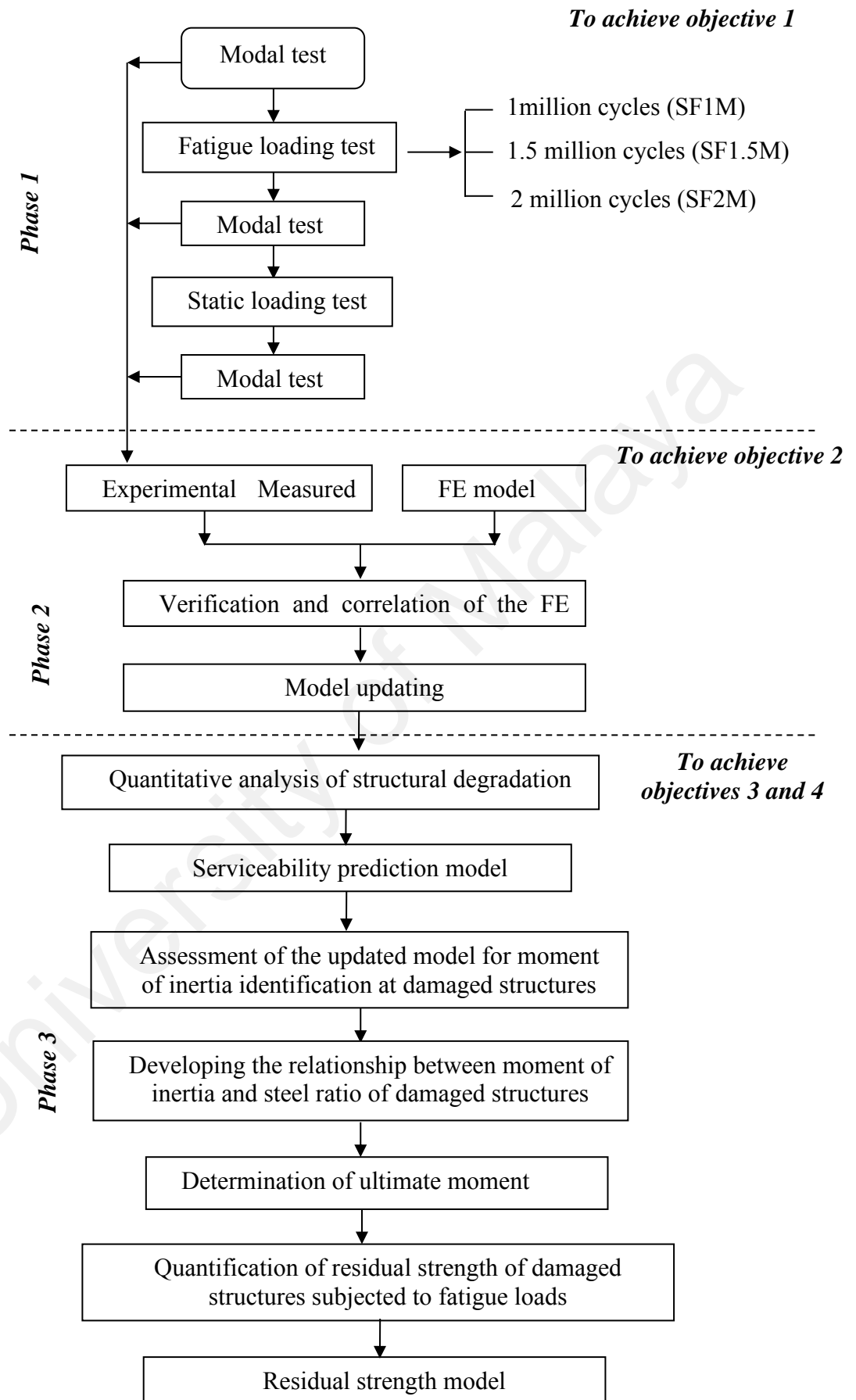
Figure 3.1: Flow chart of the research programme

3.4 Materials and specimens

There were cast and tested a total of five RC slabs. Two RC slabs SS1 was subjected to monotonic loading up to failure. The remaining three RC slabs were subject to various combinations of cyclic and monotonic load conditions with different cyclic load numbers as shown in Table 3.1 and Table 3.2. The RC slabs were unloaded in each group at the preliminary stage and started as a prerequisite for a fatigue and static test by modal testing. At each incremental load for static test and after each fatigue test, modal tests were applied to the RC slab. When the frequency measurement was recorded, the actuator was removed. Under the group of RC slabs SF1M, SF1.5M and SF2M, at the final stage of testing, static testing was imposed to observe the residual strength of the fatigued RC slabs.

The experimental testing was conducted in two phases to investigate the change in the structural dynamic characteristics of the slabs due to cyclic loads and to observe the residual strength of the fatigued RC slabs. The first phase investigated the behavior of the RC slabs up to failure under static testing. Ultimate strength results in this phase have been used as a reference in determining the loading range for fatigue load $P_{max} - P_{min}$. Furthermore, structural dynamic characteristic changes were recorded at an undamaged and damaged stage. The experimental's second phase was programmed to investigate the fatigued slabs' current load capacity. The fatigue loading was designed in this phase on the basis of the first phase findings. It was performed with a series of different cycles and ended with a static test to check the slabs' residual capacity. Similar to the first phase, structural dynamic characteristic changes were recorded at an undamaged, gradually damaged and damaged stage.

Table 3.1: The variable testing on the RC slabs with different cyclic number of fatigue testing

Slab SS1	Slab SF1M	Slab SF1.5M	Slab SF2M
Modal test	Modal test	Modal test	Modal test
+	+	+	+
Static load test	Fatigue load test (1,000,000 cyclic loads)	Fatigue load test (1,500,000 cyclic loads)	Fatigue load test (2,000,000 cyclic loads)
+			
Modal test	+	+	+
	Modal test	Modal test	Modal test
	+	+	+
	Static load test	Static load test	Static load test
	+	+	+
	Modal test	Modal test	Modal test

3.4.1 Specifications

The specimen of the slab was designed to represent a bridge deck portion. It was designed by referring to the design code used in Malaysia, which is HA and HB loading type for the live loads referred to the BD 37/01 (2001) (Appendix A). Live loads are classified as the weight of vehicles, pedestrians, riders, cyclists and all others that cross the bridges. While HA and HB are the standard normal highway loading and, respectively, the standard abnormal highway loading. The size taken for the slab specimen was 2200 mm long x 1000 mm wide x 150 mm deep to comply with the code provision (Appendix A).

3.4.2 Fabrications

All slabs had ribbed bars with a diameter of 10 mm as reinforcement of compression steel. The slabs were analyzed using Westergaard's method and designed using BS 8110 (1997) standard (Appendix A). The concrete cover for the reinforcement of tension steel was 30 mm. **Figure 3.2** shows a schematic of the concrete slab and reinforcement details.
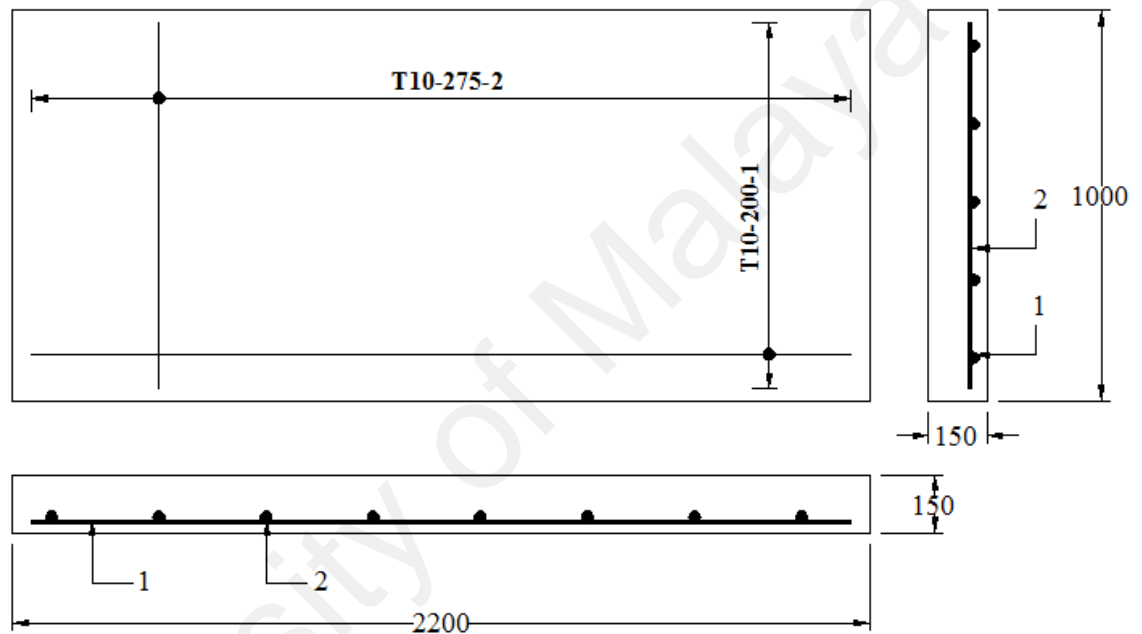
Figure 3.2: Slab and reinforcement details (unit in mm)

Wood formworks have been manufactured and used to cast the specimens. Steel bars were cut to suitable lengths and arranged as main and secondary reinforcements on the two-way side respectively. Steel wires were used to tie the steel bars together to ensure that the steel bars were in the right orientation. To ensure a constant concrete cover at 30 mm (**Figure 3.3**:a), cement cubes were inserted between the formwork and the steel bar. Before it could be used, the formworks were greased well. Truck delivered ready-mixed concrete from a batching plant (**Figure 3.3**:b).

It is necessary to check the fresh concrete workability by means of a slump test before it can pour into the formworks. The slump test had a 70 mm reading within the permitted true slump. Vibrator was used during the concreting work to ensure that the concrete mix was constantly distributed throughout the slab (**Figure 3.3**:c). The specimens were covered with wet sponge for at least three weeks after casting the concrete for a healing process (**Figure 3.3**:d).
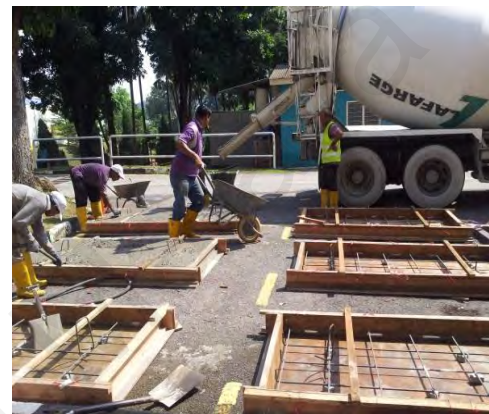
(a)	(b)
(c)	(d)

Figure 3.3: Preparation of the specimens on concreting work (a) Formwork ready for casting of concrete, (b) Pouring of concreting, (c) Using of vibrator and (d) Curing process

3.4.3   Material properties

The slabs were manufactured using ready-mixed concrete from the same concrete batching plant to control the consistency of concrete strength. The specific strength of the target was 40 MPa. The average concrete compressive strength at 28 days was about 40 MPa based on the compressive strength test. Standard cube size 100 mm x 100 mm x

100 mm was cast and tested at 7, 14 and 28 days (Figure 3.4) according to BS 1881 (1983).

Standard high yield ribbed bar steel with a diameter of 10 mm was used to reinforce tension. According to the manufacturer certificate, the steel bars had a yield strength of 500 MPa. Tensile testing was performed to determine the steel's tensile strength for a validation. The test was conducted using a universal testing machine in accordance with BS 4449 (2005). The test result shows that the steel had 550 MPa average nominal yield strength as shown in Figure 3.5.

Figure 3.4: Concrete cube test
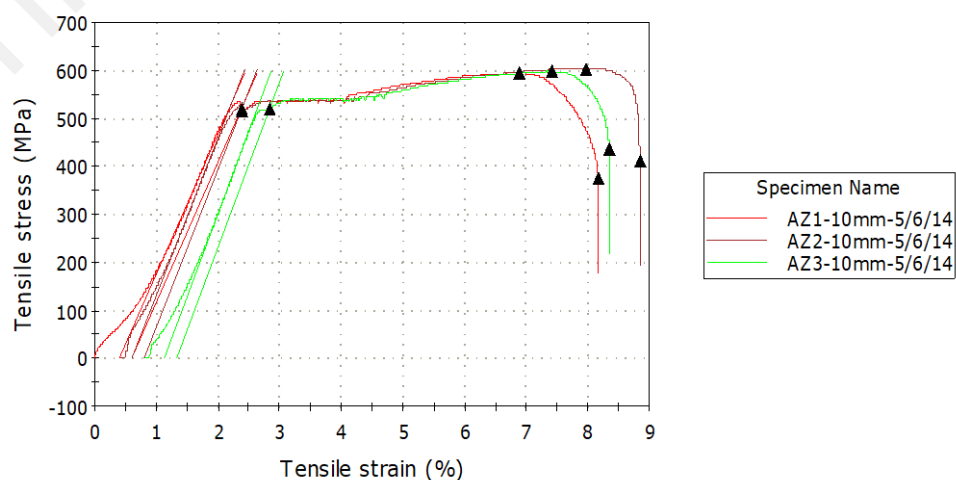
Figure 3.5: Tensile test of steel reinforcement

3.5 Instrumentations

3.5.1 Strain gauges

Two sensor types were used to measure the response to deformation and vibration. The first type is a conventional Kyowa supplied foil strain gauges. For concrete and steel reinforcement, 30 mm long gauges were used. Strain gauge resistance was 120 + - 0.3 ohms with 11 PPM / o^C thermal expansion. The slab strains were measured at their mid-span using a strain gauge and the surrounding point-load area. During the test, strain gauges attached to the mid-length bottom of the steel bar monitored the strain distribution of steel reinforcement (Figure 3.6). Before applying strain gauges, the ribs were first grinded to be flat, and then the surfaces were thinned. As described in the next sub-section, the second sensor is the accelerometer.
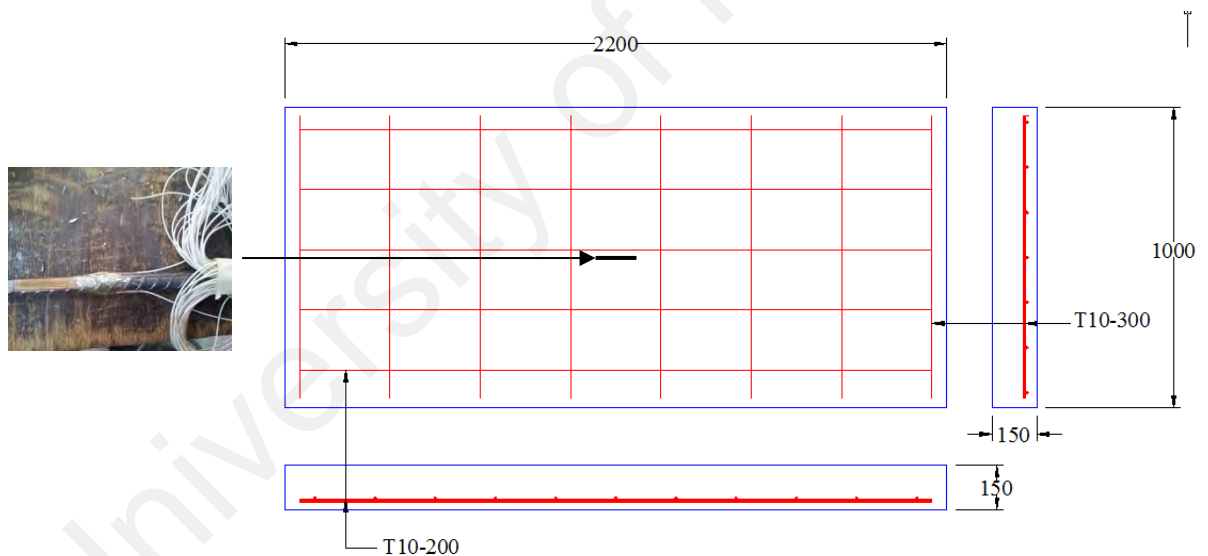
Figure 3.6: Strain gauge attached on the mid-length bottom of steel bar (unit in mm)

3.5.2 Accelerometer and electrodynamic shaker

The other type sensor used for measuring vibration response is the accelerometer. The slab's response was captured by the accelerometers. Only the slab's vertical acceleration response was measured and recorded in this dynamic measurement. The electrodynamic shaker on the top of the concrete slab was used as the input signal. The

shaker is a source of excitation directly proportional to the current provided by an amplifier. While a signal generator was used to control the excitation force. The configuration of the equipment is shown in Figure 3.7.
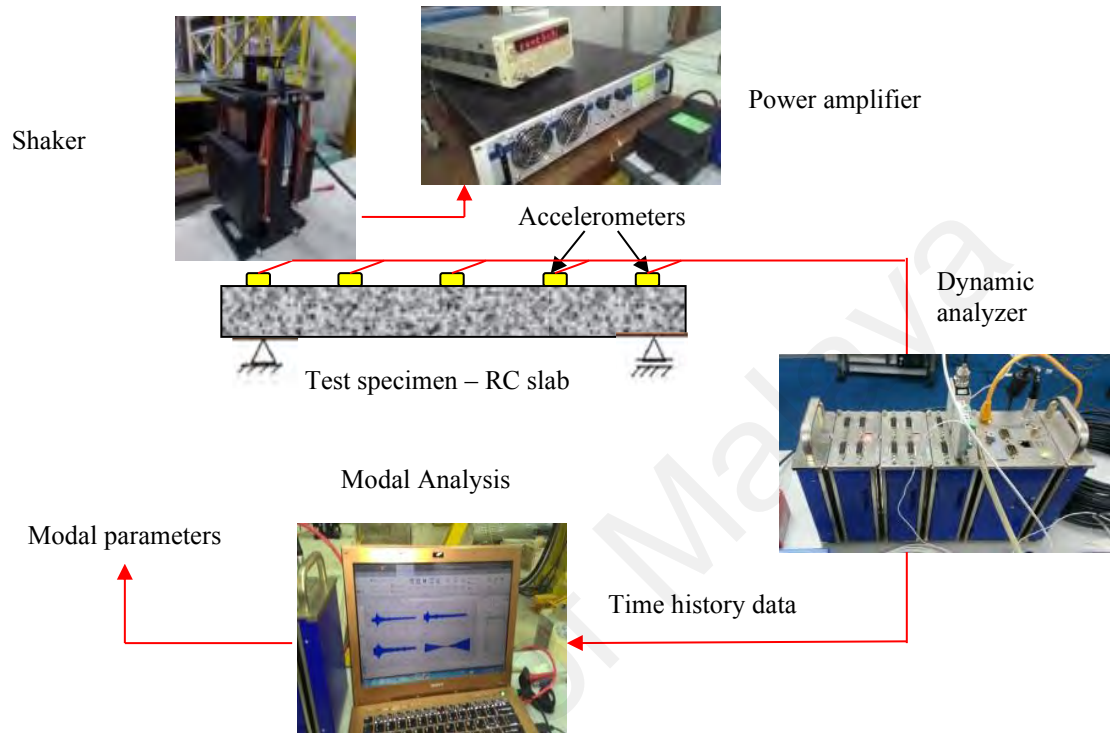
Figure 3.7: Modal testing configuration

3.5.3 Linear variable displacement transducer (LVDTs)

In order to measure the deflection as shown in Figure 3.8, two vertical Linear Variable Differential Transducer (LVDT) were fixed in the center and 500 mm from the center (under the spreader beam load point).

3.5.4 Data acquisition system

During testing, two different systems for data acquisition were used. Data logger with 20 channels used during static and fatigue testing to digitize the load signals, LVDTs and electrical strain gages (Figure 3.9a). The data output was recorded using the data logger-connected computer data system.

The other data acquisition system used is 12-channel dynamic analyzer which acquired data in time domains. This channel is suitable for recording and digitizing the accelerometer and electrodynamic shaker signal during modal testing (Figure 3.9b). The dynamic properties were determined using the modal analysis software.

Figure 3.8: Fatigue and static testing set-up and the position of the LVDTs

(a) Fatigue and static test data logger   (b) Dynamic analyser

Figure 3.9: Data loggers used during experimental works

3.6   Experimental Works

3.6.1   Testing programme

The experiment was conducted in two phases in order to investigate changes in the structural dynamic characteristics of the slabs due to cyclic loads and observe the residual load capacity of the fatigued slabs. The first phase investigated the behavior of the slabs up to failure under static testing. In determining the loading range P_{min} and P_{max} for the fatigue test, the ultimate strength (P_{ult}) for the slab obtained in this phase was used as a reference. The loading point for fatigue tests was kept the same as in static tests and cyclic load was applied at 0.6 at constant fatigue stress level, S (S= f_{max} / f_r). The slabs were tested by sinusoidal waveform fatigue load between the minimum load applied at 20% of the ultimate strength, P_{ult} to keep the actuator contact with the RC slab and the maximum load at 65% of the ultimate strength, $P_{ult,}$. It was applied with a constant 2 Hz frequency that took several days to complete the total number of cycles as shown in Table 3.2. Despite researchers establishing a range of stresses that can influence fatigue strength, the maximum stress level has an insignificant effect on concrete fatigue behavior if less than 75% of the static strength is maintained within the frequency loading range of 1 to 30 Hz (Rilem Committee, 1984).

Table 3.2 shows the test matrix. Slab SS1 was only monotonically loaded. While fatigued slabs SF1M, SF1.5M, and SF2M were placed under cyclic loading with different cycle counts, respectively 1 million, 1.5 million, and 2 million. The different number of cycles used in the fatigue tests was to represent the high cycle fatigue loading range of approximately 1000 to 10,000,000 cycles as shown in Figure 2.1 on specific categories of target structures. Following the fatigue tests, all SF1M, SF1.5M and SF2M slabs were tested to fail under monotonous load to investigate the static performance and residual strength due to accumulation of fatigue damage.

3.6.2 Supporting System

All the tests involved were conducted in the Heavy Structure Lab, Civil Engineering Department, Faculty of Engineering, University of Malaya and Heavy Structure Lab, Faculty of Civil Engineering, Universiti Teknologi MARA. To investigate the dynamic and mechanical behavior of RC slabs, a test set-up was designed. Figure 3.10 shows the test set-up. The support system was manufactured with a hinged support on one end and a roller support on the other. The supports have been spaced from center to center at 2000 mm. The support system size was sufficient to withstand the ultimate load applied to the specimens.

Table 3.2: Testing matrix

Specimen	Specimen number	Loading type	Frequency rate (Hz)	Total number of load cycles (x 10^6)	Time taken (hour)
SS1	2	Static	-	-	-
SF1M	1	Modal + Fatigue + static	2	1.0	138.89
SF1.5M	1	Modal + Fatigue + static	2	1.5	208.33
SF2M	1	Modal + Fatigue + static	2	2.0	277.78

3.6.3 Loading System

The concrete slabs were tested in four-point bending under either monotonic or cyclic loading using a Universal Testing Machine (UTM) 500 kN capacity actuator in the center of the clearly supported 2000 mm span. A computer monitored the actuator to apply load at a rate of 1 mm / min in a displacement control. The concentrated load was applied to the slab by means of a 75 mm thick steel plate measuring 365 x 365 mm and layered between the plate and the concrete surface with 20 mm thick neoprene sheet to avoid local effect on the specific concentrated loading area. These sizes simulate the wheel load footprint as indicated in BD 37/01 (2001).

Figure 3.10: Test set-up and the support system with a hinged support at one end and a roller support at the other end

3.6.4   Modal Test

In the laboratory, modal tests on RC slabs are performed to determine their dynamic characteristics that are also recognized as modal parameters including natural frequencies, mode shapes and damping ratios. The aim of these tests is to study the dynamic behavior of RC slabs at different stages; undamaged state (before any loading), fatigue state (after cyclic loading) and ultimately damaged state (after failure of the RC slabs). Table 3.1 shows the chronology of the tests. The designated testing simulated the structure's dynamic behavior at the new structure stage, under serviceability and at ultimate performance. The relationship between the degradation of stiffness in the structure of fatigue and damage and the resulting changes in modal parameters was examined.

The equipment required for modal testing on concrete slabs as set out in Figure 3.11(c) are electrodynamic shaker, power amplifier, signal generator, accelerometer, data acquisition system, and dynamic analyzer. The modal testing measurement system

consists of three major processes for extracting modal data: (i) an excitation mechanism, (ii) a structural response transducer mechanism, and (iii) an analyzer for extracting the desired output.

An electrodynamic shaker (APS Dynamics Model 113) was used as a source of excitation as the natural level of excitation in the laboratory was too low to create an acceptable magnitude signal for heavy and light structures as also implemented (Fernández et al., 2011). The shaker force is generated electrodynamically, where an amplifier provides the output directly proportional to the current. The force exerted vertically on the slab was generated by a moving mass acceleration and controlled by a signal generator. An accelerometer was mounted to the shaker armature to measure the excitation force applied to the slab. Compared to the test structure, the mass of the shaker body was assumed to be negligible.

For the acquisition of modal data, accelerometers with a sensitivity of 200 mV / g were used. The data was transmitted using an accelerometer-connecting microdot cable to the analyzer. In the longitudinal direction, ten accelerometers were mounted on the top surface of the slab along its two edges at an equal distance of 500 mm, as shown in Figure 3.11(a) and (b). Brincker & Ventura (2015) described in their textbook, the correct selection of sensors location is always uncertainty, however, the consideration should be away from any node points and in practice, it is always use at least five or six sensors.

In data acquisition of both excitation and response signals, a 12-channel IMC CRONOXflex dynamic analyzer was used. The tests were conducted at a frequency bandwidth ranging from 0 to 500 Hz with the sampling rate 1000 sps. Sampling rate defines the upper frequency band limit which can be used to analyze the recorded signals. It is a number of data samples acquired per time unit and measured as samples-

per-second (sps) and also referred to as sampling frequency. So, if the data was acquired at a 1000 Hz sampling frequency, it means data was acquired at a rate of 1000 sps. The Nyquist frequency as stated in Equation 3.1 specifies the upper limit of the frequency band (f_v) (Brincker & Ventura, 2015).

$$f_v = f_s/2; \; f_s = 1/\Delta t \qquad\qquad \text{Equation 3.1}$$

Where f_s is the sampling frequency, and Δt is the sampling time step. So if the frequency of sampling is 1000 Hz, the frequency band is limited to 500 Hz and no information exceeding this frequency can be captured. The sampling rate must be selected properly to detect the entire interest mode from the measured signals.

(a) Plan view

(b) Front elevation

Accelerometer

(c)
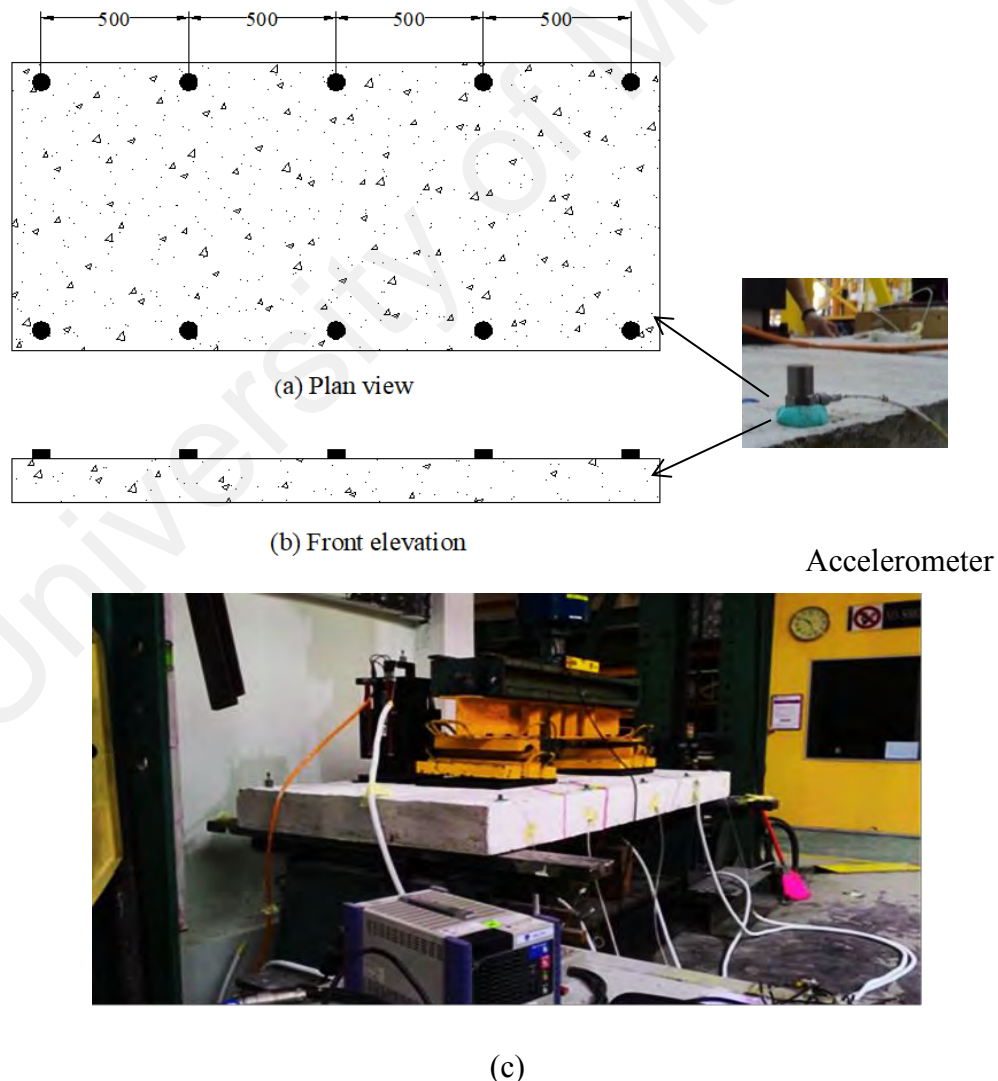
Figure 3.11: (a), (b) Position of the accelerometers on the slab (unit in mm), (c) Modal test set-up

In order to identify the reasonable variation of the structural frequency value, preliminary FE simulations could be carried out. A more practical approach, the recommended frequency of sampling must usually be greater than about 1.2 times f_v. The sampling frequency can be determined from Equation 3.1 by means of Equation 3.2 (Brincker & Ventura, 2015).

$$f_s > 2.4\, f_{max} \qquad\qquad \text{Equation 3.2}$$

Where f_{max} is the highest frequency of interest. Therefore, it is important to have an idea of the expected levels of structural vibration before performing the modal test of a structure.

The measurement durations are another important element to be considered during the data acquisition. According to ANSI S2.47 (Brincker & Ventura, 2015), a minimum time series length of the signal to be captured can be estimated about 20 times the lowest interest frequency memory as stated in T_{tot} (Equation 3.3) overall time series length.

$$T_{tot} = \frac{20}{2\xi f_{min}} = \frac{10}{\xi f_{min}} \qquad\qquad \text{Equation 3.3}$$

Where ξ is the modal damping factor. In this study, Equation 3.3 would result in a required minimum record length of 15.8s for a system of 1% damping and f_{min} of 63 Hz. Practicality, performance of modal testing is very concerned about the time and budget for the entire evaluation project commonly carried out on existing infrastructure such as bridges and buildings. Through the sensors attached to the slab surface in the time domain as plotted in Figure 3.12, the dynamic data was captured by the dynamic analyser.
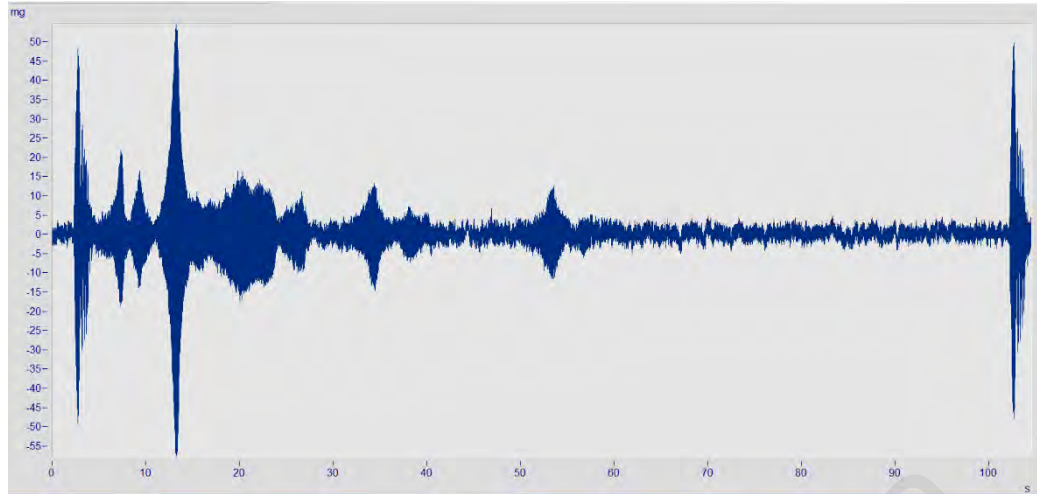
Figure 3.12: Response time history signal from a sensor during measurement

3.7 Finite Element Analysis

The FE analysis begins with a FE model being developed. FE model is a computational method used to solve the problem of engineering that includes stress analysis, dynamics, heat transfer, electromagnetism, fluid flow, etc. It is basically a numerical method and, coupled with a common algorithm, it forms a powerful unifying approach to finding a solution to a large and complex problem of engineering. By subdividing the structure into nodes and elements, the FE model breaks a complex domain into a number of simple finite elements. Each node has one or more degrees of freedom representing the structure's displacement. FE analysis is used in structural dynamics to create a virtual dynamic model of the actual structure. The system governing equation is started with the general linear movement equation as given in Equation 3.4 (Abdel Wahab, 2008).

$$[M]\{\ddot{u}\} + [C]\{\dot{u}\} + [K]\{u\} = \{F\}$$ Equation 3.4

Where M, C and K represent, respectively, the system's mass, damping and stiffness matrices. The system disregards damping by assuming free vibration. For most

engineering systems, due to its small amount, the damping value in the physical system can be ignored.

$$[M]\{\ddot{u}\} + [K]\{u\} = \{0\} \qquad \text{Equation 3.5}$$

By assuming harmonic of motion in physical system, Equation 3.6, Equation 3.7 and Equation 3.8 are substitute into Equation 3.5 and simplify to produce Equation 3.9 (Abdel Wahab, 2008).

$$\{u\} = \{\emptyset\}_i sin(\omega_i t + \theta_i) \qquad \text{Equation 3.6}$$

$$\{\dot{u}\} = \omega_i\{\emptyset\}_i cos(\omega_i t + \theta_i) \qquad \text{Equation 3.7}$$

$$\{\ddot{u}\} = -\omega_i^2\{\emptyset\}_i sin(\omega_i t + \theta_i) \qquad \text{Equation 3.8}$$

$$|\{[K] - \omega_i^2[M]\} = 0| \qquad \text{Equation 3.9}$$

From the Equation 3.9, the natural frequencies and their corresponding mode shapes are extracted through the matrix form. This is an eigenvalue problem which may be solved for up to n eigenvalues, ω_i^2 and n eigenvectors, $[\emptyset]_i$, where n is the number of degree of freedom (DOF). The square roots of the eigenvalues are ω_i, the structure's natural circular frequencies (rad/s). Natural frequencies, f_i can then calculate as in Equation 3.10 (Abdel Wahab, 2008).

$$f_i = {\omega_i}/{2\pi} \qquad \text{Equation 3.10}$$

Note that Equation 3.9 has one more unknown than equations; therefore, to find a solution, an additional equation is required. The addition equation is provided by standardization of the mode shape. Mode shapes can either be standardized to the mass matrix or unity where the vector's largest component is set to 1 as stated in Equation 3.11 (Heylen et al., 1997). Mode shape is the shape assumed by the structure when vibrating at frequency f_i.

$$\{\emptyset\}_i^T = [M]\{\emptyset\}_i = 1 \qquad\qquad \text{Equation 3.11}$$

The accuracy of the results obtained, however, depends on the modeling accuracy of the structure. This is where the experimental measurement technique is required to ensure these modal parameters. Then the results of the FE analysis are correlated with the results of the experiment. Good correlation means a good model of FE. The simulations, predictions and modifications can now be performed virtually once the FE model has been assured. This avoids any forms of' trial-and-error' solutions that may be costly and time consuming on the actual structure.

Nowadays, more attention is given to the dynamic behavior in the field of civil engineering, particularly on the lightweight structures and structures susceptible to external cyclic loading such as high-rise buildings, bridges, railway viaducts and dams. The dynamic behavior analysis is neither trivial nor straightforward. The dynamic behavior is described through a structure's modal parameters that were determined by experimental or numerical methods. It is expected that the results of both investigations will closely correlate. Experimental measurements provide information on the tested structure configuration. While FE models allow predicting the structure's dynamic behavior under different loading conditions, material type, size dimension, and boundary conditions, FE models are often not guaranteed to be reliable. To verify and correct these FE models against the experimental data, model updating technique is implemented. Further structure predictions can be made using the reliable FE model that has been improved from the updating analysis of the model. Basically, by referring to the experimental results, it involved modifying or updating the uncertainty parameters in the initial FE model. In other words, it is a process of refining a physical structure's mathematical model based on the results of the experiment. A number of FE model updating methods have been established in structural dynamics. Response surface

method (RSM) is one of the methods used in this study for the following reasons: (1) simplification of programming; (2) fast response calculation and; (3) easy reverse optimization (Fang et al., 2012). The details of this method can be found in the relevant texts (George & Draper, 1987). Figure 3.13 shows the general scheme of the FE model updating procedure.

3.8 Response Surface Based on Finite Element Model Updating

3.8.1 Background

Conceptually, during optimization iterations, FE models needed to be tuned and recalculated, which is considered to be costly computational time. As is known, the existing traditional FE model updating technique based on sensitivity involved complicated development of sensitivity matrices and it affects performance during the optimization process. A huge number of computations involved for such a large FE model, such as civil engineering structures such as bridge, dam and building, and it will expand the many iteration runs to be carried out. It can cause difficulty in convergence and consume a lot of time.

Possible solutions can therefore refer to a response surface method (RSM), which Box & Wilson (1951) Box & Wilson (1951) pioneered. RSM has demonstrated attractive ability to modify parameters of the FE model. Ren & Chen (2010) revealed that the RSM offered efficient and converged quickly compared to the traditional model updating method based on sensitivity. A good approximation of the response surface built from the FE model is demonstrated as a key to the updating method's success. A year later Ren et al. (2011) extended the study by integrating the method to accurately model complex civil structures such as bridges with the structural static response. Since then, the efficient method applied in FE model updating has been enhanced by RSM in several stages (Fang et al., 2014; Fang et al., 2012; Shan et al., 2015; Zhai et al., 2016).
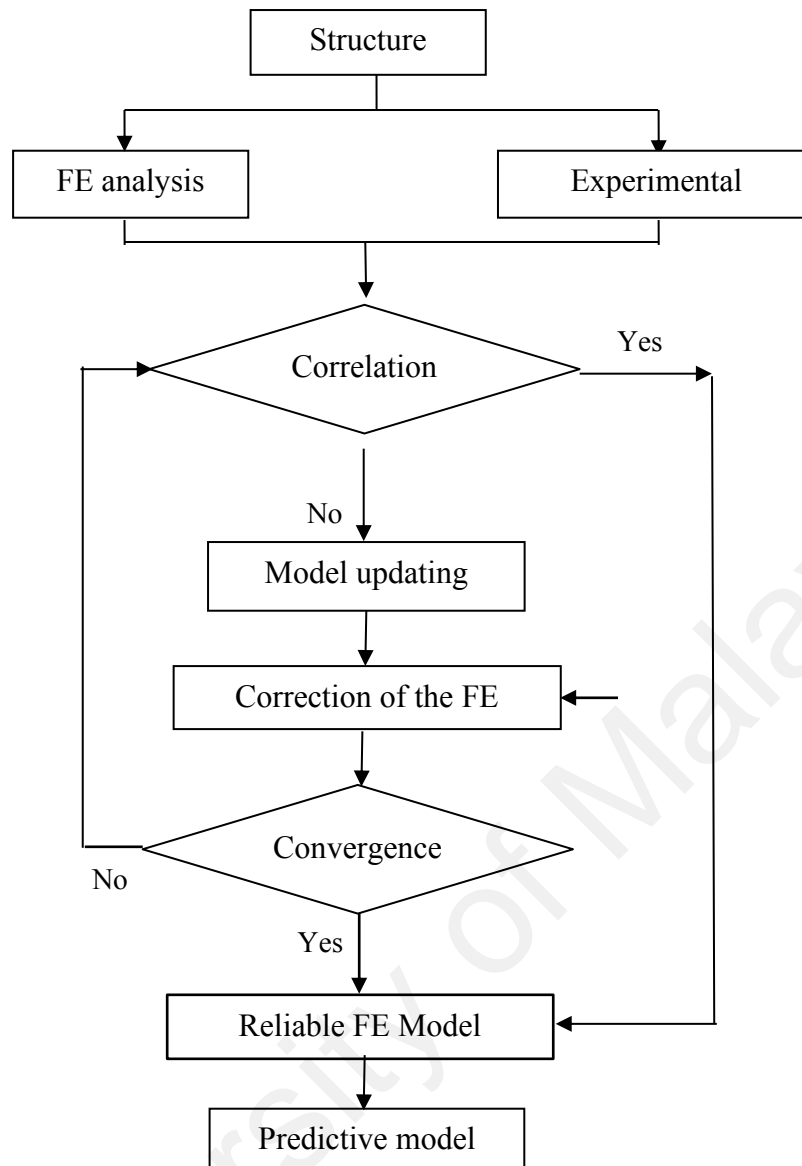
Figure 3.13: Procedure of FE model updating

In structural FE model updating, verification and validation, the RSM has been adopted extensively Zong et al., (2015). Basically, RSM is a combination of mathematical and statistical techniques. A simple relationship between parameters and a response based on limited boundary data will be expressed in the mathematical formula. It provides a response mechanism from a given input variables. The parameter is used to generate an output response as an input to be updated. A response surface equation is then developed from this approximation model, thus replacing the initial FE model for optimization purposes. The developed equation is relatively simple, as compared to a

full FE model, the optimization method operates on the surface response and not computationally intensive. Furthermore, many commercial FE analysis software are available nowadays, providing this package for ease of implementation through parallel computation, as well as calculating parameter sensitivity.

3.8.2 Response Surface-based in Structural Dynamic Finite Element Model Updating

Response surface method is a mixing technique between mathematics and statistics that is used for modeling and analysis with the aim of optimizing the response influenced by numerous variables input. The RSM process based on updating the FE model is shown in **Error! Reference source not found.**.

The procedures include the following.

- The selection of the structural parameters by using the design of experiments (DOE).

- The computation of the response by carrying out the FE analysis.

- The creation of the response surface model by performing the final regression and after that regression error.

- The development of response features of the structure through its corresponding objective functions which to be minimized.

- The updating of FE model within the developed response surface model.

- The surrogate of updated parameter to the initial FE model.

```
                    ┌─────────────┐
                    │     DOE     │
                    └─────────────┘
                           │
                           ▼
                    ┌─────────────┐
                    │     FEA     │
                    └─────────────┘
                           │
                           ▼
              ┌───────────────────────────┐
              │  Response surface creation │
              └───────────────────────────┘
                           │
                           ▼
              ┌───────────────────────────┐
              │  Response surface creation │
              └───────────────────────────┘
                           │
                           ▼
              ┌───────────────────────────┐
              │  Response surface check    │
              └───────────────────────────┘
                           │
                           ▼
              ┌───────────────────────────┐
              │     Model updating         │◄────┐
              └───────────────────────────┘     │
                           │                     │
                           ▼                     │
                    ◇─────────────◇              │
                  ◇   Convergence   ◇────────────┘
                    ◇─────────────◇        No
              Yes          │
                           ▼
              ┌───────────────────────────┐
              │      Updated FEM           │
              └───────────────────────────┘
```
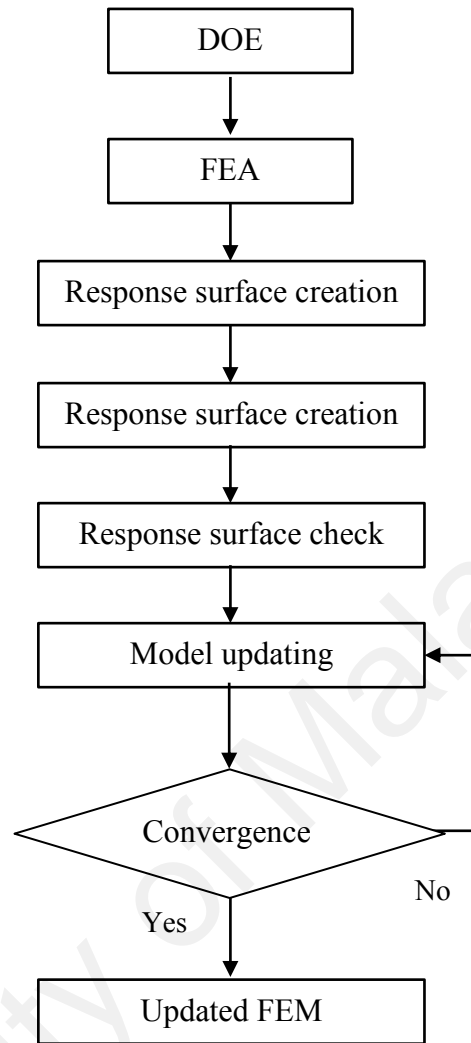
Figure 3.14: The procedure of RSM based on FE model updating

3.8.2.1 Parameter selection

DOE refers to experiment planning involving a selection of parameters to be updated as a process to generate a structure's reliable response surface. The response surface created will serve as the FE model's surrogate. However, there are several methods used in DOE. Guo & Zhang (2004) found that these two methods of central composite design (CCD) and D-optimal design were most suitable for updating FE model structural dynamics.

Similar to other updating methods, in updating the FE model, the process of selecting updating parameters is an important aspect. The criteria of how many

parameters are used in the optimization process and which parameters are used to be sensitive parameters. The selection of parameters requires considerable physical perception to avoid any conditioning during the optimization process as only a few vibration modes are commonly identifiable from the vibration test.

3.8.2.2 Response surface regression

In the case of structural dynamics, in representing a response surface, the updated FE modeling was developed using a response surface based on the polynomial mathematical approach. The Equation 3.12 expresses a typical quadratic polynomial form applied in the RSM (Ren & Chen, 2010).

$$y = \beta_o + \sum_{i=1}^{k} \beta_i x_i + \sum_{i=1}^{k} \sum_{j=1}^{k} \beta_{ij} x_i x_j \qquad \text{Equation 3.12}$$

Where β is the polynomial coefficient which was obtained from the least square estimation as stated in Equation 3.13 (Ren & Chen, 2010)..

$$\beta = [X^T X]^{-1} \{X^T Y\} \qquad \text{Equation 3.13}$$

The response y can be evaluated once the polynomial coefficient β are obtained from the input data X and Y as stated. To check the accuracy perfection of the regressed surface, the response surface should be checked before updating the structural FE model. R^2 criterion (value range from 0.0 to 0.1) and empirical integrated square error (EISE) criterion as expressed in Equation 3.14 and Equation 3.15 can be used to verify the response surface (Ren & Chen, 2010).

$$R^2 = 1 - \sum_{i=1}^{N} [y_{RS}(j) - y(j)]^2 \bigg/ \sum_{j=1}^{N} [y(j) - \bar{y}]^2 \qquad \text{Equation 3.14}$$

$$EISE = \frac{1}{N} * \sum_{j=1}^{N} [y_{RS}(j) - y(j)]^2 \qquad \text{Equation 3.15}$$

Where Y_{RS} is the response value of the confirmation samples, y is the true value of the confirmation samples and $\bar{Y}$ is the mean of all true values. The more accurate of the regressed surface is presented in the larger value of R^2. It contradicts the EISE value, the lower value is the closer data fit.

3.8.2.3 Model updating

The natural frequency is used as a response feature of your own solution in this structural dynamic FE model updating. Therefore, in terms of residuals between numerical and measured natural frequencies, the formulation for the optimized objective function is expressed as shown in Equation 3.16 (Ren & Chen, 2010).

$$\Pi(x) = \sum_{i=1}^{m} w_i(\lambda_{ai} - \lambda_{ei}) \quad 0 \leq \omega_i \leq 1$$

Equation 3.16

Where x is the design set, m is the number of modes, λ_{ai} and λ_{ei} are the numerical (finite element computed) and measured natural frequencies of the ith mode respectively. The different order of neutral frequencies is imposed by the ω_i weight factor.

Then the updating of the FE model can be modelled as a restricted problem of minimization to obtain the satisfied set of design as subject to Equation 3.17 (Ren & Chen, 2010).

$$x_{lk} \leq x_k \leq x_{uk,} \qquad k = 1,2,3, ...$$

Equation 3.17

Where X_{lk} and X_{uk} are the upper and lower bounds on the kth design variable to be set. N is the total number of design variables also known as updated parameters.

3.9   Summary

This chapter described the details of the laboratory program. The main goal of this program is to evaluate the structural dynamic behavior including the natural frequency and damping ratio of typical RC slabs under constant cyclic loads at the level of variety

fatigue damage using vibration measurement. Repeated loading of the cyclic load will result in structural degradation of the stiffness and load carrying capacity. Therefore, on these fatigued RC slabs monotonic static load tests are performed to continuously monitor the dynamic behavior of the damaged RC slabs. The work related to FE modeling, correlation and updating of tested RC slabs under fatigue and damage condition is also presented in this chapter 3. The main purpose of updating the model is to obtain calibrated FE models against experimental data.

CHAPTER 4: RESULTS AND DISCUSSIONS

4.1   Introduction

This chapter presents the results finding from the experimental testing and finite element (FE) modeling and updating. The updated FE models will be used later to quantify the fatigued structure's serviceability that is simulated to the existing structure. Updated FE models are usually used in dynamic structures in civil engineering, such as damage detection, structural heat monitoring, and structural assessment and evaluation. This chapter begins by present the experimental results, and then updated FE modeling. Based on these finding, analytical investigation on stiffness degradation and residual strength was carried out to develop a relationship between these parameters in producing the serviceability prediction model.

4.2   The effects of Fatigue Damage on Dynamic Response

The modal parameter estimates using enhanced frequency domain decomposition (EFDD) techniques introduced by Brincker et al. (2001) through operational modal analysis (OMA). The main part of this technique is to perform Power Spectral Density (PSD) output singular value decomposition (SVD). The natural frequencies were directly based on the peaks of the SVD plots and the corresponding singular vectors can be used to obtain mode shapes. EFDD is an enhanced FDD technique intended to obtain the coefficients of damping through the technique of logarithmic decrement. This paper will not provide the detailed process of this technique, it is provided in Zhang et al. (2010). As mentioned above, for this AVT, ten accelerometers were used for each measurement set-up. Modal parameter was identified in this research using the EFDD method as used in commercial software for modal analysis. The data was captured by the dynamic analyzer during the experimental and extracted automatically in time histories as shown in Figure 4.1.
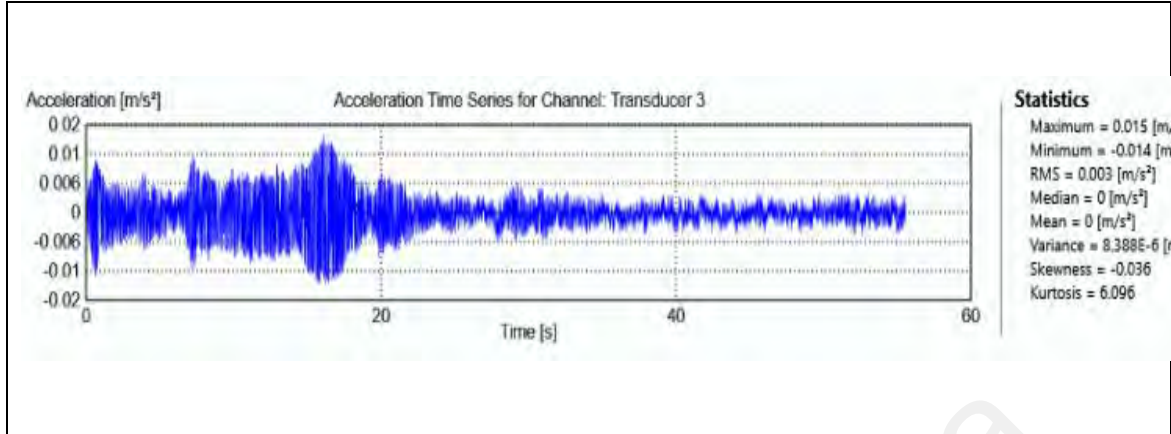
Figure 4.1: Typical time history signal of slab during measurement

The software has an option to import asci type as input file before the pre-processing and analysis stage can be carried out. The asci file was developed by specimen degree information and geometry, sampling interval and set-up of measurement. The software processed and recognized the measurement set-up file and was to be transformed into a graphical view to show the geometry position and measurement set-up as shown in Figure 4.2. The data was filtered after the pre-processing before the spectral density matrices could produce the SVD.

Figure 4.3 presents the measurement of SVD on the spectral density matrix. The top curve shows the largest value representing the most significant singular values to be used to determine the modal parameter from the five singular values obtained. The significant frequencies and corresponding modes were identified as the structural modes by applying peak-picking to the specific peaks of the singular values as shown in Figure 4.3.
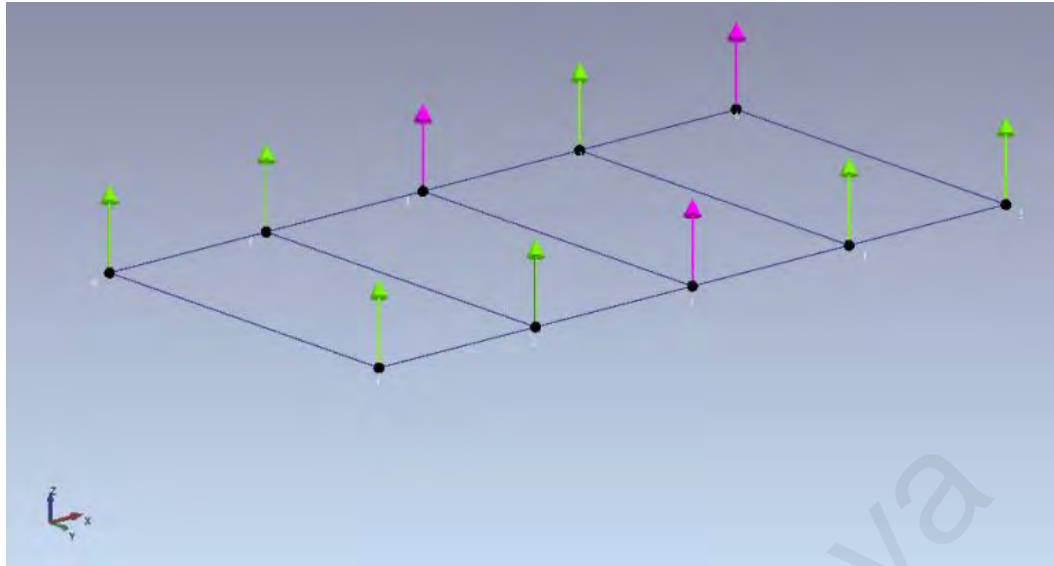
Figure 4.2: Geometrical arrangement of transducers in AVT of RC slab

Despite the fact that there are close-spaced modes in the top SVD curve, using this peak-picking of EFDD technique, it is possible to identify the close modes and even repeated modes by not including the harmonic components. Note that a typical resonating system response is declining exponentially as shown on Figure 4.4, the red region specifies the part of the correlation function used to recognize possible modes without harmonic components. The frequency obtained has been validated by crossing the zero axis by the correlation function as shown in Figure 4.5.

The damping estimate was determined from the correlation function logarithm envelope performed by a linear regression technique representing the red line as shown in Figure 4.6. This natural frequency and damping estimation process was carried out by averaging all sets of measurement data together. Table 4.1 show the first three natural frequencies identified by the AVT on the different level of damage of the SF1M, SF1.5M and SF2M slabs.
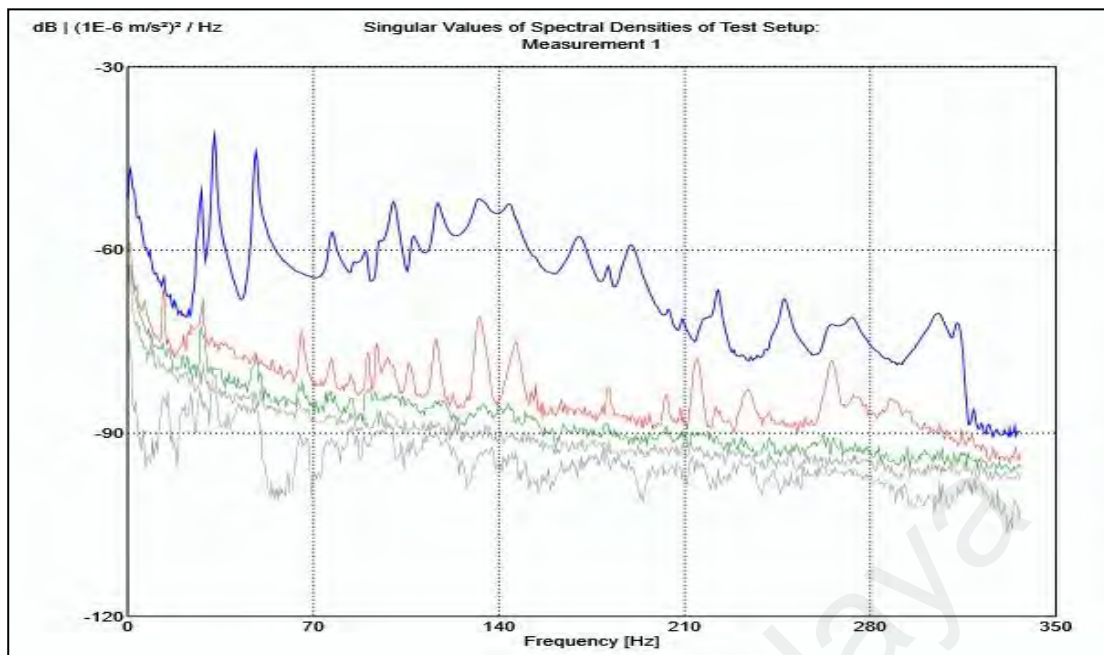
Figure 4.3: Peak-picking of the SVD
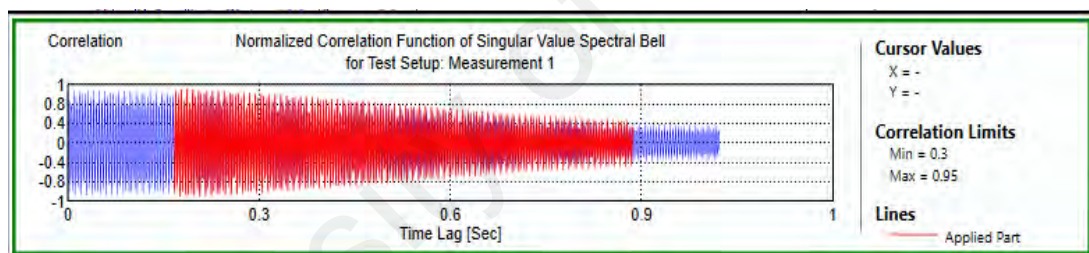
Figure 4.4: Normalized correlation function for mode at specific frequency from the data set
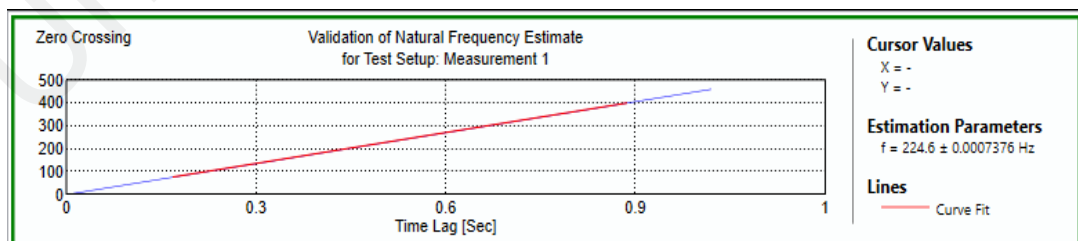
Figure 4.5: Natural frequency identification by zero-crossing counting
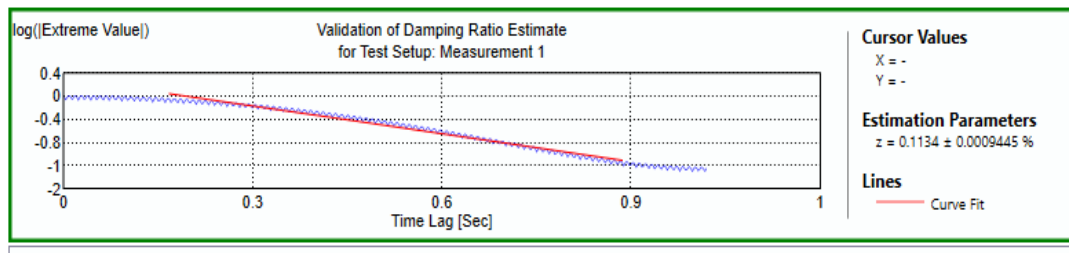
Figure 4.6: Damping ratio estimation from the decay of the correlation function

Table 4.1: First three measured natural frequencies of the RC slabs at the level of undamaged, fatigued due to 1.0 (SF1M), 1.5 (SF1.5M) and 2.0 (SF2M) million cyclic loads and damaged due to static load

Natural frequencies, f (Hz)							
Mode number	Undamaged slab	Fatigue scenario			Damage scenario		
		SF1M	SF1.5M	SF2M	SF1M	SF1.5M	SF2M
1	63.5	48.2	41.0	39.0	38.6	36	29.2
2	159.2	170.0	153.0	128.7	155.0	132.3	124.7
3	199.4	189.0	203.6	183.4	247.0	153.1	133.3
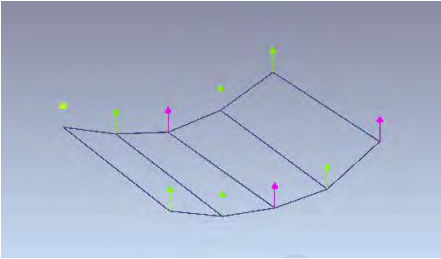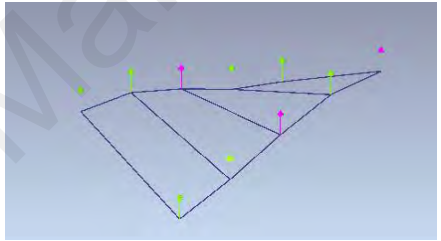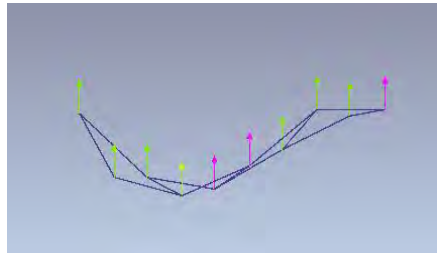
Table 4.2 corresponds to the slab SF1M, SF1.5M and SF2M measured damping ratio respectively. These ratios characterize the slab's damping, which is closely related to the system's energy dissipation or energy loss. It can be observed that the trend in the measured damping ratio has increased as the level or severity of damage has increased, which is consistent with the fact that damage in the slabs affects the change in the damping ratio, but the changes in SF1.5M and SF2M have been inconsistent and previous researchers have concluded a relatively unreliable damage indicator (Prasad & Seshu, 2010; Razak & Choi, 2001). Figure 4.7, Figure 4.8 and Figure 4.9, respectively, show the measured mode shapes of undamaged, fatigued (SF1M, SF1.5M and SF2M) and damaged RC slabs.

Table 4.2: First three measured damping ratio of the RC slabs at the level of undamaged, fatigued due to 1.0 (SF1M), 1.5 (SF1.5M) and 2.0 (SF2M) million cyclic loads and damaged due to static load
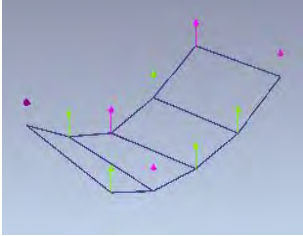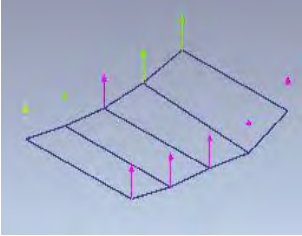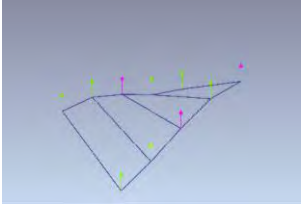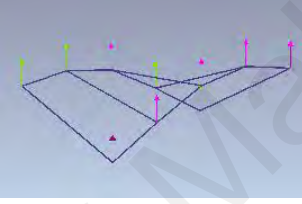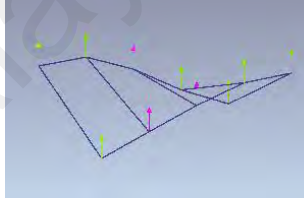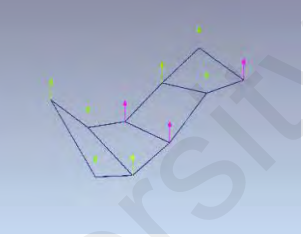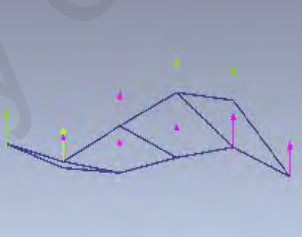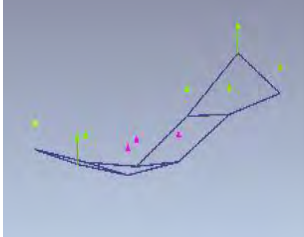
Damping ratio, ζ (%)							
Mode number	Undamaged slab	Fatigue scenario			Damage scenario		
		SF1M	SF1.5M	SF2M	SF1M	SF1.5M	SF2M
1	1.95	1.36	1.60	2.43	1.57	2.27	1.95
2	1.09	1.44	0.97	1.84	2.37	1.37	1.56
3	0.67	1.21	0.44	2.45	2.57	1.28	1.33

Figure 4.10 presents the normalized natural frequency variation as ($\Delta f = f^i_{1T} - f^0_{1T})*100/f^0_{1T}$) a function of the number of cycles. f^0_{1T} is referred to frequency obtained at undamaged slab before applying any load, and subsequently after each certain number of cycles, the measured frequency is represented by f^i_{1T}, where i is the number of cycles. The curve in the graph shows that the natural frequency significantly decreases over the first 1.5 million cycles, but remains almost consistent afterwards, which is consistent with Nieto et al. (2006)'s findings as influenced by the elastic module.
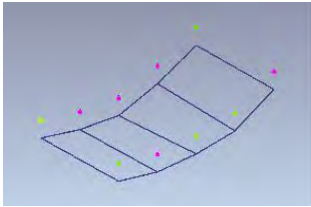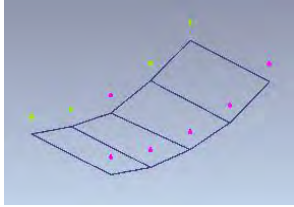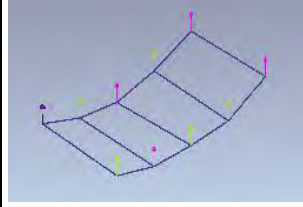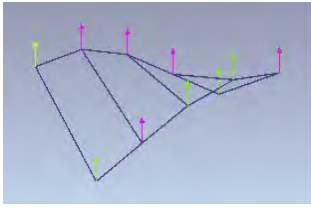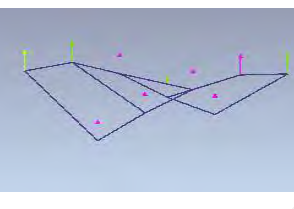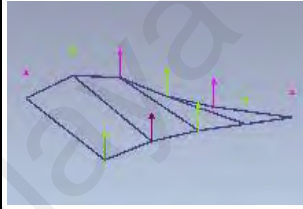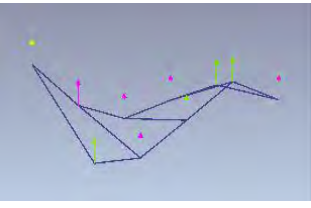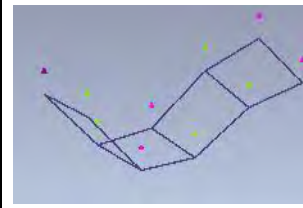
Referring to Figure 4.11, the results of the natural frequencies of all modes of the slabs are depicted by a bar graph against the damaged level. The downward trend in the graph indicates that by comparison, the two parameters from different non-destructive and destructive techniques is proportional to the stiffness of RC slabs. The magnitude of degradation may also become an indicator to the severity of damage induced onto the structure.

Mode number	Mode shape	Undamaged slab
1	First bending	f = 63.5Hz, ξ = 1.95%
2	First torsion	f = 159.2Hz, ξ = 1.09%
3	Second bending	f = 199.4Hz, ξ = 0.67%

Figure 4.7: Mode shapes of undamaged RC slab, identified as 1st and 2nd bending (mode 1, mode 3) and 1st torsion (mode 2)

Mode number	Fatigue scenario		
	SF1M	**SF1.5M**	**SF2M**
1	f = 48.2Hz, ξ = 1.36%	f = 41.0Hz, ξ = 1.6%	f = 39.0Hz, ξ = 2.43%
2	f=170.0Hz, ξ = 1.44%	f = 153.0Hz, ξ = 0.97%	f = 128.7Hz, ξ = 1.84%
3	f=189.0Hz, ξ = 1.21%	f = 203.6Hz, ξ = 0.44%	f = 183.0Hz, ξ = 2.45%

Figure 4.8: Mode shapes of fatigued RC slabs; SF1M, SF1.5M and SF2M, identified as 1st and 2nd bending (mode 1, mode 3) and 1st torsion (mode 2)

Mode number	Damage scenario		
	SF1M	SF1.5M	SF2M
1	f = 38.6Hz, ξ = 1.57%	f = 36.0Hz, ξ = 2.27%	29.2Hz, ξ = 1.95%
2	f = 155.0Hz, ξ = 2.37%	f = 132.3Hz, ξ = 1.37%	f = 124.7Hz, ξ = 1.56%
3	f = 247.0Hz, ξ = 2.57%	f = 153.1Hz, ξ = 1.28%	f = 133.3Hz, ξ = 1.33%

Figure 4.9: Mode shapes of damaged RC slabs; SF1M, SF1.5M and SF2M due to static load, identified as 1st and 2nd bending (mode 1, mode 3) and 1st torsion (mode 2)
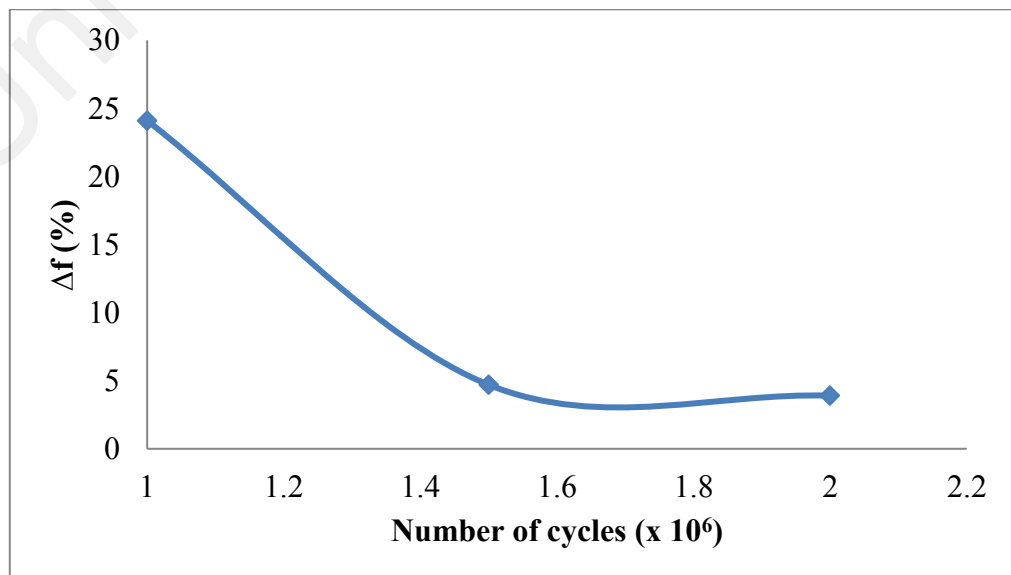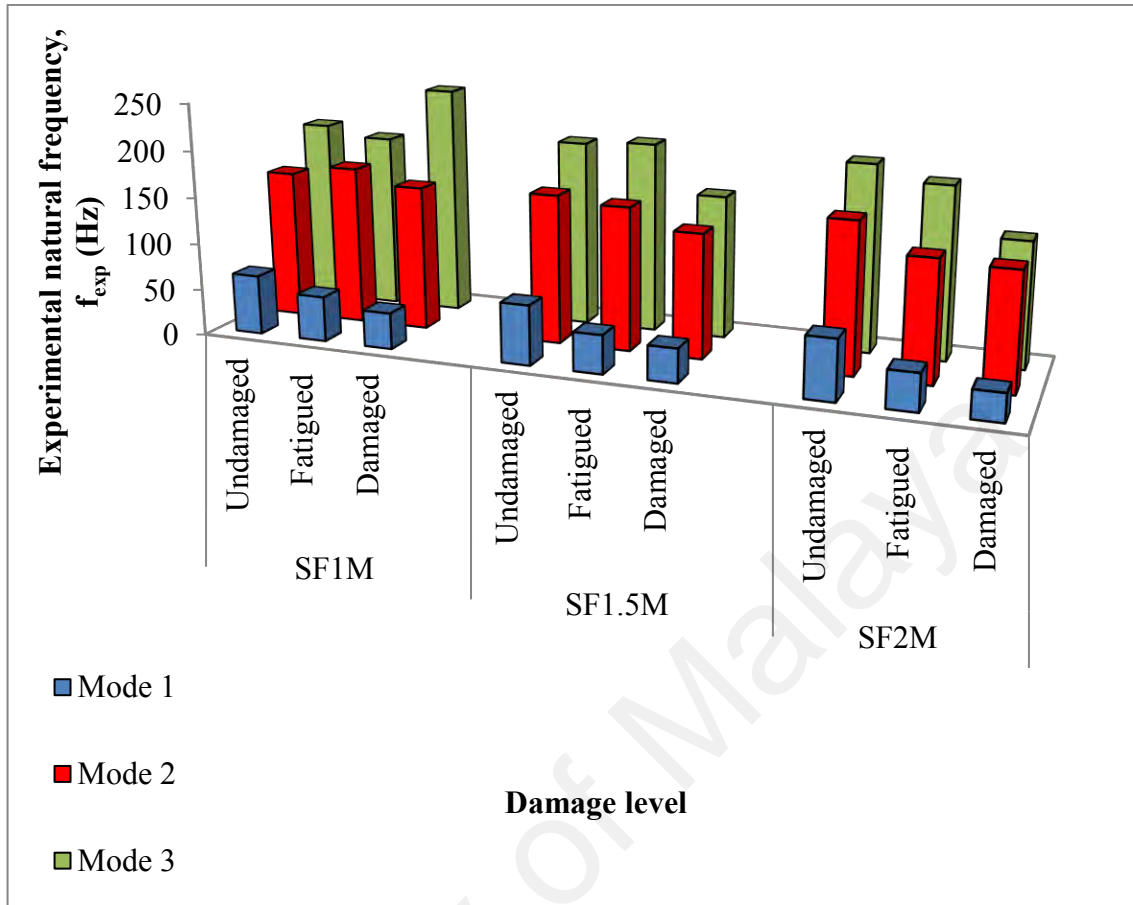
Figure 4.11: Effect of undamaged, fatigued and damaged structures on natural frequency

4.3 Finite Element Modelling, Ccorrelation and Updating of Tested Reinforced Concrete Slab Structures

This section describes the overall FE analysis and process of updating the tested RC slab structures. In the previous chapter, the detailed explanation on the experimental part was described.

4.3.1 Finite Element Modelling and Analysis

First of all, the initial FE model was developed using Ansys Workbench 16.2. To characterize the properties of the RC slab, a line element with user-integrated cross section was selected for geometry properties. User-integrated cross-section type is used by defining the geometry through the cross-section area, A (mm^2) and the inertia

moment, I (mm^4), as shown in Figure 4.12. The RC slab ends were modelled as pin and roller supports as a boundary condition by setting the appropriate displacement at the global coordinate system.

Initially, the model was developed using specific initial value of material properties to represent the undamaged slab. The concrete modulus of elasticity, $E_{c,s}$ is 29915 MPa, estimated using the empirical expression as calculated from Equation 4.1 (Nawy, 2005) and the Poisson's ratio, υ_c is 1.0.

$$E_{c,s} = 4730\sqrt{f_c}$$ Equation 4.1

Where f_c = 40 N/mm^2 is the compressive concrete stress.
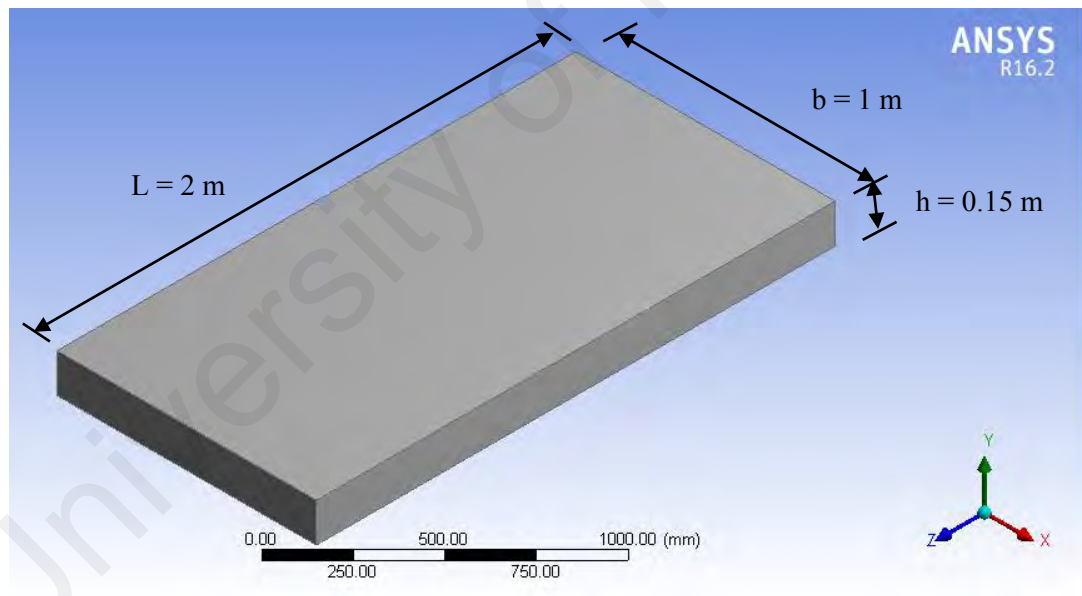
Figure 4.12: FE model of RC slab structure

According to BS 1881-209 (1990) for equivalent static modulus of concrete $(E_{c,s})$ between 13 to 52 GPa, the value of dynamic modulus of concrete $(E_{c,d})$ could vary between 24 to 58 GPa. In addition, the formula for calculation of $E_{c,d}$ can also be found

in other relevant text (Neville, 2009; BS 1881-209, 1990). In this research, Equation 4.2 (Neville, 2009) was used for the calculation of $E_{c,d}$.

$$E_{c,d} = \frac{1}{0.83} E_{c,s}$$ Equation 4.2

The numerical modeling calculated the first three natural frequency modes for the initial FE model of the RC slab structure corresponding respectively to the first bending and second bending mode shapes for mode 1 and mode 3 as shown in comparison with the natural frequencies Figure 4.13.
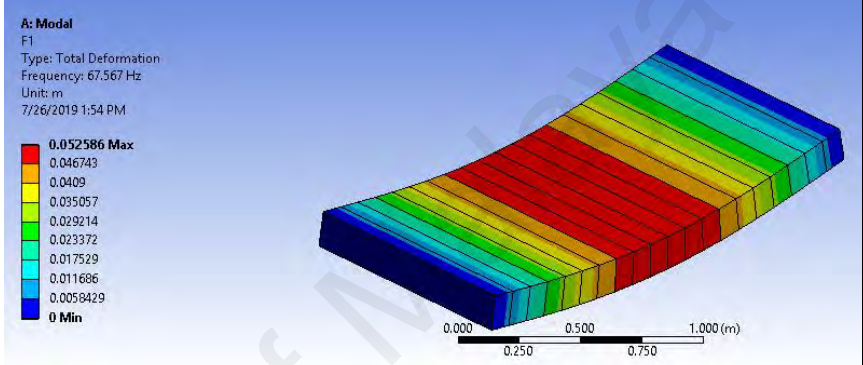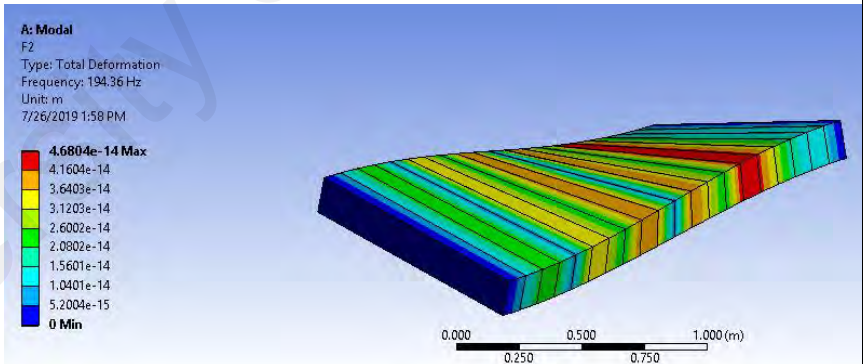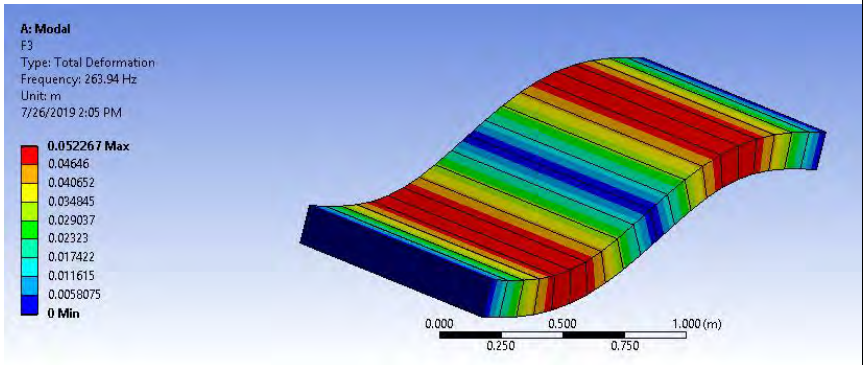
Through the correlation analysis, the degree of similarity of modal parameters can be examined qualitatively and quantitatively. The process of updating begins with the matching step of the model. In general, the most common method of direct comparison used by analysts is through specific natural frequencies matched between numerical and experimental models.. This is often done by using the simple Equation 4.3. The relative error (Δ_f) of the numerical natural frequency (f_{fem}) is calculated against the experimental measured (f_{exp}).

$$\Delta_f = \frac{f_{fem} - f_{exp}}{f_{exp}}$$ Equation 4.3

Table 4.3 presents the comparison of experimental and numerical outcome of neutral frequencies at the initial undamaged state. The reasons for the deviation between the two methods may be that in simulation, the boundary condition, geometry and material characteristics are not completely the same as that of the structures being tested. Equation 4.17 quantifies the difference between natural and experimental frequencies and the number of the first mode is 6.30%.

A linear graph by plotting the experimental value for each of the modes against the numerical has been used for correlation. The good matching correlation between the two result sets is shown as a straight line on the graph with a regression value of 0.9916 (Figure 4.14).

Mode	Natural frequency, f (Hz)	Mode shape
1	67.57	
2	194.36	
3	263.94	

Figure 4.13: The first three natural frequencies and the corresponding mode shapes of the initial RC slab FE model

Table 4.3: Natural frequencies correlation between experimental (f_{exp}) and initial numerical ($f_{fem,int}$) of the undamaged RC slab

Mode	Experimental, f_{exp} (Hz)	FEM, $f_{fem,int}$ (Hz)	Error $\Delta f=(f_{exp} - f_{fem,int})/f_{exp}$ (%)
1	63.5	67.57	6.30
2	159.0	194.36	22.96
3	199.0	263.94	32.63
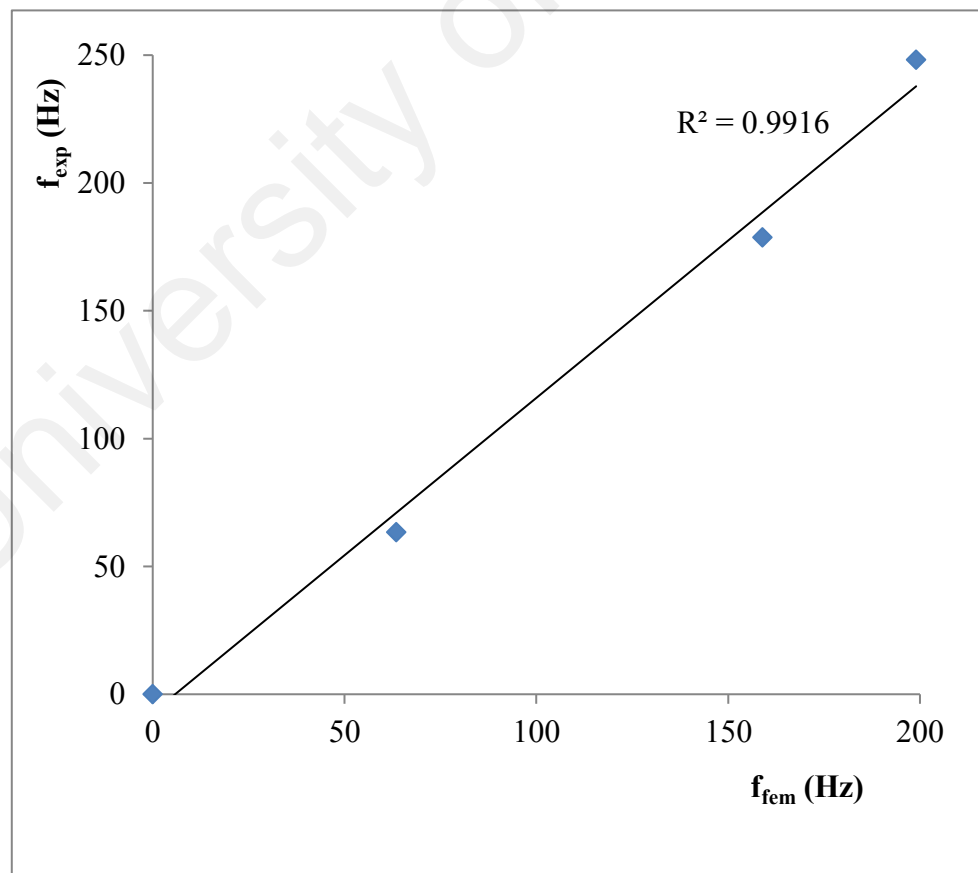
Figure 4.14: Comparison between initial numerically calculated (f_{fem}) and experimentally estimated (f_{exp}) natural frequencies

4.3.2 Finite Element Model Updating Technique

It can be seen in the previous section, the method of correlation provides information about the existence of differences between the two models without describing whether the mass of stiffness influences them. Overall, by applying some uncertain changes in sensitive parameters, the model updating process is enhanced by the presence of model updating technique using RSM, an updated FE model can imitate the structure's measured response.

The same initial FE mode is used to update the FE model. The initial FE model needs to be updated by varying the material and geometry properties of the slab structure to match the experimental natural frequencies. The updating exercise was carried out with the parametric optimization of Ansys Workbench FE software. Traditionally, optimization tasks were performed mostly through trial and error in order to achieve a suitable parameter goal. For today's computer technologies, using numerical optimization techniques to guide the evaluation of target results is a more productive and cost-effective practice.

In model updating process, the most sensitive parameters are highly considered, otherwise the impact of variation of parameters on the structure's dynamic properties is difficult to accurately measure. Due to insufficient information, this will make the updating process unconditional.

However, preparation of a FE model to be a candidate for updating requires some specific considerations of additional factors not normally taken into account in conventional FE model construction. Of these, an important one is that uncertainties in a structure must be expressed quantitatively as parameters. When damage is known to

exist in a localised area in a structure, one way to simulate the damage is to incorporate some 'weak' elements (Brownjohn and Xia, 2000; Xia and Brownjohn, 2004) into an FE model. This avoids the problem of damage detection that would require far more unknowns. For the purpose, beam elements were used to represent the damage zones at the midspan. If the parameters take the real values for the damage zones, then the FE model is taken to represent the damaged RC slab, but if the parameters match those for the rest of the slab the FE model represents the undamaged slab. By estimating the parameters of the 'weak' beam elements through model updating based on measured data, the damage is quantified and the residual stiffness and load-carrying capacity could be determined.

To illustrate the sensitivity of the response to the variations of the parameters, three parameters were investigated: the moment of inertia (I), the module of Young (E) and the density (π) by conducting the RSM procedure. This consideration for the simply supported uniform beam as expressed in the already known equation as shown in Equation 4.4, in accordance with the theoretical of flexural frequencies (Daniel, 2008).

$$f_n = \frac{n^2 \pi}{2L^2} \sqrt{\frac{EI}{\rho A}}$$

Equation 4.4

Where f_n is the natural frequency in Hz, n is the mode order, L is the structure length in m, E is the Young's modulus in N/m^2 or Pa, ρ is the density in kg/m^3 and A is the cross-section area in m^2. The geometry properties of I and A related to the parameter t. Therefore, the selected sensitive parameters indicate their significance contributions to the natural frequencies.

In the updating process, the selected uncertain parameters were restricted based on engineering judgment with upper and lower limit values to ensure the physical

significance that reflects the real structure. The updated FE model and experimental's natural frequencies and mode shapes that presented in Figure 4.15 are highly correlated with $R^2 = 0.9916$ as shown in Figure 4.16.

Table 4.4 presents the comparison of experimental and updated numerical outcomes at undamaged state. It shows that the first frequency differences were reflected in the actual dynamic behavior of the structure from 6.50 percent to 0.16 percent which explains the updated FE model. The other way of correlating the difference is to show some pairing of both results by showing the linear regression values close to 1.0, as shown in Figure 4.16. However, the error can be seen high in the second and third mode compared to the first mode, because both numerical and experimental modal data. Modal data for higher modes may affect by the ambient effects which vibration sources used in modal testing contaminate the signal with noise. When using ambient methods the response peak in the frequency domain is decreased and slightly flattened by noise, distorting the mode shape. Problems of bias, resolution, noise and averaging are acute for large civil structures with low frequencies, non-stationary inputs and (often) inhospitable conditions (Brownjohn et al., 2001).

The updated FE models are good candidates to be used for the next FE model prediction for fatigued and damaged structures from the correlation analysis. Thereafter, the updated FE model is further validated against measured frequencies from the experimental results.

Mode	Natural frequency, f (Hz)	Mode shape
1	63.6	
2	182.9	
3	248.4	
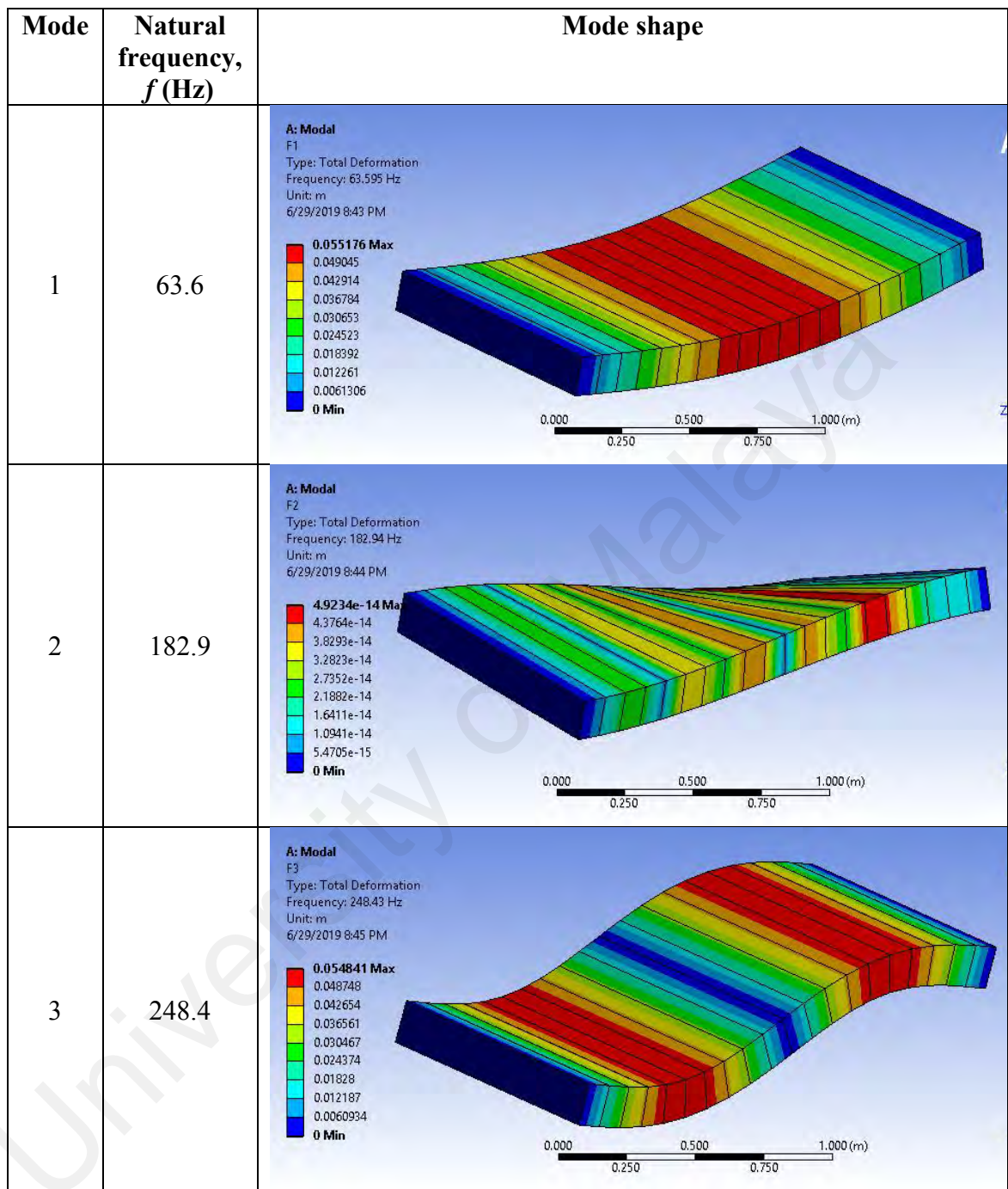
Figure 4.15: The first three natural frequencies and the corresponding mode shapes

of the updated undamaged RC slab FE model

Table 4.4: Natural frequencies correlation between experimental (f_{exp}) and updated numerical ($f_{fem,updt}$) of the undamaged RC slab (SS1)

Mode	Experimental, f_{exp} (Hz)	FEM, $f_{fem,updt}$ (Hz)	Error $\Delta f=(f_{exp} - f_{fem,updt})/f_{exp}$ (%)
1	63.5	63.6	0.16
2	159	182.9	15.03
3	199	248.4	24.82
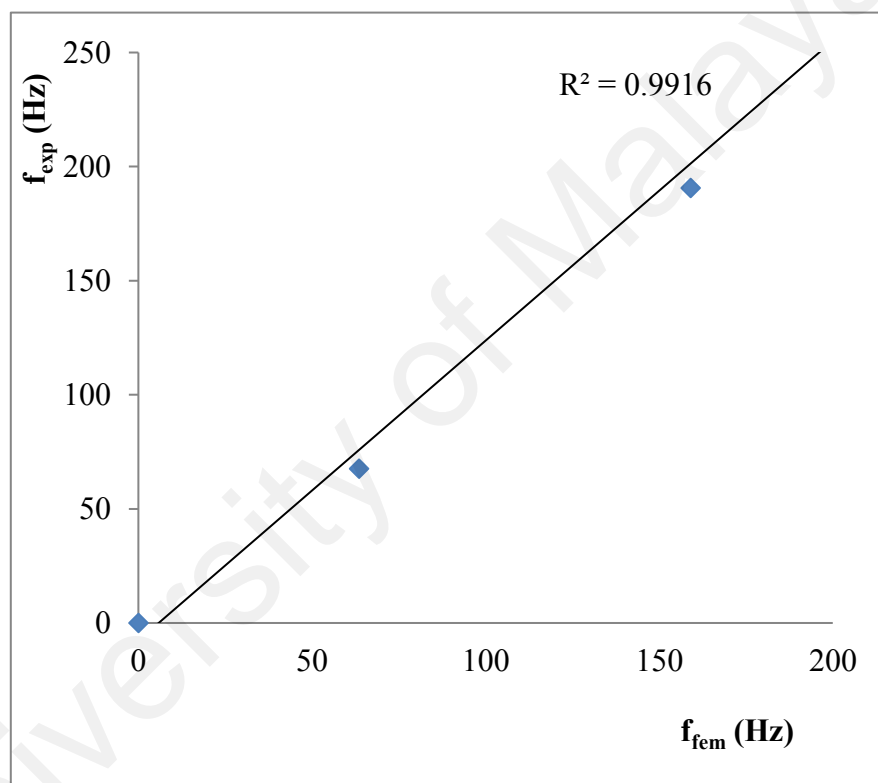
Figure 4.16 : Correlation of updated numerical (f_{fem}) and experimental measured (f_{exp}) natural frequencies of undamaged RC slab

Figure 4.17 shows the sensitivity of input parameters consisting of geometry and material properties influencing the natural frequency output parameter. Table 4.5 shows the change to closely match the measured experimental frequencies of selected parameters in the updated natural frequencies of the FE model.
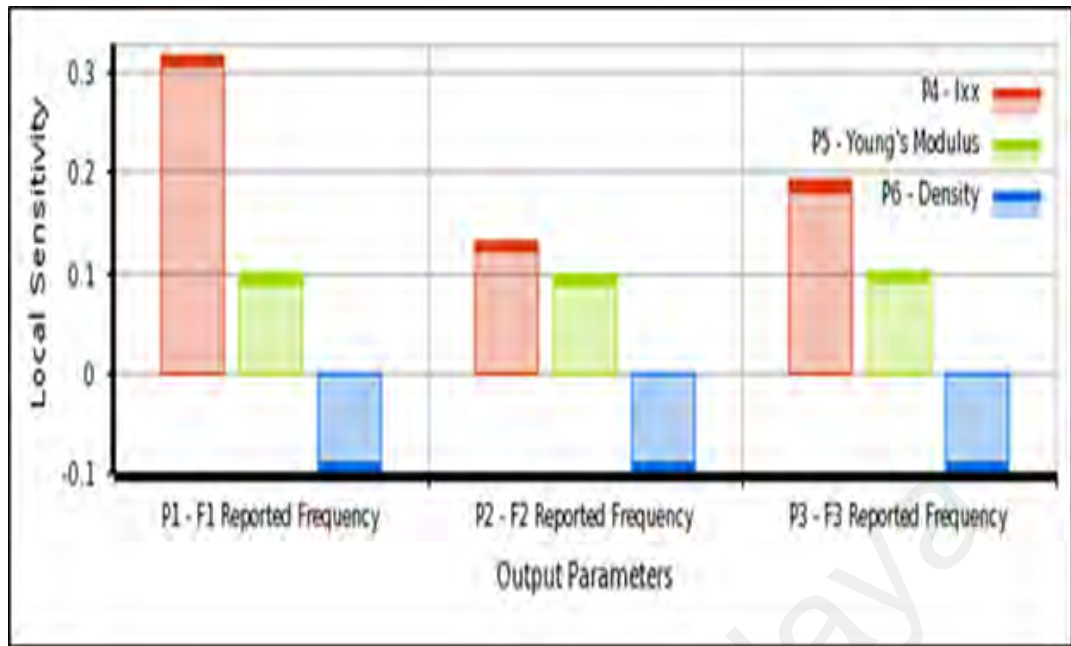
Figure 4.17: Sensitivity parameter

Table 4.5: The change of selected parameters after model updating for undamaged RC slab structure

Parameter	Initial value	Updated value
Density, ρ (kg/m^3)	2400	2180
Young's Modulus, E (MPa)	38524	31000
Moment of inertia, I (mm^4)	2.81E8	2.81E8

4.3.3 Model Updating of Fatigued and Damaged Reinforced Concrete Slabs
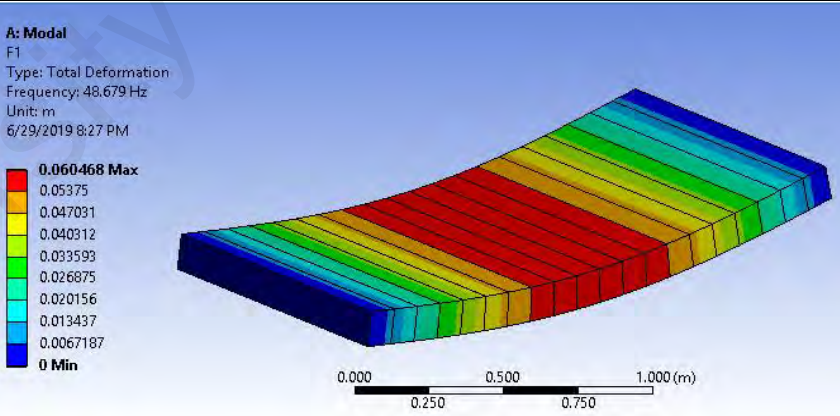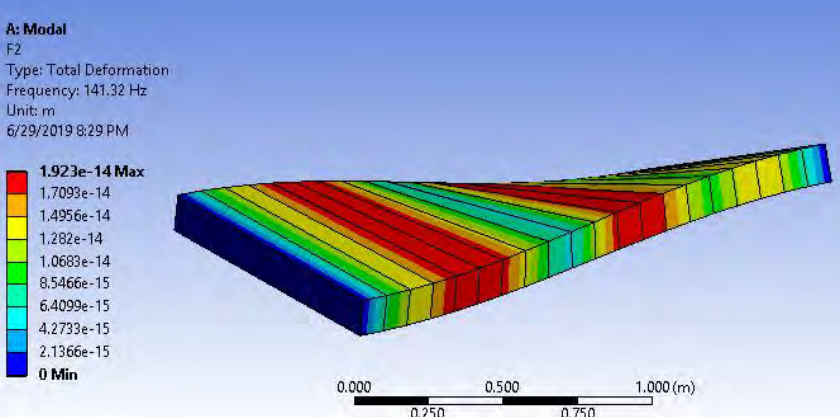
Model updating's main objective is to enhance further correlation and minimize the discrepancies between numerical and experimental dynamic characteristics taking into account sensitive parameters.

The updated undamaged FE model was used as the numerical reference against the measured frequencies obtained from the experimental to further modify the FE modeling for the fatigued structures. Thus, to represent the fatigued condition, the updated undamaged FE model has been adjusted to match the natural frequencies with experimental measurements in terms of its uncertain parameters. Table 4.6 shows the numerical (f$_{fem}$) and experimental measured (f$_{exp}$) natural frequencies for fatigued slab

structures (SF1M) undergoing 1 million load cycles as the result of the model updating. The frequency differences showing a low value of 0.41% and 0.89% for bending mode 1 and 3 respectively. The correlated data between the natural frequencies of the pairing f_{fem} and f_{exp} is still satisfactory by showing a good regression value near 1.0 as shown in Figure 4.18. Figure 4.19 shows the natural frequencies and corresponding mode shapes by modeling for fatigued slab SF1M. The FE model was reflected in the fatigued structure's real dynamic behavior.

Due to 1,500,000 (SF1.5M) and 2,000,000 (SF2M) cycle numbers, the FE model was also used to model the fatigued RC slabs. As uncertain updating parameters, the same parameters of Young's module and moment of inertia are selected.

Mode	Natural frequency, f (Hz)	Mode shape
1	48.7	
2	141.3	

| 3 | 191.5 | |

Figure 4.19: The first three natural frequencies and the corresponding mode shapes of the fatigued RC slab FE model (SF1M)

Table 4.7 and Table 4.8 show the numerical (f_{fem}) and experimental measured (f_{exp}) natural frequencies for fatigued slab structures undergoing 1.5 and 2 million load cycles as the result of the model updating. Even though there are some differences between the values of the natural frequencies between the numerical (f_{fem}) and experimental (f_{exp}) of the undamaged/damaged/fatigued RC slabs, they are considered acceptable in FE model updating because of the high correlation values of R^2 which ranges between 0.964 to 0.998 as illustrated in Figures 4.16, 4.18, 4.20, 4.21, 4.24, 4.25, 4.26.

Table 4.6: Natural frequencies correlation between experimental (f_{exp}) and updated numerical ($f_{fem,updt}$) of the fatigued RC slab (SF1M) subjected to 1 million load cycles

Mode	Experimental, f_{exp} (Hz)	FEM, $f_{fem,updt}$ (Hz)	Error $\Delta f=(f_{exp} - f_{fem,updt})/f_{exp}$ (%)
1	48.5	48.7	0.41
2	170	141.3	16.88
3	189.8	191.5	0.89
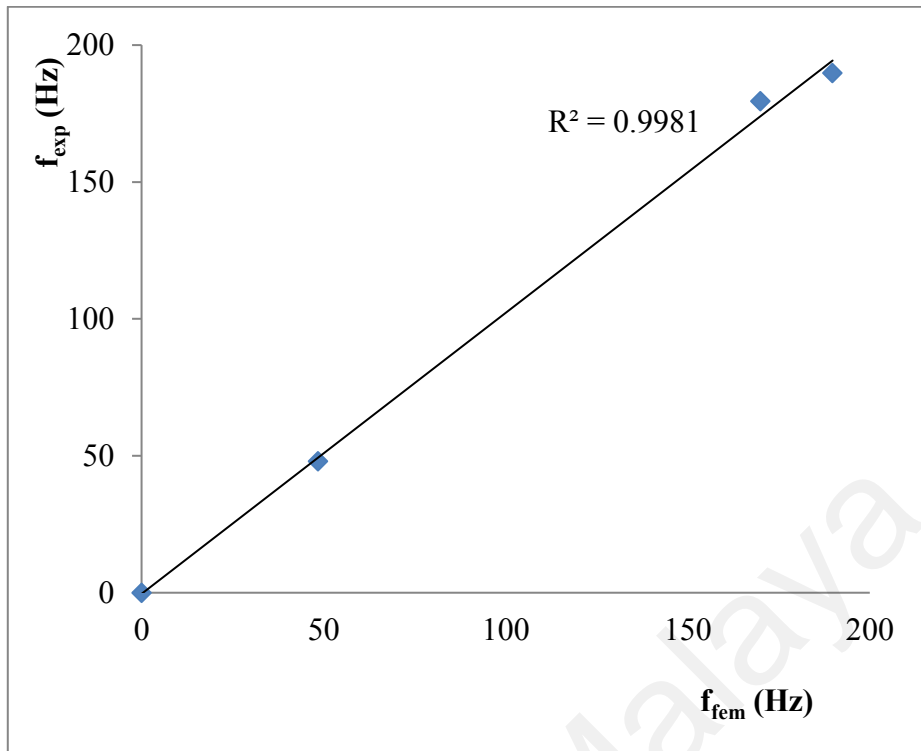
Figure 4.18 : Correlation of numerical (f_{fem}) and experimental measured (f_{exp}) natural frequencies of fatigued RC slab (SF1M)

The frequency differences in RC slab SF1M, SF1.5M and SF2M showing a small error of 0.41 percent, 1.95 percent and 2.31 percent respectively for mode 1 which is more stable compared to higher mode 2 and 3 as described above. Figure 4.20 and Figure 4.21, respectively for RC slab SF1.5M and SF2M, however, the correlated data between the pairing f_{fem} and f_{exp} natural frequencies is still satisfactory by showing a good regression value close to 1.0. Figure 4.22 and Figure 4.23 show the natural frequencies and corresponding mode shapes for fatigued RC slab SF1.5M and SF2M by modeling. The FE model was reflected in the fatigue structure's real dynamic behavior.
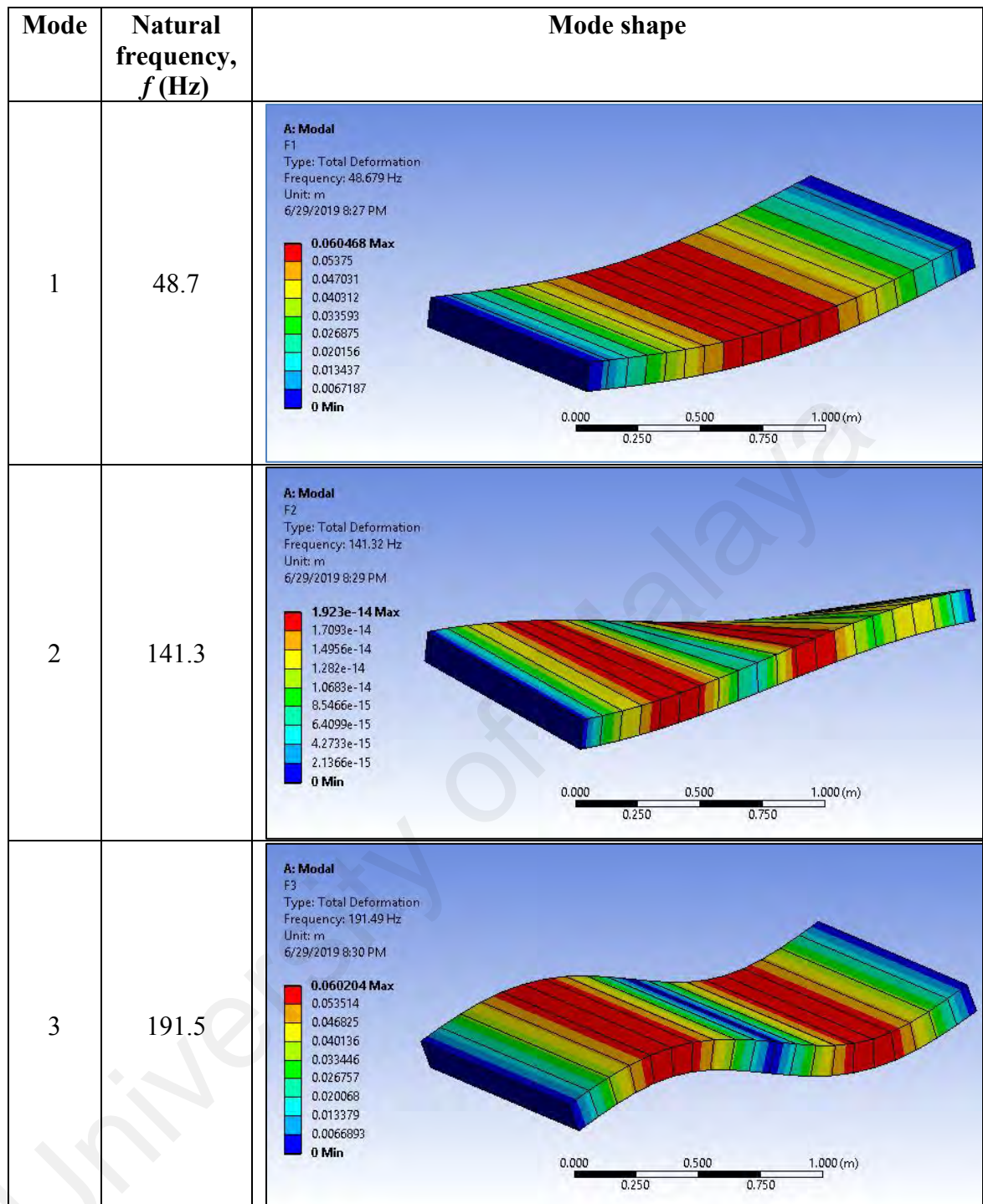
Mode	Natural frequency, f (Hz)	Mode shape
1	48.7	
2	141.3	
3	191.5	

Figure 4.19: The first three natural frequencies and the corresponding mode shapes of the fatigued RC slab FE model (SF1M)

Table 4.7: Natural frequencies correlation between experimental (f_{exp}) and updated numerical ($f_{fem,updt}$) of the fatigued RC slab (SF1.5M) subjected to 1.5 million load cycles

| Mode	Experimental, f_{exp} (Hz)	FEM, $f_{fem,updt}$ (Hz)	Error $\Delta f=(f_{exp} - f_{fem,updt})/f_{exp}$ (%)
1	41.0	41.8	1.95
2	153.0	121.6	20.52
3	203.6	164.7	19.11

Table 4.8: Natural frequencies correlation between experimental (f_{exp}) and updated numerical ($f_{fem,updt}$) of the fatigued RC slab (SF2M) subjected to 2.0 million load cycles

Mode	Experimental, f_{exp} (Hz)	FEM, $f_{fem,updt}$ (Hz)	Error $\Delta f=(f_{exp} - f_{fem,updt})/f_{exp}$ (%)
1	39.0	39.9	2.31
2	128.7	116.4	9.56
3	183.0	157.6	13.88

Modeling the damaged structure was later used with the FE model. As uncertain updating parameters, the same parameters of Young's module and moment of inertia are selected. The selected parameters are constantly reviewed during the model updating process, and the modeling is constantly revised until the acceptable percentage of accuracy is reached. Using the user-integrated line geometric model in Ansys Workbench, the parameters must be optimized when modifying the model.

The natural frequencies were measured experimentally after the monotonic load had been imposed until the fatigued RC slab reached the level of yield load.

Table 4.9, Table 4.10 and Table 4.11, respectively, present the experimental measured and updated numerical natural frequencies of RC slabs SF1M, SF1.5M and SF2M after updating based on the measured natural frequencies at damaged structure. A good regression value as shown in Figure 4.24, Figure 4.25 and Figure 4.26 represents the correlations between these measurements.
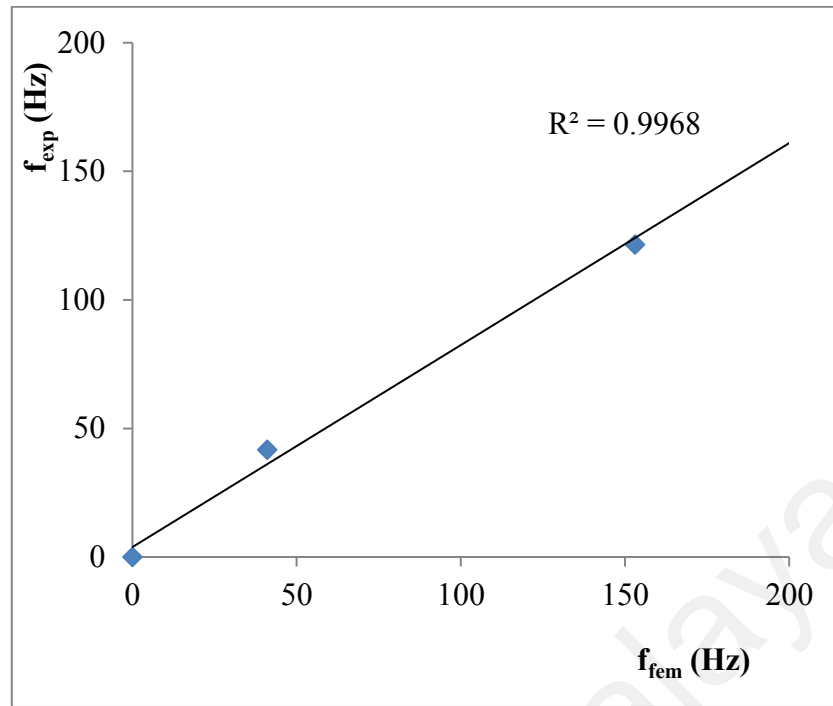
Figure 4.20 : Correlation of numerical (f_{fem}) and experimental measured (f_{exp}) natural frequencies of fatigued RC slab (SF1.5M)
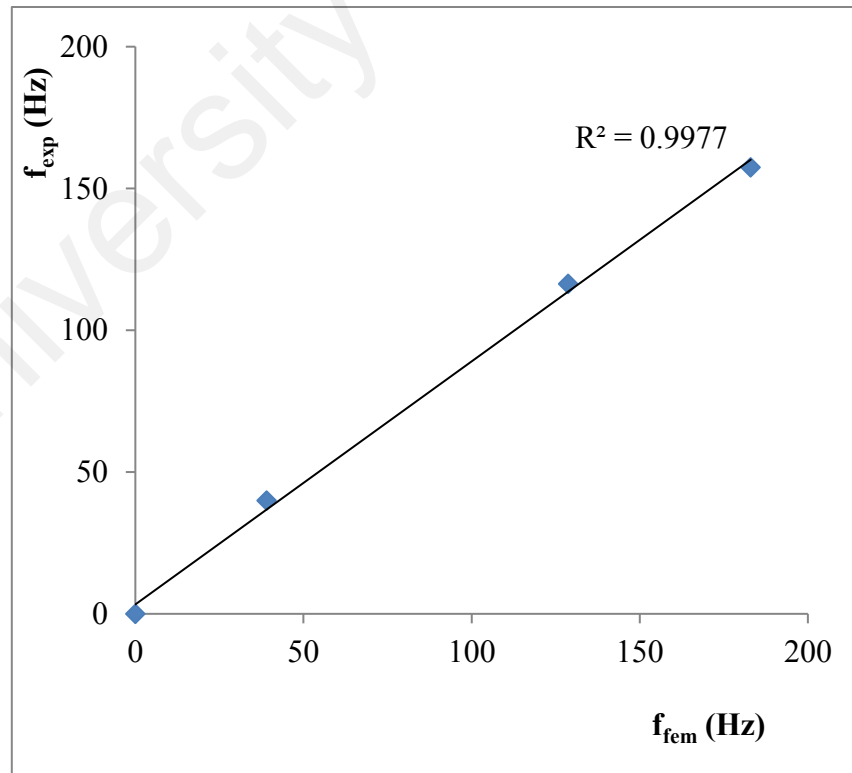
Figure 4.21 : Correlation of numerical (f_{fem}) and experimental measured (f_{exp}) natural frequencies of fatigued RC slab (SF2M)

Mode	Natural frequency, f (Hz)	Mode shape
1	41.8	A: Modal F1 Type: Total Deformation Frequency: 41.77 Hz Unit: m 6/29/2019 3:19 PM 0.062644 Max 0.055684 0.048723 0.041763 0.034802 0.027842 0.020881 0.013921 0.0069605 0 Min
2	121.6	A: Modal F2 Type: Total Deformation Frequency: 121.61 Hz Unit: m 6/29/2019 3:20 PM 2.3523e-13 Max 2.0909e-13 1.8296e-13 1.5682e-13 1.3068e-13 1.0455e-13 7.841e-14 5.2273e-14 2.6137e-14 0 Min
3	164.7	A: Modal F3 Type: Total Deformation Frequency: 164.66 Hz Unit: m 6/29/2019 3:21 PM 0.062404 Max 0.05547 0.048536 0.041602 0.034669 0.027735 0.020801 0.013867 0.0069937 0 Min

Figure 4.22 : The first three natural frequencies and the corresponding mode shapes of the fatigued RC slab FE model (SF1.5M)

Mode	Natural frequency, f (Hz)	Mode shape
1	39.9	
2	116.4	
3	157.6	
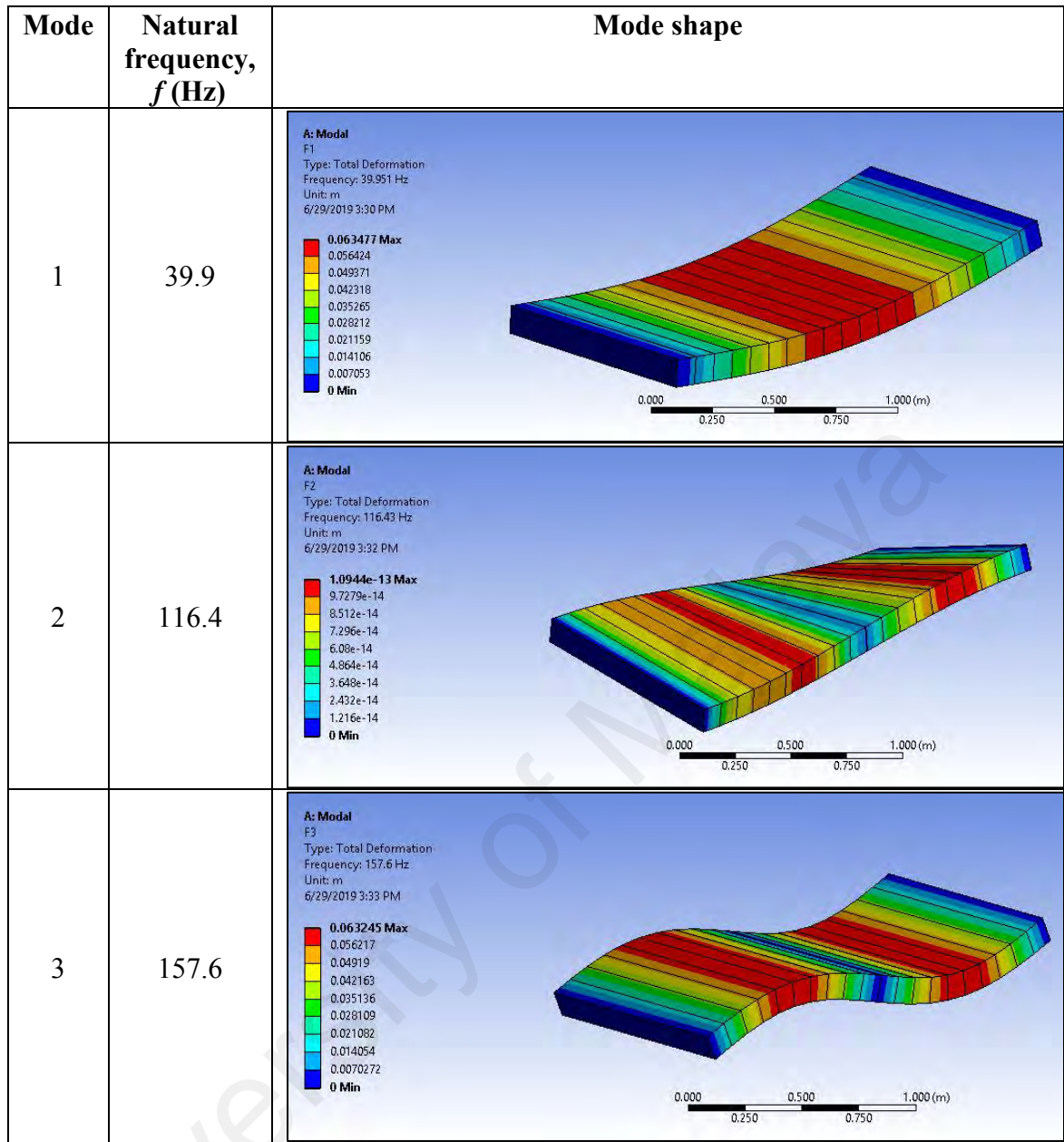
Figure 4.23: The first three natural frequencies and the corresponding mode shapes of the fatigued RC slab FE model (SF2M)

Table 4.9: Natural frequencies correlation between experimental (f_{exp}) and updated numerical ($f_{fem,updt}$) of the damaged RC slab (SF1M)

Mode	Experimental, f_{exp} (Hz)	FEM, $f_{fem,updt}$ (Hz)	Error, $\Delta f = (f_{exp} - f_{fem,updt})/f_{exp}$ (%)
1	38.6	38.7	0.26
2	155.0	144.5	6.77
3	247.0	152.8	38.14

Table 4.10: Natural frequencies correlation between experimental (f_{exp}) and updated numerical ($f_{fem,updt}$) of the damaged RC slab (SF1.5M)

Mode	Experimental, f_{exp} (Hz)	FEM, $f_{fem,updt}$ (Hz)	Error, $\Delta f=(f_{exp}-f_{fem,updt})/f_{exp}$ (%)
1	36.0	36.5	1.39
2	132.3	136.4	3.10
3	153.1	144.2	5.81

Table 4.11: Natural frequencies correlation between experimental (f_{exp}) and updated numerical ($f_{fem,updt}$) of the damaged RC slab (SF2M)

Mode	Experimental, f_{exp} (Hz)	FEM, $f_{fem,updt}$ (Hz)	Error, $\Delta f=(f_{exp}-f_{fem,updt})/f_{exp}$ (%)
1	29.2	30.0	2.74
2	124.7	112.6	9.70
3	133.3	119.0	10.73
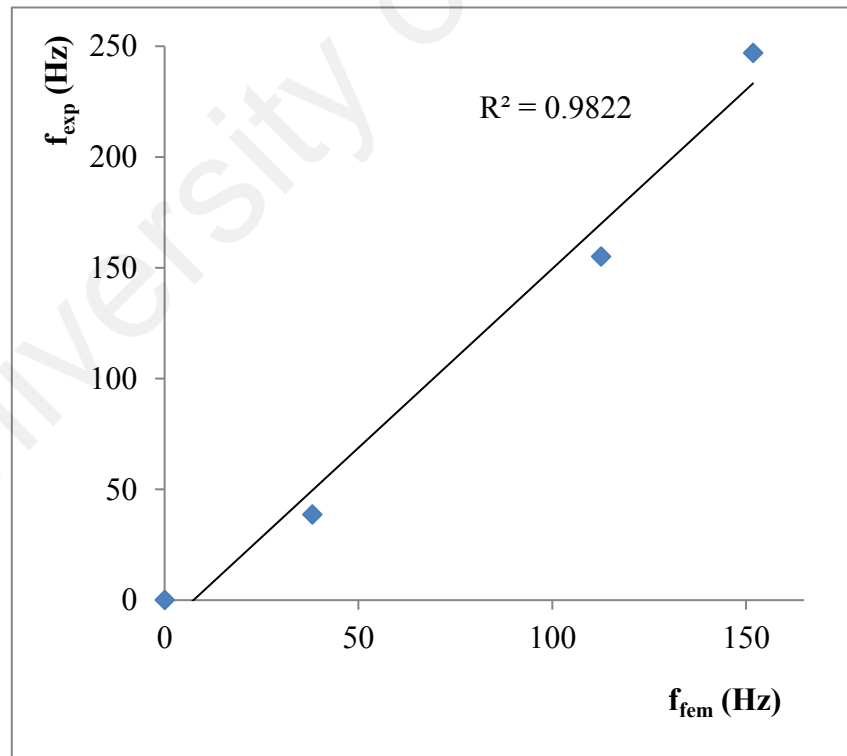
Figure 4.24 : Correlation of numerical (f_{fem}) and experimental measured (f_{exp}) natural frequencies of damaged RC slab (SF1M)
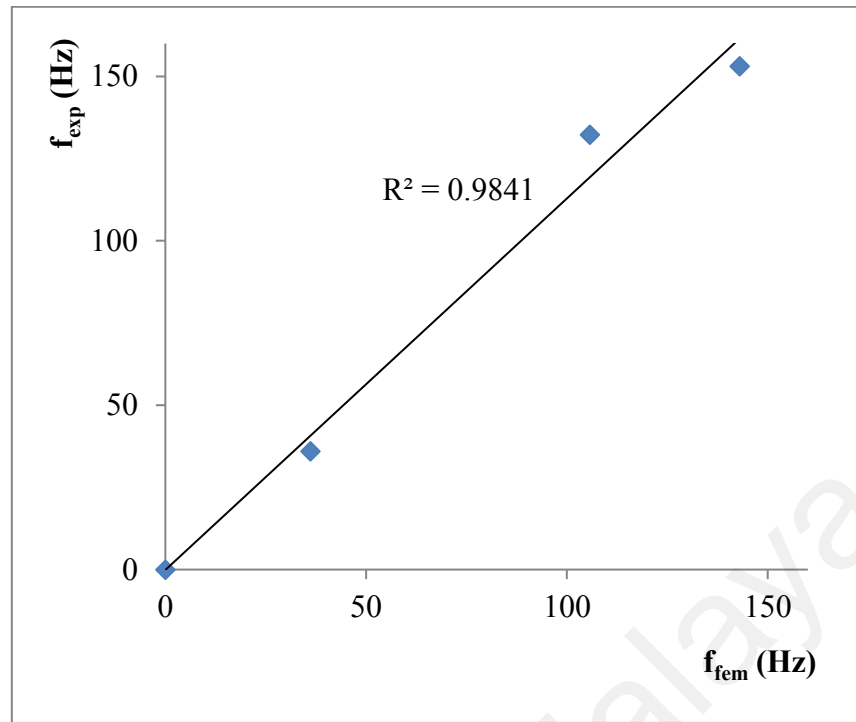
Figure 4.25: Correlation of numerical (f_{fem}) and experimental measured (f_{exp}) natural frequencies of damaged RC slab (SF1.5M)
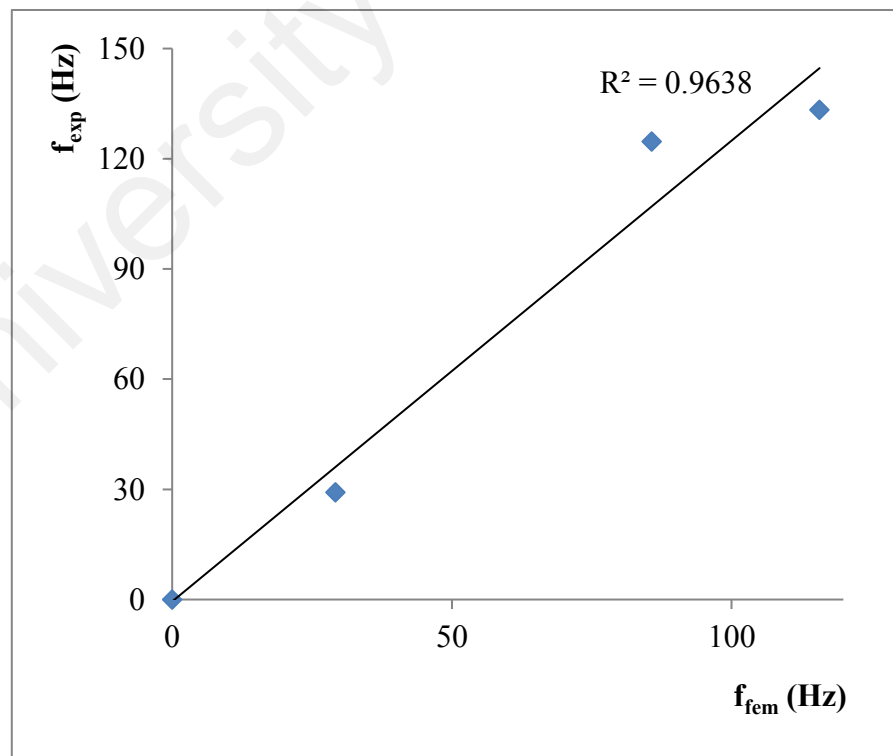
Figure 4.26: Correlation of numerical (f_{fem}) and experimental measured (f_{exp}) natural frequencies of damaged RC slab (SF2M)

In general, the natural frequency trend was associated with the increase in the level of damage to cyclic loads as shown in Table 4.12, Figure 4.27 and Figure 4.28. A decrease in natural frequency was observed damaged by fatigue and continuously damaged by RC slabs at the state of static failure, it could be concluded that the structure experienced a loss of stiffness and subsequently a decrease in natural frequencies. Referring to Figure 4.29, the results of the updated natural frequencies of all modes of the slabs are depicted by a bar graph against the structural conditions. The downward trend in the graph indicates the severity of damage induced onto the structure influence the stiffness of RC slabs.

Table 4.12: The updated natural frequencies and the corresponding modes of the undamaged, fatigued and damaged RC slabs

Mode number	Undamaged slab, $f_{fem,updt}$ (Hz)	Fatigue scenario, $f_{fem,updt}$			Damage scenario, $f_{fem,updt}$		
		SF1M (Hz)	SF1.5M (Hz)	SF2M (Hz)	SF1M (Hz)	SF1.5M (Hz)	SF2M (Hz)
1	63.36	48.7	41.8	39.9	38.7	36.5	30.0
2	182.1	141.3	121.6	116.4	144.5	136.4	112.6
3	247.3	191.5	164.7	157.6	152.8	144.2	119.0
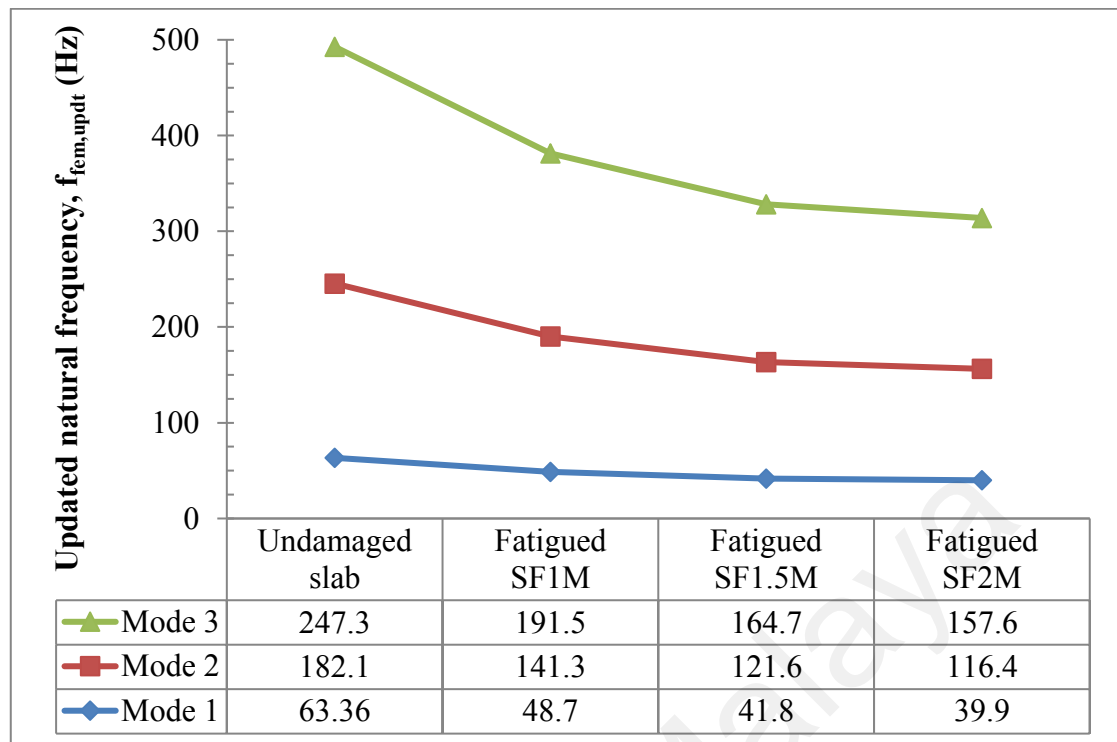
Figure 4.27: The updated natural frequencies and the corresponding modes of the undamaged and fatigued RC slabs

	Undamaged slab	Fatigued SF1M	Fatigued SF1.5M	Fatigued SF2M
Mode 3	247.3	191.5	164.7	157.6
Mode 2	182.1	141.3	121.6	116.4
Mode 1	63.36	48.7	41.8	39.9
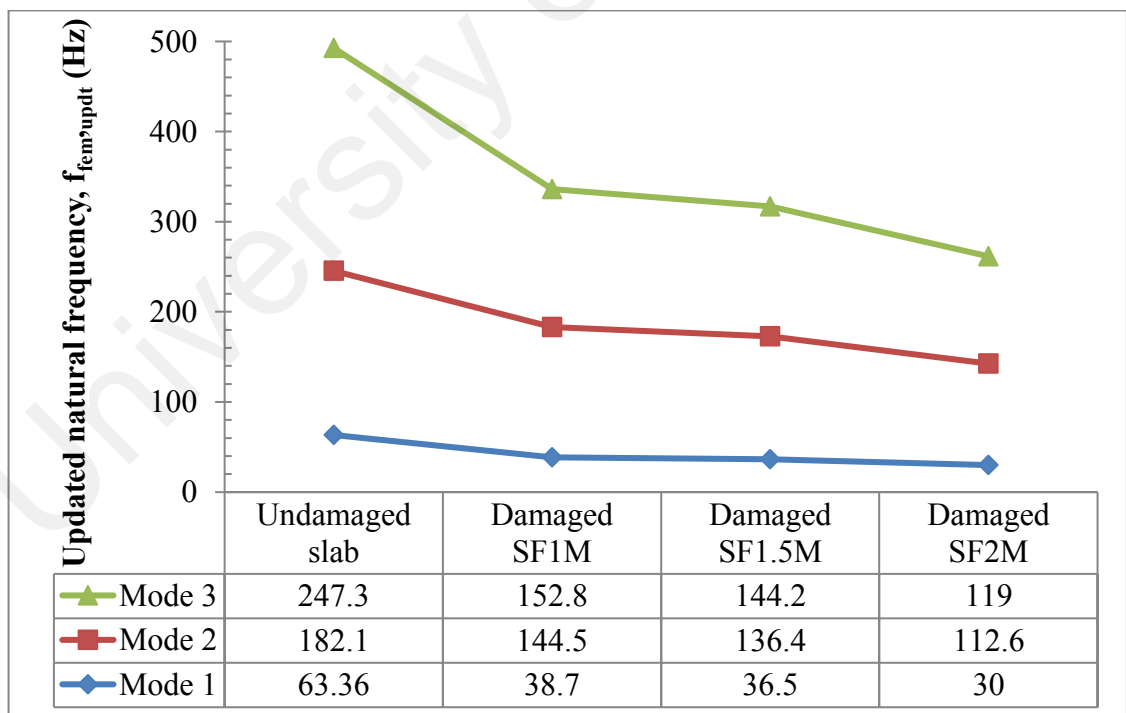
Figure 4.28: The updated natural frequencies and the corresponding modes of the undamaged and damaged RC slabs

	Undamaged slab	Damaged SF1M	Damaged SF1.5M	Damaged SF2M
Mode 3	247.3	152.8	144.2	119
Mode 2	182.1	144.5	136.4	112.6
Mode 1	63.36	38.7	36.5	30
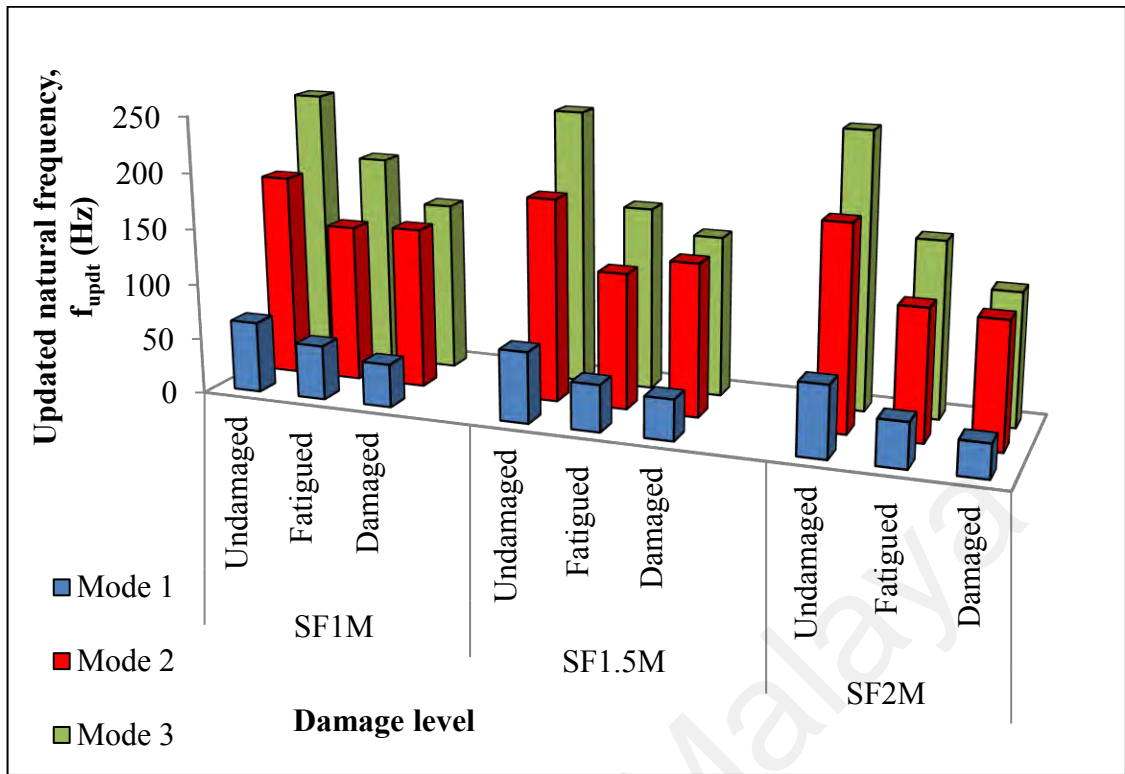
Figure 4.29: Effect of undamaged, fatigued and damaged structures on updated natural frequency

4.4 Stiffness Degradation

Composite fatigue damage shows a complicated mechanism compared to homogeneous materials, as they normally involve various modes of damage including debonding, cracking, and fiber breakage. Because of this, there is still ongoing study in this field to enhance research and enhance existing knowledge. Due to the variety of damage modes, in terms of residual strength and stiffness, material properties were affected. Measuring the change in these properties during the service life is therefore essential. Therefore, a feasible non-destructive technique in monitoring structural health would be desirable. Due to their non-destructive technique, modal analysis is one of the structural health monitoring techniques that can be used. Modal parameter can be obtained by vibration testing and modeling of finite elements. Natural frequency is one of the modal parameters that depends on the stiffness of the material. The degradation of stiffness will be captured in different times of fatigue to differentiate the damage caused by fatigue. Since the vibration testing is carried out on the basis of the ambient

force, modal parameter can be measured in-situ without interrupting the operation of the site, e.g. in bridge building and building existing structures, making it a more effective technique.

4.4.1 Predictive Modelling

The updated stiffness parameters include the Young's modulus and moment of inertia was obtained from the FE analysis after updating based on the measured natural frequencies against the fatigued and damaged structures. Figure 4.30 to Figure 4.35 shows the results on the updated stiffness parameters of RC slabs SF1M, SF1.5M and SF2M.
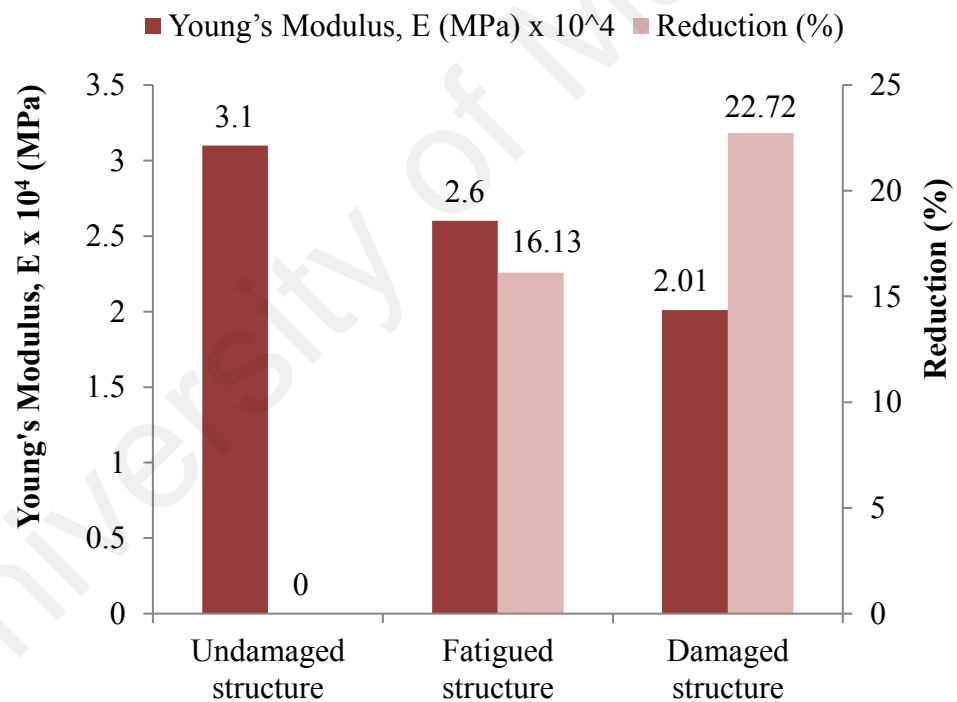
Figure 4.30: Reduction of Young's modulus after model updating for RC slab SF1M due to 1 million fatigue loads at different level condition of structure
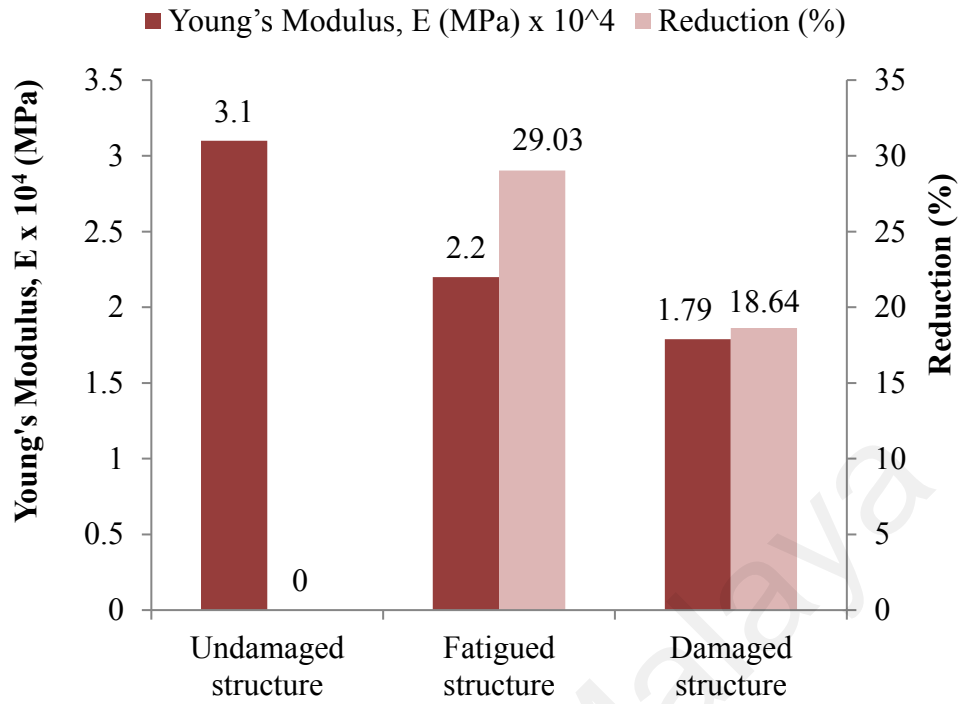
Figure 4.31: Reduction of Young's modulus after model updating for RC slab SF1.5M due to 1.5 million fatigue loads at different level condition of structure
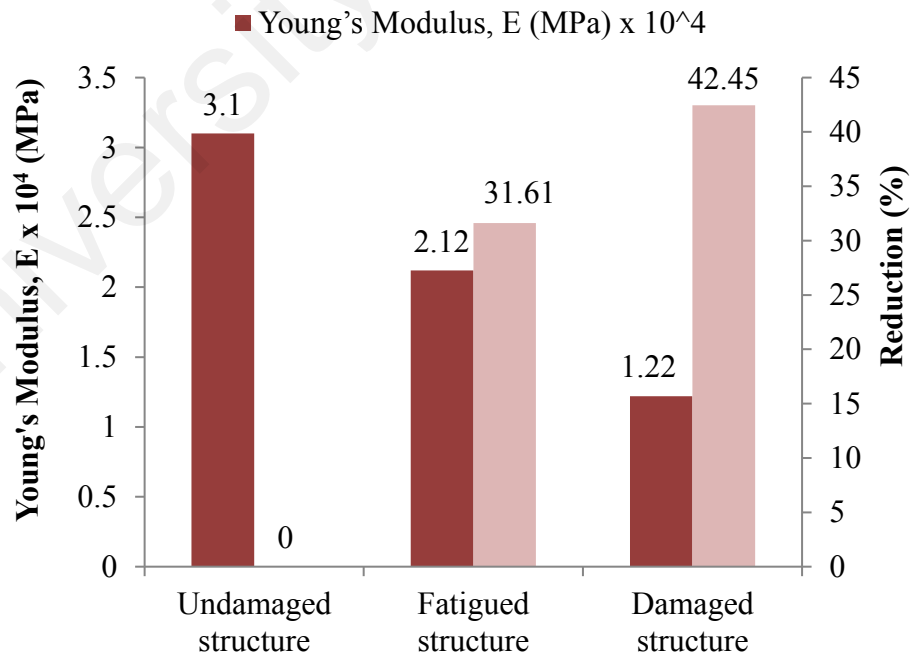
Figure 4.32: Reduction of Young's modulus after model updating for RC slab SF2M due to 2 million fatigue loads at different level condition of structure
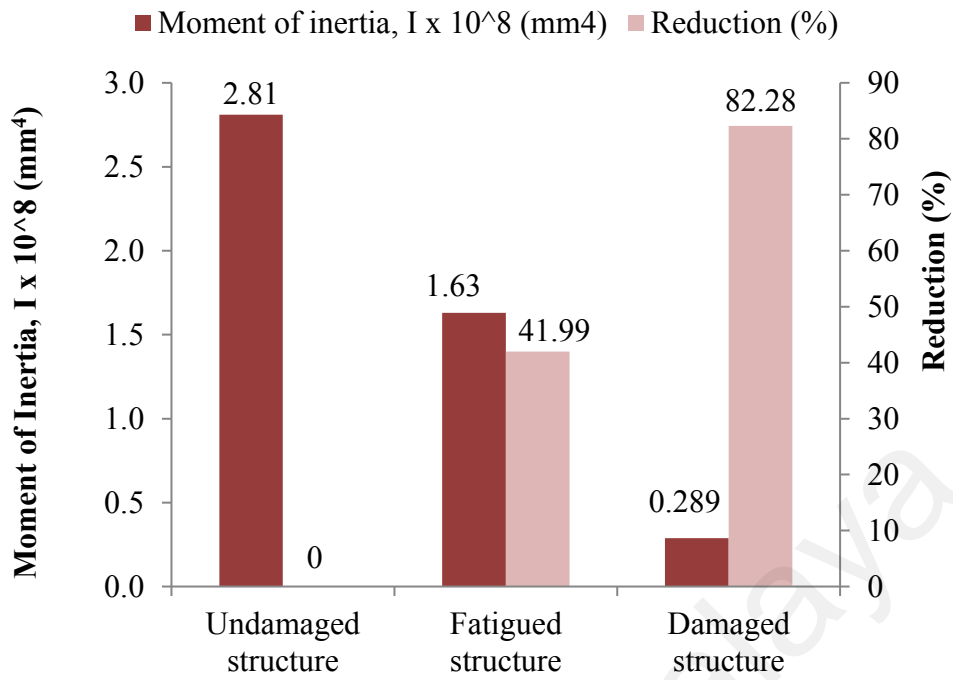
Figure 4.33: Reduction of moment of inertia after model updating for RC slab SF1M due to 1 million fatigue loads at different level condition of structure
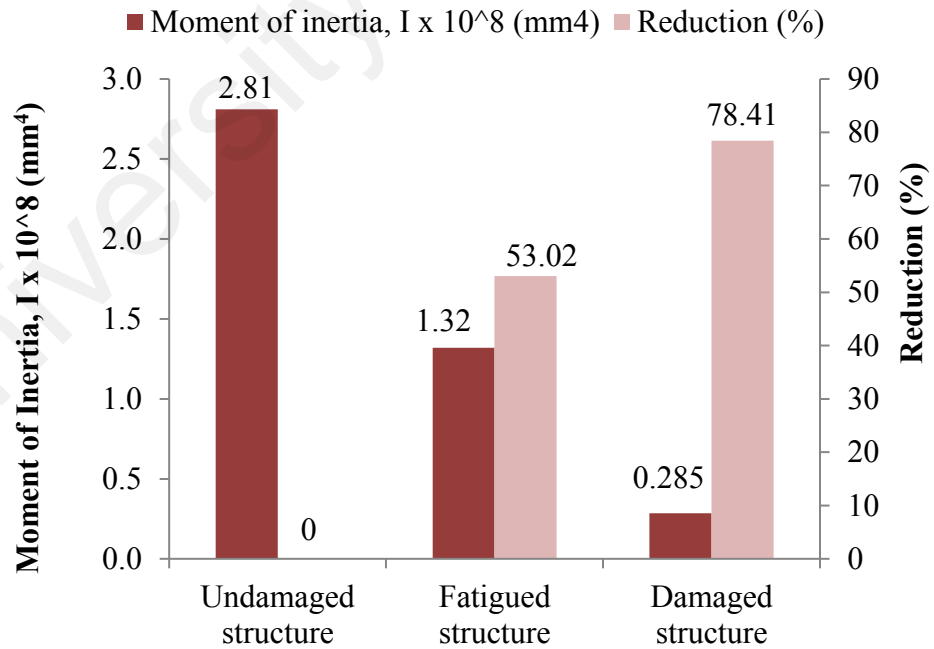
Figure 4.34: Reduction of moment of inertia after model updating for RC slab SF1.5M due to 1.5 million fatigue loads at different level condition of structure
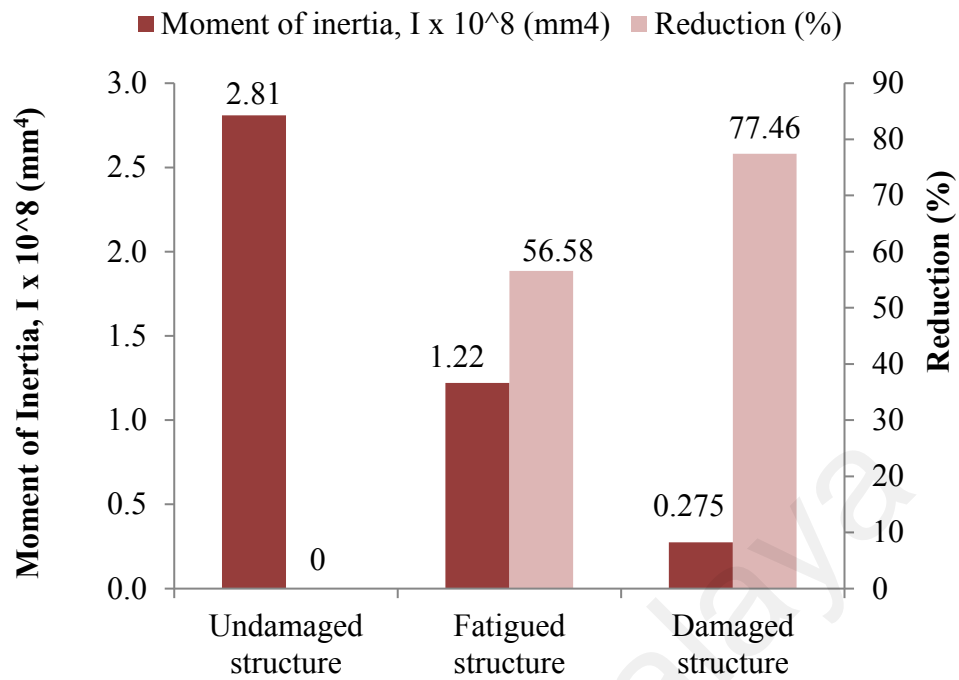
Figure 4.35: Reduction of moment of inertia after model updating for RC slab SF2M due to 2 million fatigue loads at different level condition of structure

The relationship between parameters of stiffness; introduces the moment of inertia and Young modulus at each condition of RC slabs in different levels of fatigue and damage. Figure 4.36 and Figure 4.37 show changes in the stiffness parameters of undamaged, fatigued and damaged RC slabs due to 1 million (SF1M), 1.5 million (SF1.5M) and 2 million (SF2M) cycles associated with updated FE model natural frequencies to meet the experimental frequency requirements.

	Undamaged	Fatigued	Damaged
SF1M	31000	26000	20093
SF1.5M	31000	22000	17900
SF2M	31000	21200	12200
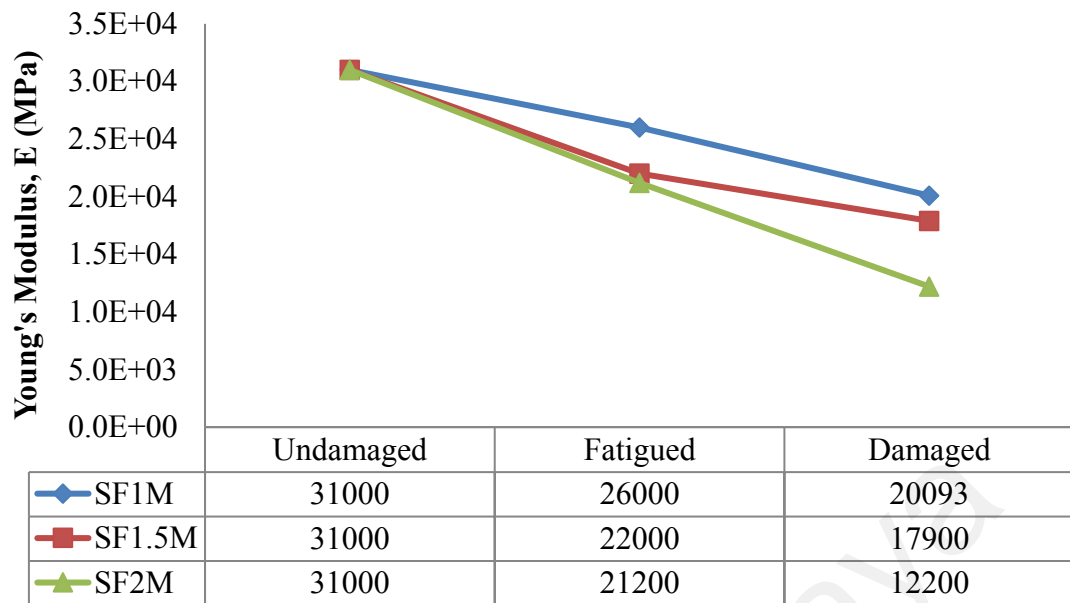
Figure 4.36: The change of Young's modulus after model updating of RC slab structures at various level of fatigue and damage

	Undamaged	Fatigued	Damaged
SF1M	2.81E+08	1.63E+08	2.89E+07
SF1.5M	2.81E+08	1.32E+08	2.85E+07
SF2M	2.81E+08	1.22E+08	2.75E+07
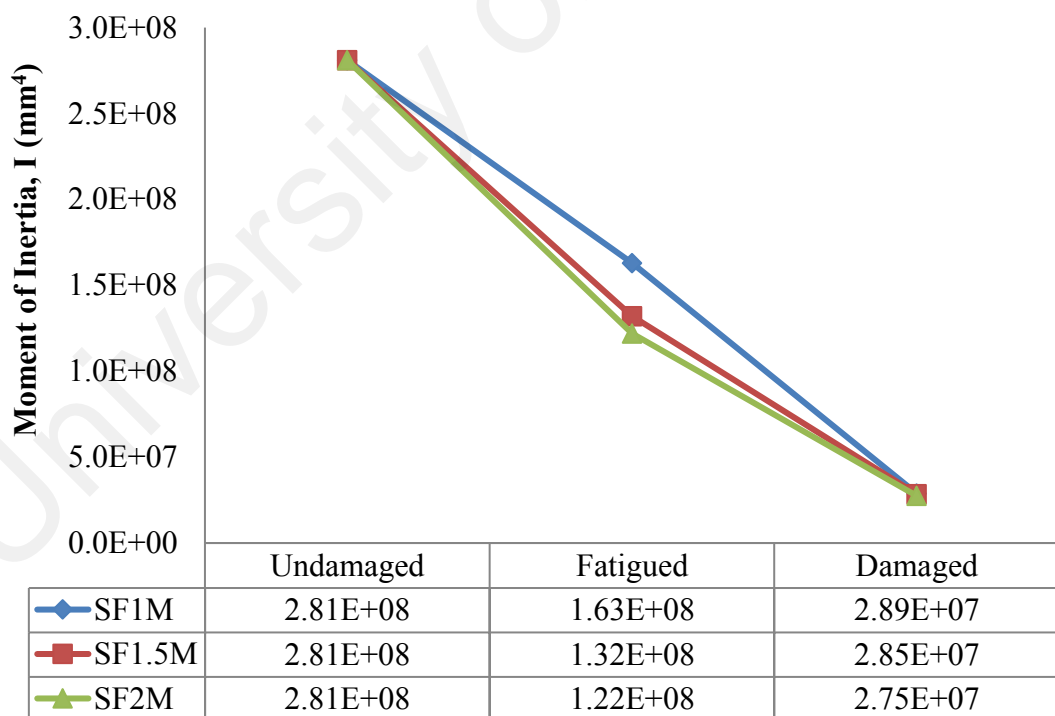
Figure 4.37: The change of moment of inertia after model updating of RC slab structures at various level of fatigue and damage

The relationship between stiffness, load cycles and dynamic response of natural frequency is established based on the results of the experimental and FE analysis. Based on the updated structural stiffness values at each condition; fatigue and RC slab damage (Figure 4.38), it can be seen prominently that the percentage of stiffness reduction increases as the fatigue level increases. This study presents the relationship between the stiffness parameter as an indicator in the structural fatigue condition. It can be observed that under the structure's serviceability, the relationship can identify the stiffness index level. It is worth mentioning that Young's modulus and moment of inertia are capable parameters in assessing existing structural performance by integrating modal analysis and model finite element updating to quantify structural damage. Figure 4.39 illustrates the result. It can be seen that with increasing numbers of cycles, stiffness decreases. The predictive model is studied and expressed as Equation 4.5 to estimate the stiffness under the serviceability of fatigued RC slab structure.

$$K = 8.3209e^{-0.633x} \qquad \text{Equation 4.5}$$

The stiffness (K) deficiency of fatigued structure can be identified through the index of the fatigue level, D_i which is defined as stated in Equation 4.6.

$$D_i = \frac{\Delta K}{K_0} \qquad \text{Equation 4.6}$$

Where ΔK indicates the stiffness change between undamaged and fatigued of the RC slab and K_0 signifies the original stiffness of undamaged structure. Figure 4.40 shows the percentage reduction in stiffness. At 2 million load cycles, the reduction in stiffness reaches 70.26 percent. The result is a useful prediction for evaluating the fatigue-bearing capacity of fatigued structures likely to be exposed to increased loads in the future.

4.4.2 Analytical Investigation as the Model Validation

There are concrete structures that are susceptible to continuous cyclic loads that contribute to the structures' deficient service life. The dynamic properties principles indicate that natural frequency measurement can be reduced due to the influence of stiffness. A similar principle can be made from the same parameter for a mechanical property, which is stiffness, also affects the slab structure's residual load capacity. Therefore, this method based on that key parameter was developed through experimental dynamic measurements and FE modeling and updating provides practically safety information that can quantify the fatigued structure's serviceability. It can be noticed that the process of stiffness reduction begins with the first cyclic load applied to the structure, so the service life will decrease from that moment on. The degradation of the stiffness in fatigue structure is because of the time-dependent on cyclic creep strain of concrete, ε_c (Equation 4.7) after certain number of fatigue cycles, N which dependent to Young's modulus, E_N (Equation 4.10) for concrete in compression. As a response from a given number of cyclic loads, the effective moment of inertia, $I_{E,N}$ also changed (Equation 4.11) (ACI 318-77).

	Undamaged	Fatigued	Damaged
SF1M	8.71E+12	4.24E+12	5.80E+11
SF1.5M	8.71E+12	2.90E+12	5.10E+11
SF2M	8.71E+12	2.59E+12	3.36E+11
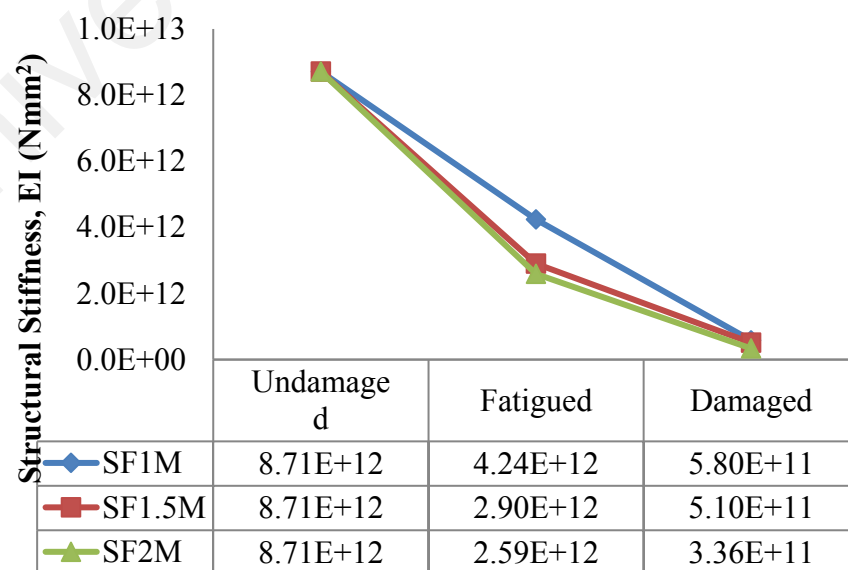
Figure 4.38 : The updated values of the structural stiffness at each condition of the RC slabs
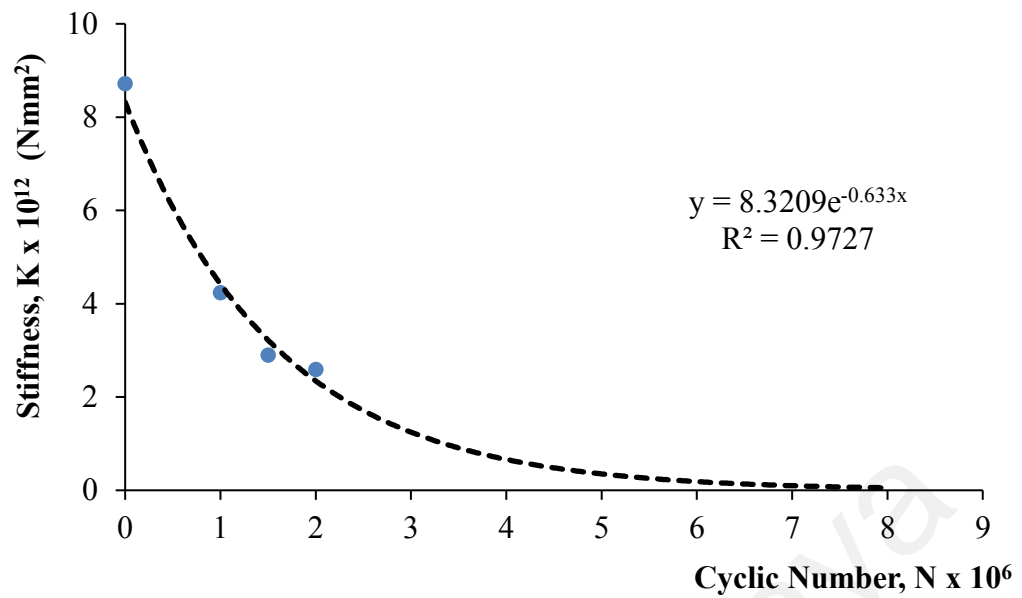
Figure 4.39 : Predictive model for stiffness serviceability of fatigued RC slab structure
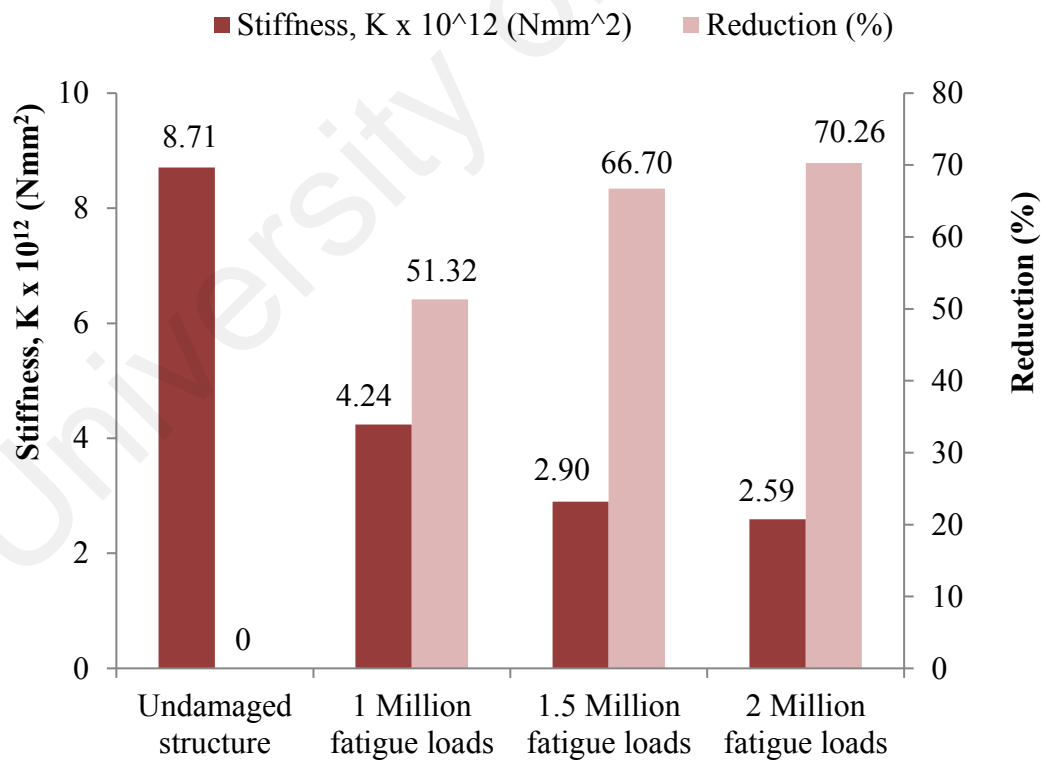
Figure 4.40 : Stiffness reductions of fatigued RC slab at each fatigue level

$$\varepsilon_c = 129\sigma_m t^{1/3} + 17.8\sigma_m \Delta N^{1/3} \qquad \text{Equation 4.7}$$

$$\sigma_m = \left[\frac{(\sigma_{max} + \sigma_{min})/2}{f_c}\right] \qquad \text{Equation 4.8}$$

$$\Delta = (\sigma_{max} - \sigma_{min})/f_c \qquad \text{Equation 4.9}$$

$$E_N = \frac{\sigma_{max}}{\frac{\sigma_{max}}{E} + \varepsilon_c} \qquad \text{Equation 4.10}$$

$$I_{E,N} = I_{cr,N} + \left(\frac{M_{cr,N}}{M_a}\right)^3 (I_g - I_{cr,N}) < I_g \qquad \text{Equation 4.11}$$

$$I_{cr,N} = \left(\frac{by^3}{3}\right) + n_N \rho b d (d - y)^2 \qquad \text{Equation 4.12}$$

$$n_N = \frac{E_s}{E_N} \qquad \text{Equation 4.13}$$

$$M_{cr,N} = \frac{I_g}{(h - y)} f_{r,N} \qquad \text{Equation 4.14}$$

Where $I_{cr,N}$ (Equation 4.12) is the cracked moment of inertia after N^{th} cycle, $M_{cr,N}$ (Equation 4.14) is the cracked moment after N^{th} cycle, M_a is maximum applied moment, I_g is gross moment of inertia, $f_{r,N}$ is the reduced modulus of moment rupture due to cyclic loading and can be computed from Equation 4.15. While f_r (Equation 4.16) is the modulus of rupture of concrete and N is number of load cycles (Cheng, 2011).

$$f_{r,N} = f_r \left(1 - \frac{\log N}{10.954}\right) \qquad \text{Equation 4.15}$$

$$f_r = 0.623\sqrt{f_{cu}} \qquad \text{Equation 4.16}$$

Where $E_N I_{E,N}$ is the stiffness of the slab after N cyclic number.

Through the model updating of measured and numerical natural frequencies of fatigued RC slabs, these stiffness parameters of Young's modulus, E_N and moment of inertia, $I_{E,N}$ were computed based on the dynamic fundamental concept of natural frequency. Analytical natural frequency estimation, especially for beam bending, can be found from the fundamental frequency of vibration. The neutral frequencies are calculated using Equation 4.17 and Equation 4.18 (Daniel, 2008).

$$\omega = \left(\frac{n\pi}{L}\right)^2 \sqrt{\frac{EI}{\rho A}}$$

Equation 4.17

$$f = \frac{\omega}{2\pi}$$

Equation 4.18

Where ω is the natural frequency in rad/sec, n is the mode shape, L is the length of the slab, E is modulus of elasticity, I is moment of inertia, ρ is concrete density, A is the area of the slab cross section and f is neutral frequency in hertz (Hz).

The data presented in Table 4.13 and Table 4.14 are the validation of the stiffness parameter of the fatigued RC slab SF1 M, SF1.5 M and SF2 M obtained from the FE model updating to the theoretical results in Equation 4.7 to Equation 4.16.

Table 4.13: Validation of structural stiffness of fatigued RC slabs

Specimen	Stiffness, K (Nmm^2)	
	FE model updating	Analytical
SF1M	4.24E12	3.56E12
SF1.5M	2.90E12	3.00E12
SF2M	2.59E12	2.68E12

Table 4.14: Validation of structural stiffness of damaged RC slabs

Specimen	Stiffness, K (Nmm^2)	
	FE model updating	Analytical
SF1M	5.80E11	5.803E+11
SF1.5M	5.10E11	5.102E+11
SF2M	3.36E11	3.356E+11

From Figure 4.41, it is observed that there is not much difference in this study regarding the results of stiffness measured by updating and analytically calculated FE model. The predictive model developed had therefore been validated. As shown in Figure 4.42, the percentage error of these values is well correlated with the linear regression graph. It is possible to see good agreement with the behavior of the stiffness-load cycles observed in analytics with that obtained from the updating of the FE model. The proposed predictive model could be used confidently to predict the fatigued structures' serviceability.
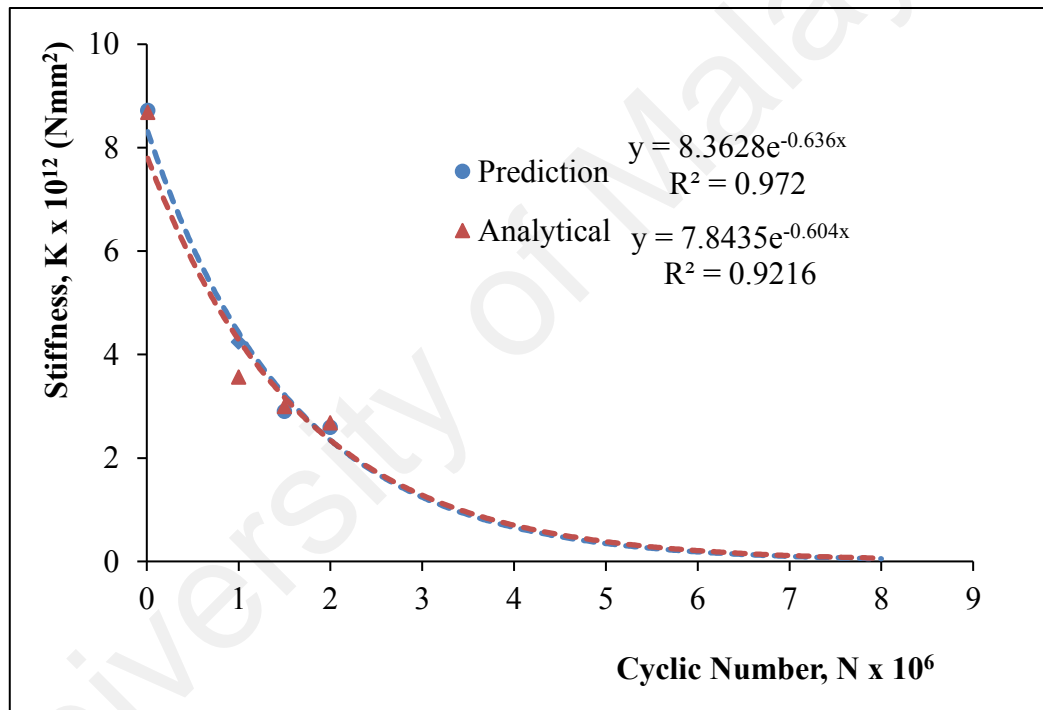
Figure 4.41: Validation of predictive model for stiffness serviceability of fatigued RC slabs
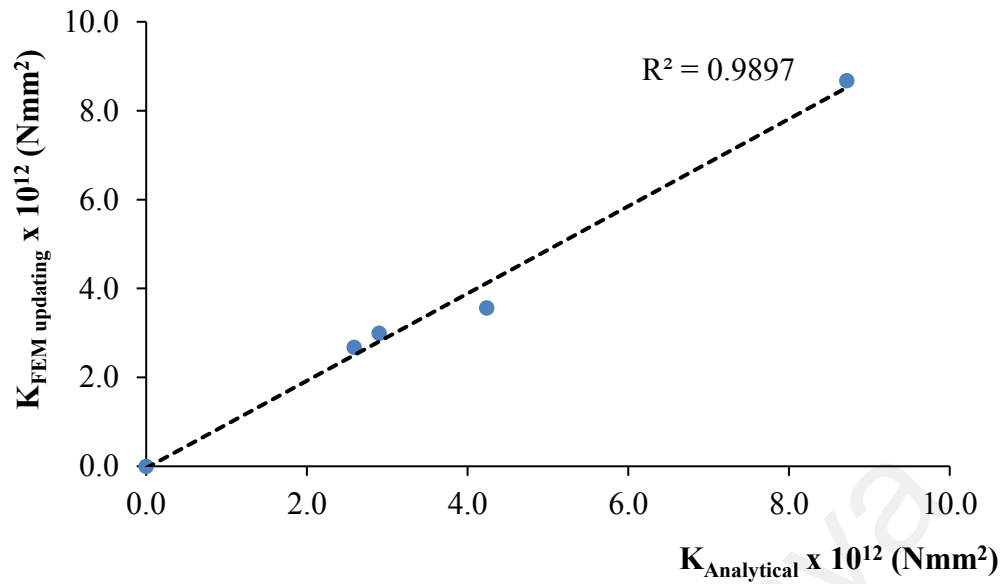
Figure 4.42: Correlation of FEM model updating and analytical stiffness of fatigued RC slabs

4.4.3 Relationship between Structural Stiffness and Natural Frequency

The model for predicting degradation of stiffness is validated in the previous sub-section based on the experimental data and established theoretical. When a structure is subjected to some degree of fatigue damage or deterioration, the stiffness has changed, and the natural frequencies shift as well. It is shown in the simple beam relationship as expressed in Equation 4.17 and Equation 4.18. The magnitude of the changes becomes an indicator of the damage's severity. It is evident from these equations that the RC slab's natural frequency is proportional to its structural stiffness, K (EI). From the results presented in Table 4.15 and Table 4.16, the relationship was demonstrated as the two percent change in stiffness would result in a one percent change in natural frequency or the natural frequency to stiffness ratio could represent 0.5. Razak & Choi (2001) also demonstrated that relationship in their corrosion effect study to the change in stiffness and natural frequency in RC beam. They made changes in the natural frequencies of the corroded beams compared to the control beam by using a simple supported beam's free vibration formula.

Table 4.15: The effect of structural stiffness on fatigued RC slabs to its natural frequency

Specimen	Stiffness		Natural frequency		Ratio of reduction, f/K
	K (Nmm^2)	K Reduction (%)	f (Hz) 1st mode	f Reduction (%)	
SS1	8.71E12	0	63.36	0	0
SF1M	4.24E12	51.32	48.04	24.18	0.47
SF1.5M	2.90E12	66.70	40.65	35.84	0.54
SF2M	2.59E12	70.26	39.91	37.01	0.53

Table 4.16: The effect of structural stiffness on damaged RC slabs to its natural frequency

Specimen	Stiffness		Natural frequency		Ratio of reduction, f/K
	K (Nmm^2)	K Reduction (%)	f (Hz) 1st mode	f Reduction (%)	
SS1	8.71E12	0	63.36	0	0
SF1M	5.80E11	93.34	38.7	38.92	0.42
SF1.5M	5.10E11	94.14	36.5	42.39	0.45
SF2M	3.36E11	96.14	30	52.65	0.55

4.5   Residual Strength

This sub-section describes analyzes performed to evaluate the effects of fatigue damage on RC slabs' current performance. The performance behavior was characterized by its capacity for residual strength. This required the RC slabs that were subjected to varying loads of fatigue and then tested through the statically increasing load to failure. The residual strength measured was compared with the analytical as validation of the proposed efficient method for evaluating RC structures for fatigue damage. Details are presented on the analysis, methods, results and conclusions.

4.5.1   Load-deflection Behaviour

Figure 4.43 shows the load deflection curve obtained from the static flexural test. All the slabs behaved linearly between the load and deflection applied until their yield

point was reached. Slab SF1M's residual load capacity was 98.1 kN. Slab SF1.5M's residual load capacity was 96.0 kN, which is 1.4 percent lower than slab SF1M's because of the higher load cycles applied to it. Slab SF2M had the lowest residual load capacity of the slabs, which was placed under the highest number of load cycles of 2 million. SF2M's residual load capacity was 92.1 kN, which is 4.75 percent lower than slab SF1.5M and slab SF1M respectively and 6.1 percent lower. The results indicated a decrease in the strength of the fatigued RC slabs as the fatigue level on the RC slabs increased, which shows a decrease in the structural stiffness. This decreasing stiffness value is due to steel tensile yield. It is also noted that the fatigued slabs ' residual load capacity is lower than the unfatigued SS1 RC slab. It can be concluded that the accumulated fatigue damage significantly influenced the residual load capacities of the fatigued slabs, although it should be noted that all the slabs did not fail because of fatigue.

Figure 4.44 shows the slab deflection change as cyclic load numbers increase. It can be seen that with the total cycles applied, the amount of slab deflection increases, with the slab deflection recorded at 1 million, 1.5 million and 2 million cycles being 12.7 mm, 17 mm and 22.62 mm respectively. The flexural crack was observed near the position of the load actuator and propagated as shown in Figure 4.45 to the support of the slab. The slabs' deflection behavior under cyclic loading shows a uniform percentage increase of 34% and 33%, corresponding to 1.5 million and 2 million cyclic loads, respectively. In the investigations conducted by Carvelli et al. (2010); Cheng (2011); Foglar & Göringer (2015); Peng et al. (2016), similar trends have also been reported.

4.5.2 Residual Strength Model

The real structures could experience fatigue in their service life due to the continuous cyclic loads and causes the material properties to deteriorate in strength or stiffness. The established traditional approach to total life expressed the number of cycles as the function of amplitude or maximum load or fatigue stress (S-N curves) without intuition of the level of deterioration. Mechanical and phenomenological approaches were thus frequently referred to as the solution to this problem in the literature. However, in the engineering application, phenomenological offered more practical approach to the prediction of fatigue life of existing structures by taking into account the more useful material properties of strength and deterioration of stiffness.
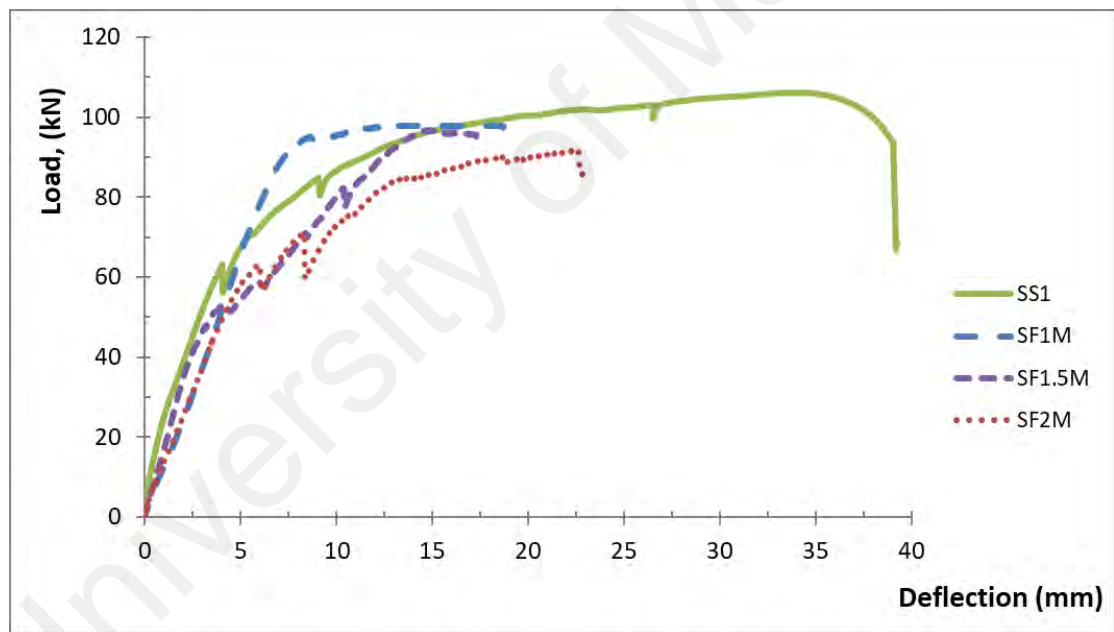
Figure 4.43: Residual strength of slabs SF1M, SF1.5M, and SF2M due to fatigue, compared with control slab SS1 that is not preloaded with fatigue load.
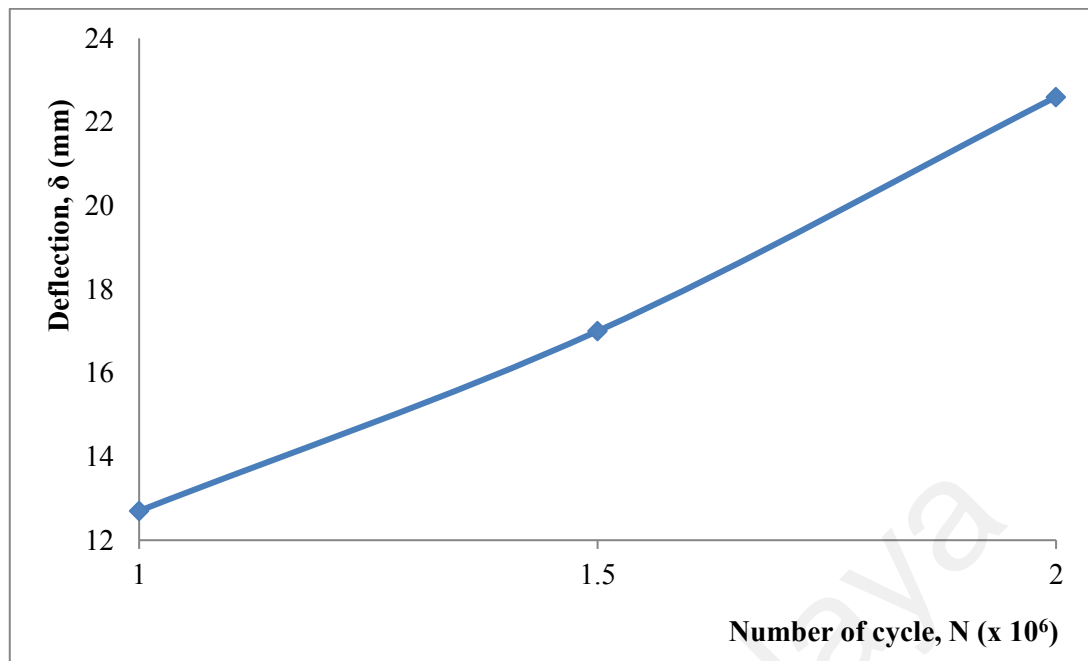
Figure 4.44: Deflection of the slab appropriate to the number of cycles
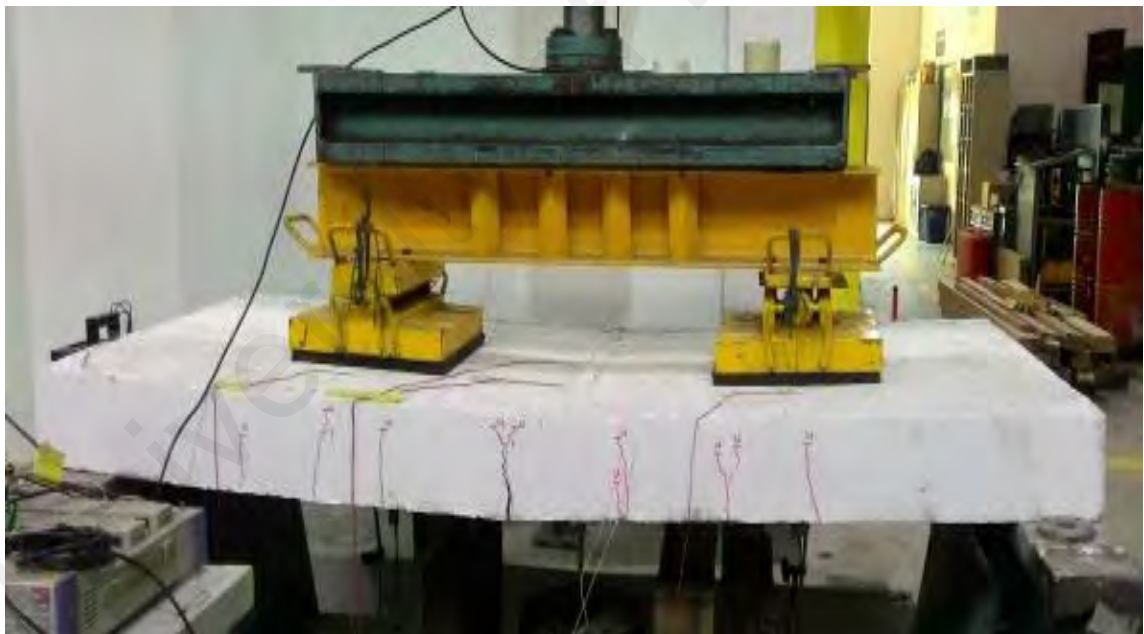
Figure 4.45: Flexural crack near the load actuator position and propagated towards the support of the slab

The residual strength approach is therefore largely used in the prediction of fatigue life. Under a probabilistic and deterministic technique, this approach served as the basis for developing more residual strength models for the prediction of fatigue life. The prediction models were originally based on the degradation of strength that developed under constant fatigue loading of the amplitude. Figure 4.46 illustrates the residual strength model philosophy (Stojković et al., 2017). Conceptually, during the constant amplitude fatigue loading, the accumulation of damage occurs in the material. S_R is the main parameter in assessing the level of damage. As the number of cycles increased, n deteriorated the residual strength due to increased accumulation of damage. When the residual strength reaches the same value of the maximum cyclic load or stress, S_{max}, the structural element considered failing, and the number of cycles at that point is characterized by fatigue life, N.
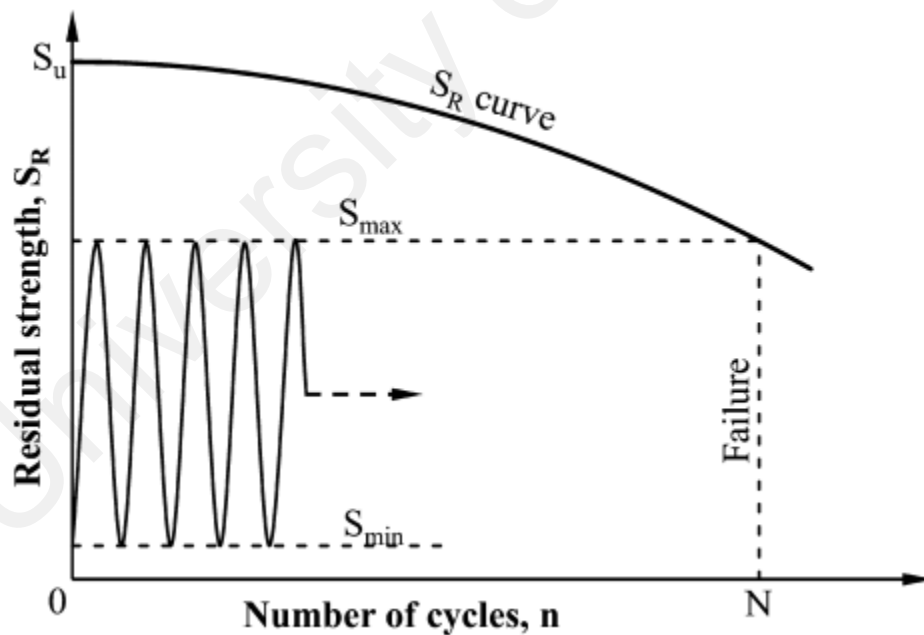
Figure 4.46: Residual strength model philosophy (Stojković et al., 2017)

As one of the objectives of this research is to establish a predictive model for evaluating the fatigue-carrying capacity of fatigued RC slabs, the residual strength

approach could be the most compatible method to be applied. The experimental program was designed to obtain the remaining static load (residual strength) on the development of the residual strength model for the prediction of fatigue life under different fatigue damage levels. Four identical RC slabs have been built and tested, Chapter 3 specifies the detailed description. The first slab was tested under a monotonous increase in load until the ultimate static load capacity was not obtained. The remaining three RC slabs were tested under different load cycles and subsequently the fatigued RC slabs were tested under the monotonic load to establish the residual strength and fatigue cycles relationship. The results investigated in this study for the residual strength of fatigued RC slabs are presented in Table 4.17. It has been observed that the percentage of the reduction in residual strength increases from 7.45 percent to 13.11 percent as cyclic load and fatigue damage increases.

Table 4.17: Details of loading of test RC slabs and the residual strength

Specimens	Test Objective	Number of cycles, N	Fatigue min load, S_{min} (kN)	Fatigue max load, S_{max} (kN)	Residual strength, S_R (kN)
SS1	Static	N/A	N/A	N/A	106
SF1M	Residual	1 million	20	65	98.1
SF1.5M	Residual	1.5 million	20	65	96.0
SF2M	Residual	2 million	20	65	92.1

The results obtained from the experimental were plotted in the graph of residual strength versus number of cycles when presenting the residual strength degradation with regard to the number of cycles as the fatigue life model (Figure 4.47 to Figure 4.49). The experimental data was plotted in the vicinity of the fitted curves with the points lying. The high determination coefficient values, R^2 shows that the model of fatigue life (S-N) is very well correlated and can be used to predict fatigue life, N. The fatigue life was predicted as listed in Table 5.6 from the developed fatigue life model shown in Figure 4.47 to Figure 4.49. Thus, the number of experimental works on fatigue testing

as well as the cost and time consumption could be reduced by having this prediction model.

The residual strength, S_R is expressed as the function of maximum cyclic load or stress, S_{max}, static strength, S_U, fatigue life, N, and number of cycles, n, Equation 4.19). Here, $f(S_{max}, S_U, N)$ function defines the rate of strength decrease associated with cyclic loading. The residual strength, S_R initially equals to the static strength, S_U. The general form of the assumed residual strength relation expressed in the Equation 4.20. Where α is strength degradation parameter which can be attained from the curve fitting. The function $f(S_{max}, S_U, N)$ is developed through a failure criterion. The assumption has been made when the residual strength equals the maximum cyclic load or stress magnitude, the failure will occur. By explanation, when the failure happens, the number of loading cycles, n, equals the fatigue life, N. Applying this conditions into Equation 4.20, Equation 4.21 could be formulated. Then, when Equation 4.21 was substituting into Equation 4.20, Equation 4.22 was established. $\frac{n}{N}$ is represented as normalized number of cycles, n with respect to fatigue life, N and α is the strength degradation. By using the predicted fatigue life listed in Table 4.18, parameter α can be calculated. The α value obtained as 0.997 which was determined based on the same maximum cyclic stress level. Hence, the formulated residual strength expressed in Equation 4.24, could successfully predict the fatigue-carrying capacity of fatigued RC slab (Stojković et al., 2017).

$$S_R = f(S_{max}, S_U, N)$$
Equation 4.19

$$S_R = S_U - f(S_{max}, S_U, N)n^{\alpha}$$
Equation 4.20

$$f(S_{max}, S_U, N) = \frac{S_U - S_{max}}{N^{\alpha}}$$
Equation 4.21

$$S_R = S_U - (S_U - S_{max}) \left(\frac{n}{N}\right)^{\alpha} \qquad \text{Equation 4.22}$$

$$\frac{n}{N} = n_n \qquad \text{Equation 4.23}$$

$$S_R = S_U - (S_U - S_{max})(n_n)^{0.997} \qquad \text{Equation 4.24}$$

Observing the trend of residual strength degradation, the exhibiting fatigued RC slabs decreased as the fatigue level on the RC slabs increased. It can also be seen that the residual strength of fatigued slabs is lower than that of unfatigued RC slab SS1. It can be concluded that the residual strength of the fatigued RC structures was significantly influenced by the fatigue damage accumulated, although it should be noted that all the slabs did not fail due to fatigue. During cyclic loading, the concrete between the surrounding reinforcements undergoes tensile fatigue and subsequently causes structural stiffness changes.
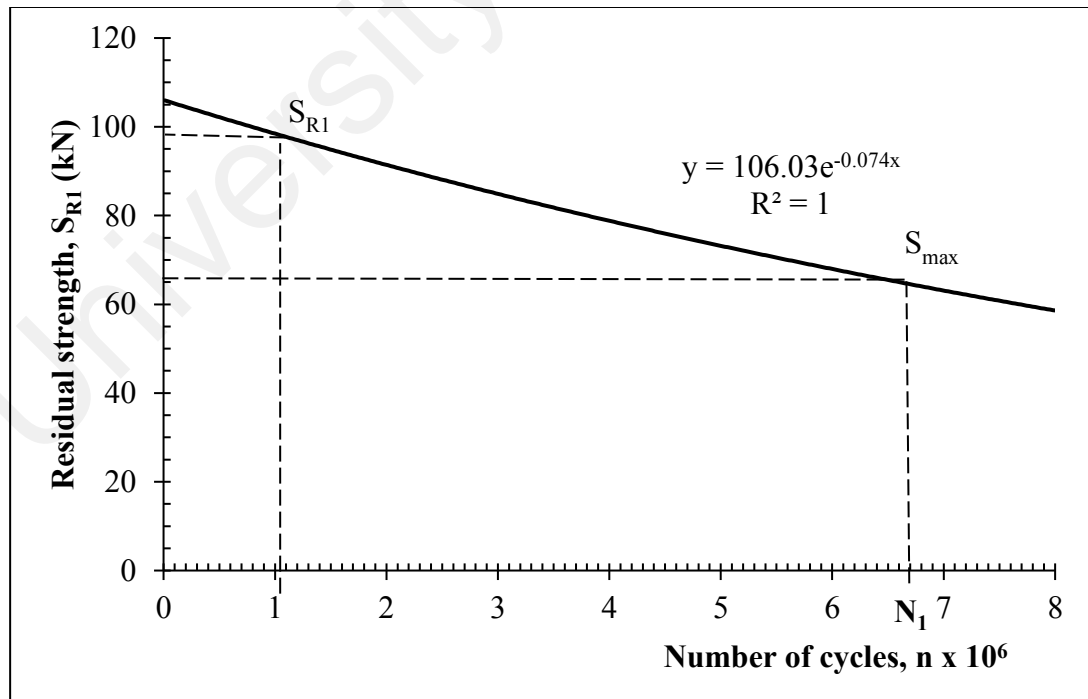
Figure 4.47: Residual strength, S_{R1} and fatigue life, N_1 of slab SF1M
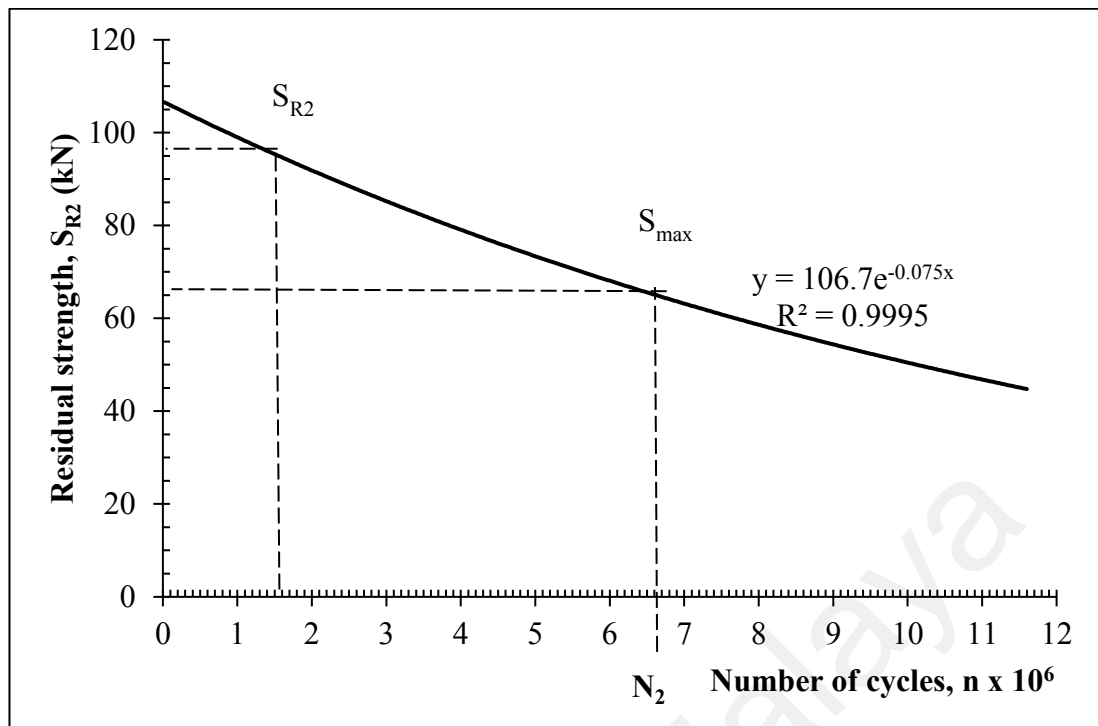
Figure 4.48: Residual strength, S_{R2} and fatigue life, N_2 of slab SF1.5M
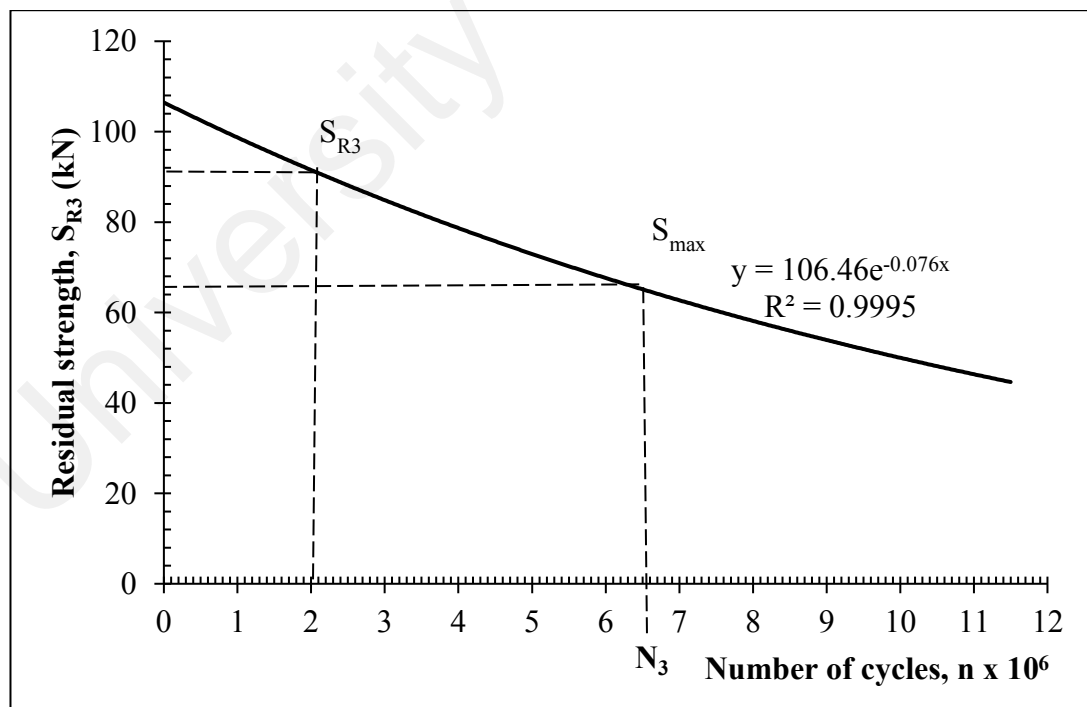
Figure 4.49: Residual strength, S_{R3} and fatigue life, N_3 of slab SF2M

Table 4.18: Fatigue life prediction from the developed fatigue life model

Specimens	Number of cycles, n x 10^6	Fatigue life, N x 10^6	Coefficient of determination, R^2
SS1	1	6.70	1
SF1M	1.5	6.60	0.9995
SF1.5M	2	6.50	0.9995

4.5.3 Analytical Methods

Due to its structural stiffness, the performance of the RC structure under fatigue loads could be observed. It is noted that when exposed to fatigue loading due to concrete fatigue in the tension zone, the stiffness of the RC structure will decrease. The resistance reduction process begins with the first cyclic load applied to the structure, so the service life will decrease from that moment on. The reduction of the strength is related to the stiffness degradation in fatigue structure which is because of the time-dependent on cyclic creep strain of concrete, ε_c (Equation 4.7) after certain number of fatigue cycles, N which dependent to Young's modulus, E_N (Equation 4.10) of concrete. As a response from a given number of cyclic loads, the strength also changed.

Based on the known effective moment of inertia, $I_{E,N}$, the cracked moment of inertia, $I_{cr,N}$ can be determined. Under the cracked section analysis, the relationship between the moment of inertia and the effective steel ratio of the damaged slab was developed, hence residual load carrying capacity of the fatigued RC slab can be quantified. In bending at the ultimate limit state, the development of that relationship is basically referring to the reinforced concrete slab analysis. This analysis is by assuming redistribution for zero moment according to the requirement of the Eurocodes 2 design (Mosley, 2012). Figure 4.50(b) shows the strain distribution along the depth of section where ε_c and ε_s represent the compressive concrete and tensile steel strains. The ultimate concrete strain is 0.0035 typical for classes of concrete less or equal than concrete grade C50/60. It is assumed that the plane section remain plane after straining, so that the

section is in a linear distribution of strain. Figure 4.50 shows the simplified rectangular stress block distribution, with f_{ck} and f_{st} representing concrete compressive and steel tensile strengths and $\gamma_c = 1.5$ is the usual partial safety factor for the concrete strength. The ultimate design stress $0.85 f_{ck} / \gamma_c$ is acting over the upper area at the depth of $0.8c_u$, which is does not extend to the neutral axis of the section. For the equilibrium, the ultimate design moment, M_u must be balanced by the moment of resistance of the section as given in the Equation 4.25 (Nawy, 2005).

$$M_u = 0.87 f_{yk} \rho bd \left(d - \frac{\beta y}{2} \right)$$

Equation 4.25

Where β is coefficient of concrete, normally used 0.8, y is the neutral axis depth at ultimate state can be calculated using the horizontal force equilibrium on the cross section as given in Equation 4.26 and Equation 4.27. ρ is the effective steel ratio and formulated by A_s/bd. As a structural flexural element, slab has an ability to resist the applied loads through the reinforcing steel embedded in the tension zones. Hence, the effective steel ratio becomes an important element in this investigation on serviceability and capacity of fatigued and damaged structure (Nawy, 2005).

$$I_{cr} = \frac{1}{3} by^3 + n\rho bd(d - y)^2$$

Equation 4.26

$$\frac{1}{2} by^2 + n\rho bdy - n\rho bd^2 = 0$$

Equation 4.27

Where y is the neutral axis depth at the cracking state, $\rho = A_s/bd$ is the effective steel ratio, $n = E_s/E_c$, E_s and E_c are steel and concrete modulus of elasticity. E_s is 2.0×10^5 N/mm^2 and E_c is 31,000 N/mm^2. When the ultimate moment of the damaged structure was identified, the ultimate load carrying capacity can be determined by using Equation 4.28 (Nawy, 2005).
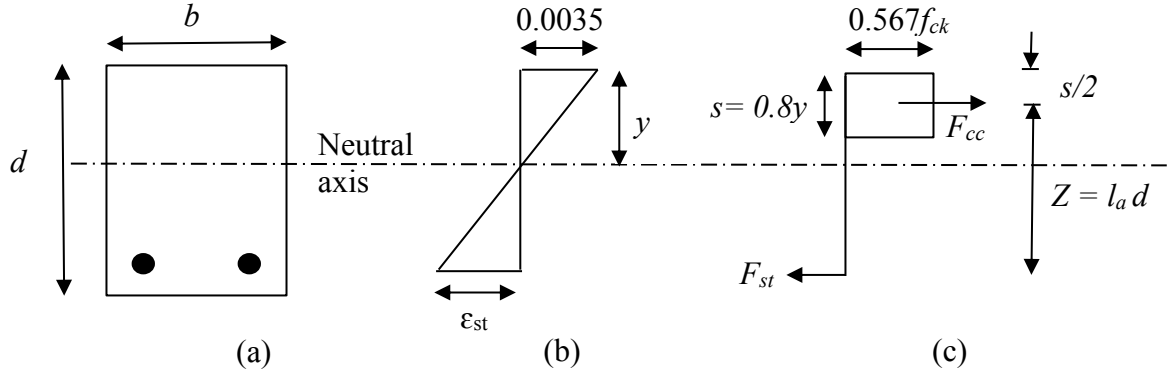
Figure 4.50: Singly reinforced section analysis; (a) Cross section, (b) Strain at ultimate strain, (c) Concrete-steel ultimate stress block (Nawy, 2005).

$$P_u = \frac{8M_u}{L} \qquad \text{Equation 4.28}$$

The ability of the flexural structure to withstand the bending moment exerted by the loads applied is primarily through a sufficient capacity of load carrying. Thus, the tension zones of the concrete structure needed to be strengthened by a certain amount of steel bars in order to have an adequate capacity to carry the load. Consequently, the RC slab's load carrying capacity cannot be evaluated directly from the updated results of the FE model. The cross section needed to be designed in the design of a RC structure for specific geometric dimensions and steel bar area based on the given moment from the load applied and the properties of the given material. Obviously seen here, there is a relationship between the stiffness and the evaluation of the load capacity whereby the effective steel ratio is influenced by the determination of the stiffness and the final moment of the structure as indicated in Equation 4.26 and Equation 4.27. Using Equation 4.28, the load carrying capacity can be determined by referring to the once the final moment is calculated.

An existing serviceability structure is simulated by the specimen of fatigued RC slab. Physically, it is hard to determine the effective steel ratio on the real structure if damage has been identified by the RC structure. However, as mentioned earlier, through

the integrated dynamic testing and model updating, the relationship between the effective steel ratio and the stiffness can be developed. The effective steel ratio can be identified from that relationship, leading to the ultimate moment quantification and load carrying capacity. Equation 4.26 and Equation 4.27 show how the relationship between moment of inertia, I and effective steel ratio, ρ is developed.

Using the updated value of the moment of inertia, the final moment is calculated for the damaged RC slab SF1M structure by using Equation 4.25 as 24.46 kNm. The resulting load carrying capacity of the damaged structure was 97.8 kN. The maximum load of the RC slab SF1M was maintained up to 98.1 kN, reduced by 7.17 percent compared with the ultimate load of the 106 kN unfatigued RC slab. The ultimate load from the experimental can be seen close to the analytical load with a minimum error of 0.31% and a maximum error of up to 0.52% as shown in Table 4.19. As shown in Figure 4.51, the percentage error of these values is well correlated with the linear regression graph. The model was therefore validated and it was possible to use the method with confidence to assess the fatigue damage caused by RC structures.

The data presented in Table 4.20 is the validation of the damaged RC slab SF1M, SF1.5M and SF2M stiffness parameter obtained from the FE model updating to analytical results based on the theoretical results in Equation 4.26 and Equation 4.27 and the validation showed a good correlation of $R^2 = 1$ (Figure 4.52).

Table 4.19: Comparison of the ultimate loads obtained from the experimental and analytical calculation

Specimens	M_u (kNm)	Residual strength analytical, S_{RA} (kN)	Residual strength experimental, S_{RE} (kN)	$S_{R,error}$ (%)
SF1M	24.46	97.8	98.1	0.31
SF1.5M	24.09	96.37	96.0	0.90
SF2M	23.15	92.58	92.1	0.52

Table 4.20: Validation of structural stiffness of damaged RC slabs

Specimen	Stiffness, K (Nmm^2)		
	FE model updating, K_{upd}	Analytical, K_{anl}	$K_{,error}$ (%)
SF1M	5.80E11	5.803E11	0.052
SF1.5M	5.10E11	5.102E11	0.039
SF2M	3.36E11	3.356E11	0.11
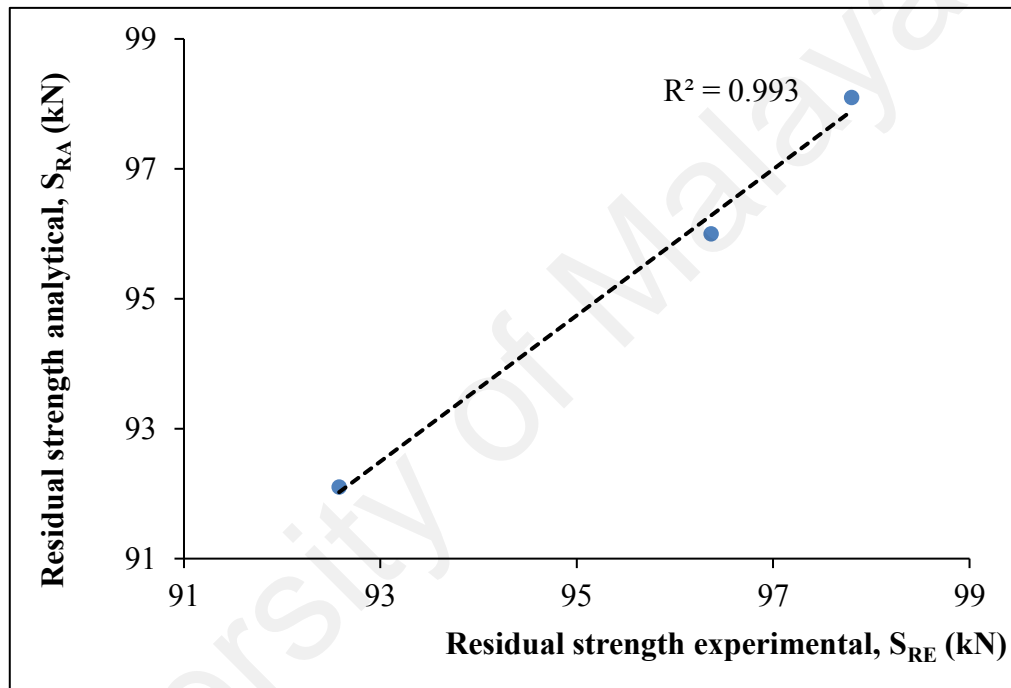
Figure 4.51: Correlation of residual strength analytical and experimental of fatigued RC slabs
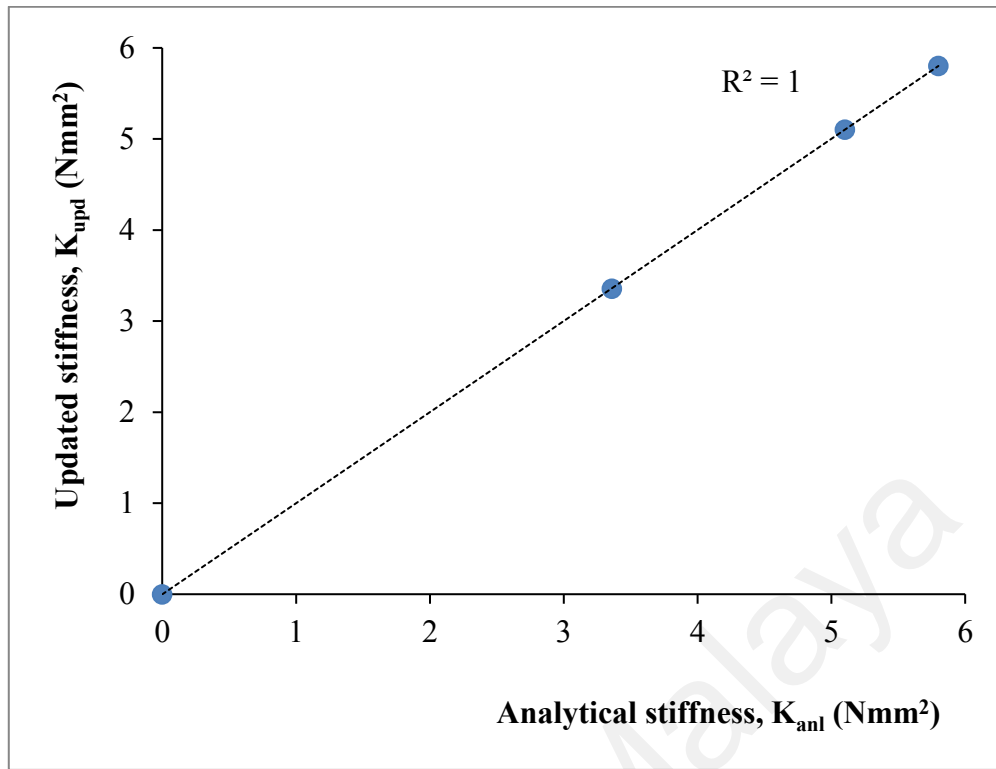
Figure 4.52: Correlation of updated and analytical stiffness of damaged RC slabs

4.6 Relationship between Stiffness Degradation and Residual Strength

Due to its current load capacity, the structural stiffness and residual strength deteriorated conceptually with increasing number of loading cycles. The relationship between stiffness degradation and residual strength is presented and discussed in this section with the condition of fatigue damage in RC slabs.

The relationship between the two damage modes can be defined as in Equation 4.29 by analyzing the above material characteristics.

$$D_K = \left(D_{S_R}\right)^{\beta}$$ Equation 4.29

D_K and D_{S_R} are monotone increasing function, where D_K is the stiffness damage under fatigue load, D_{S_R} is the residual strength damage under fatigue load and β is a model parameter obtained from the fitted curve presented in Figure 4.53.

$$D_K = 34.422 D_{S_R}{}^{0.0379}$$

The graph describes the residual strength and structural stiffness behavior with respect to fatigue damage, the stiffness has changed and subsequently the residual strength shifts as well. In Equation 4.30 the relationship has been formulated. The magnitude of the changes becomes an indicator of the damage's severity. The relationship was demonstrated as proportional from the results presented in Table 4.21, the change approximately represented by the ratio of structural stiffness to residual strength is 0.1. Compared to the control specimen, it performed changes in the RC slab's structural stiffness and residual strength.
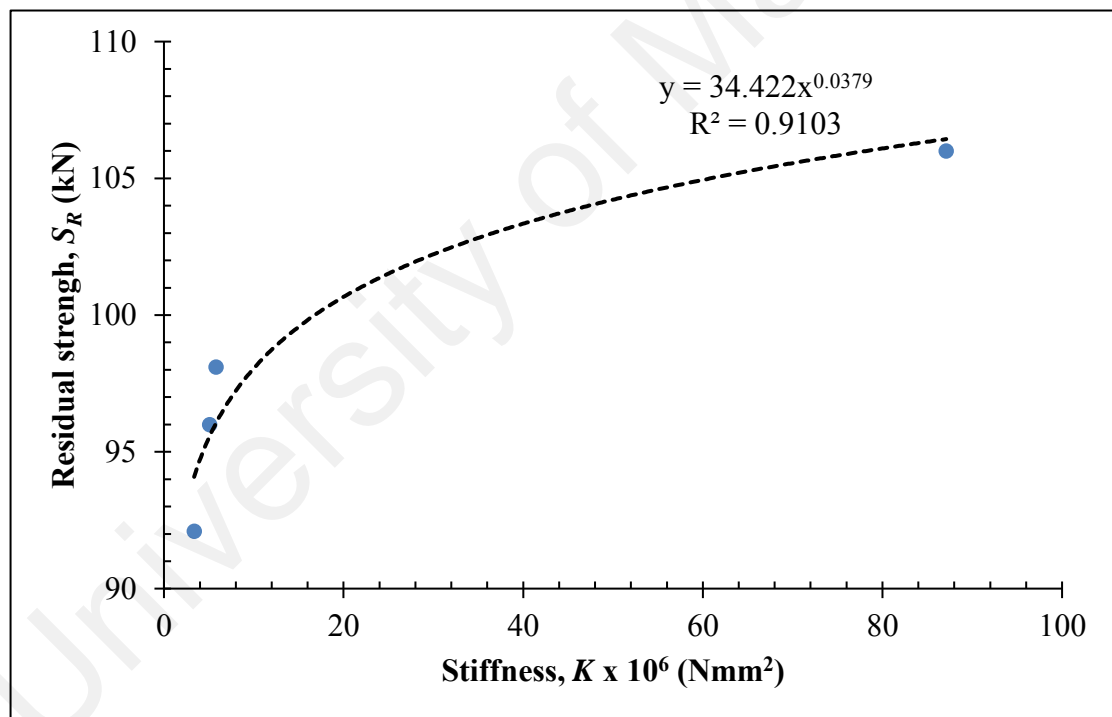
Figure 4.53: Residual strength and structural stiffness of damaged RC slabs

Table 4.21: The effect of structural stiffness on fatigued RC slabs to its residual strength

Specimen	Strength		Stiffness		
	S_R (kN)	K_{dam} reduction (%)	K_{dam} (Nmm²)	K_{dam} reduction (%)	Ratio of reduction, S_R to K_{dam}
SS1	106.0	0	8.71E+12	0	0
SF1M	98.1	7.45	5.80E+11	93.34	0.080
SF1.5M	96.0	9.43	5.10E+11	94.14	0.100
SF2M	92.1	13.11	3.36E+11	96.14	0.136

4.7 Summary

This chapter described the finding from laboratory testing, and FE modelling and updating. Based on the results, the natural frequency of fatigued RC slabs decreased with the increased level of fatigue damage and is considered an index of the performance of structural fatigue reflecting the degree of degradation. This relationship explains the principle of using natural frequency changes to characterize structural fatigue damage. The presence of damage is acknowledged to cause changes in structural dynamic properties including natural frequencies, mode shapes, and damping, and thus a change in the damping ratio may reflect the damage. The damping ratio, however, shows inconsistent results in this study. The fact that the damping estimate was influenced by the uncertainty factor contributes to this result. Cao et al. (2017) reported that uncertainty was attributed to three aspects of the damping mechanism's complexity, difficulties in properly characterizing the damping due to the lack of universal mathematical models, and the factors in selecting the damping estimation method also induce error in estimating. Therefore, it is acknowledged that the use of damping ratio to identify structural damage is an unresolved research topic and is recommended to be further explored. The law of stiffness degradation under a fatigue load is examined by identifying the relationship between fatigue damage and natural frequency parameter.

The serviceability performance could be monitored and predicted based on the quantitative description of this vibration measurement on the fatigued structures.

In the second phase of the results, the correlated and updated FE model had reflect the actual condition of RC slabs. It has been shown that, compared to the initial models, the updated FE models have smaller errors and therefore better improvements in terms of agreement on natural frequencies. It can be seen that the updated FE models ' natural frequencies were close to the experimental data measured. Using the parametric optimization applied through the commercial FE software of ANSYS Workbench, the updated process was carried out using the Design of Experiments (DoE) approach. The result of an updated FE model is more reliable to use against experimental results for the next FE model prediction for fatigued and damaged structures.

The last phase of the results is about the assessment of fatigue damage based on structural stiffness that includes the module and moment of inertia of the Young. Results have shown that fatigued structure intensity causes significant changes in structural stiffness and residual strength. It has also been identified that the structural stiffness changes are consistent with the degradation of residual strength. The magnitude of changes may indicate the severity of the damage. The quantification of structural stiffness and residual strength of fatigued structures was demonstrated by the evaluation of fatigue-bearing capacity of existing structures. The results validate that the proposed method is efficient and practical, so the potential for evaluating existing structures that are susceptible to continuous cyclic load could be very good. In managing repair and maintenance plans, predicting the structural performance that subjected to increased loads in the future would be helpful.

CHAPTER 5: CONCLUSIONS AND RECOMMENDATIONS

5.1 Conclusions

In this study, non-destructive vibration-based evaluation methodology is established for the evaluation of the serviceability of RC slabs under three different structural conditions; undamaged, fatigued and damaged through integrated dynamic testing; modal testing, fatigue and static loading testing and simulation. The methodology consists of the measurement process and the analysis of results, which was studied by means of a series of experimental measurement works and numerical simulations. Conclusion can be drawn as follows:

(1) Experimental work was carried out on the RC slab specimens with different fatigued and damaged levels to determine the dynamic characteristics. The obtained natural frequencies decreased as the level of fatigue and damage on the RC slabs increases, based on the experimental investigations. The results showed that the intensity of fatigued structures causes significant changes in the modal parameters and the remaining capacity for structural loading. It is associated as the stiffness of the structure decreases and the vibration frequencies decrease.

(2) Simulating successfully the FE models of the tested RC slabs using Ansys software. The FE model simulation has been experimentally validated. It was found that with the experimental data, the updated results showed satisfactory agreement. The result was a firming of both experimental and updated FE model data with a good linear correlation. Thus, the simulations of fatigued RC slab structures according to their real conditions were performed with confidence by having a reliable updated FE model.

(3) Modeling the serviceability performance of RC slabs under fatigue load successfully developed a constitutive model using a stiffness degradation model. The predictive

model proposed could be used to evaluate the serviceability of existing RC slab structures.

(4) A method for detecting damage has been proposed using the three parameters of the relationship (stiffness, natural frequency and residual strength) to detect progressive damage in fatigued RC slabs.

(5) Methodology for residual strength (load carrying capacity) of the RC structures at a particular level of fatigue using an integrated static and dynamic testing has been presented. The effect of residual strength due to accumulative fatigue load is approximated mathematically through updated stiffness degradation model. The model has been validated by analytical values and comparing with the corresponding experimental results. It is observed the developed model is in good agreement with the corresponding experimental values. Residual strength has also can be predicted using that developed model. The proposed model is suitable for high cycle of vibrating structures such as bridges and dams.

The results show that the dynamic behavior was significantly influenced by the fatigued and damaged RC slab structures. The relationship has been established between the structures ' mechanical and dynamic behavior in terms of natural frequency, structural stiffness, and residual strength. It shows the importance of understanding the fatigue load interaction and the dynamic characteristics of the existing structures ' serviceability. The findings have thus enhanced the viability of integrated non-destructive techniques and simulation for damage detection and quantification whereby it is not limited to damage condition alone but can also be assessed in progressive damage phase.

5.2   Recommendations

Some of the recommendations are based on the findings of the research.

1. Additional research on the fatigue load test of RC slabs is recommended up to fatigue failure to study the estimation of the remaining fatigue life. This helps develop procedures for statistical analysis that can establish the probabilistic model of reliability.

2. For future work, the work presented in this thesis report must be continued by conducting an ambient vibration test with a field test on the actual RC bridge deck slab. This type of testing uses traffic and wind-induced disturbances as natural or environmental excitement to extract the modal parameters of the real structural element.

3. Insufficient information on the overall structural bridge system, including substructure and foundation, can lead to significant uncertainties regarding structural safety and serviceability. It is a suggestion to leverage the technique of structural identification to characterize the dynamic behavior of existing bridges on the substructure or foundation system.

REFERENCES

Abdel Wahab, M. (2008). *Dynamics and vibration: an introduction*. John Wiley.

ACI 318-77. (2008). Building Code Requirements for Reinforced Concrete. *(American Concrete Institute)*, *552*.

Agardh, L. (1994). Impact Excitations of Concrete Highway Bridges. In *Proceedings of the 12th International Modal Analysis,* 2251, 1329.

Aktan, A. E., Farhey, D. N., Brown, D. L., Dalal, V., Helmicki, A. J., Hunt, V. J., & Shelley, S. J. (1996). Condition Assessment for Bridge Management. *Journal of Infrastructure Systems*, *2*(3), 108–117.

Aktan, A. E., Farhey, D. N., Helmicki, A. J., Brown, D. L., Hunt, V. J., Lee, K. L., & Levi, A. (1997). Structural identification for condition assessment: Experimental arts. *Journal of Structural Engineering*, *123*(12), 1674–1684.

Al-Rousan, R., & Issa, M. (2011). Fatigue performance of reinforced concrete beams strengthened with CFRP sheets. *Construction and Building Materials*, *25*(8), 3520–3529.

Alexander, M., & Beushausen, H. (2019). Durability, service life prediction, and modelling for reinforced concrete structures – review and critique. *Cement and Concrete Research*, 122, 17-29.

Alexander, M., & Thomas, M. (2015). Service life prediction and performance testing - Current developments and practical applications. *Cement and Concrete Research*, 78, 155-164.

Aljazaeri, Z. R., & Myers, J. J. (2015). Fatigue and Flexural Behavior of Reinforced Concrete Beams Strengthened With a Fiber Reinforced Cementitious Matrix. *Journal of Composites for Construction*, *21*, 1–7.

Allemang, R. J., & Brown, D. L. (1982). A correlation coefficient for modal vector analysis. *First International Modal Analysis Conference*, 110–116.

Altunişik, A. C., Bayraktar, A., & Sevim, B. (2012). Operational modal analysis of a scaled bridge model using EFDD and SSI methods. *Indian Journal of Engineering and Materials Sciences (IJEMS)*, *19*(5), 320–330.

Altunişik, A. C., Karahasan, O. Ş., Genç, A. F., Okur, F. Y., Günaydin, M., & Adanur, S. (2018). Sensitivity-based model updating of building frames using modal test data. *KSCE Journal of Civil Engineering*, *22*(10), 4038-4046.

Andersen, P., Brincker, R., Ventura, C., & Cantieni, R. (2008). Modal estimation of civil structures subject to ambient and harmonic excitation. *Proc. XXVI IMAC*, 4-7.

Baptista, M. A., Mendes, P., Costa, A. C., Sousa, C., Afilhado, A., & Silva, P. (2004). Use of ambient vibration testing for modal evaluation of a 16 floor reinforced concrete building in Lisbon. *13th World Conference on Earthquake Engineering*,

Vancouver.

Bayraktar, A., Türker, T., ALTUNIşIK, A. C., Sevim, B., Şahin, A., & Özcan, D. M. (2010). Determination of dynamic parameters of buildings by operational modal analysis. *Teknik Dergi/Technical Journal of Turkish Chamber of Civil Engineers*, *21*(4).

Bayraktar, Alemdar, Altunişik, A. C., & Türker, T. (2016). Structural condition assessment of Birecik highway bridge using operational modal analysis. *International Journal of Civil Engineering*, *14*(1), 35–46.

Bayraktar, Alemdar, Can Altunişik, A., Sevim, B., & Türker, T. (2010). Ambient vibration tests of a steel footbridge. *Journal of Nondestructive Evaluation*, *29*(1), 14–24.

BD 37/01. (2001). Loads for Highway Bridges. *The Highways Agency*.

Benmokrane, B., El-Salakawy, E., El-Ragaby, A., & Lackey, T. (2006). Designing and testing of concrete bridge decks reinforced with glass FRP bars. *Journal of Bridge Engineering*, *11*(2), 217–229.

Berman, A., & Nagy, E. J. (1983). Improvement of a large analytical model using test data. *AIAA Journal*, *21*(8), 1168–1173.

Bien, J., & Zwolski, J. (2007). Dynamic Tests in Bridge Monitoring--Systematics and Applications. In *IMAC-XXV: conference & exposition on structural dynamics, Orlando*, 1–10.

Box, G.E.P., & Wilson, K. B. (1951). On the experimental attainment of optimum conditions. *Journal of the Royal Statistical Society*, *13*(1), 1–45.

Box, G.E.P., & Draper, N. R. (1987). *Empirical model-building and response surfaces* (Vol. 424). New York: Wiley.

Brincker, R., Andersen, P., & Moller, N. (2000). An indicator for separation of structural and harmonic modes in output-only modal testing. *18th International Modal Analysis Conference*, 1649–1654.

Brincker, R., Frandsen, J., B., A., & Palle. (2000). Ambient response analysis of the Great Belt Bridge. *Proceedings of the International Modal Analysis Conference - IMAC*, *1*, 26–32.

Brincker, R., & Ventura, C. E. (2015). *Introduction to Operational Modal Analysis*. *Introduction to Operational Modal Analysis*. John Wiley & Sons.

Brincker, R., Zhang, L., & Andersen, P. (2001). Modal identification from ambient responses using frequency domain decomposition. *Smart Materials and Structures*, *10*(3), 441.

Brownjohn, J. M.W., Magalhaes, F., Caetano, E., & Cunha, A. (2010). Ambient vibration re-testing and operational modal analysis of the Humber Bridge. *Engineering Structures*, *32*(8), 2003–2018.

Brownjohn, J.M.W., Xia, P. Q., Hao, H., & Xia, Y. (2001). Civil structure condition assessment by FE model updating: methodology and case studies. *Finite Elements in Analysis and Design*, 37, 761–775.

Brownjohn, J. M., De Stefano, A., Xu, Y. L., Wenzel, H., & Aktan, A. E. (2011). Vibration-based monitoring of civil infrastructure: challenges and successes. *Journal of Civil Structural Health Monitoring*, 1(3-4), 79-95.

Brownjohn, James M W, Hao, H., & Pan, T. C. (2001). *Assessment of structural condition of bridges by dynamic measurements*. Nanyang Technological University, Applied Research Project RG (Vol. 5).

Brownjohn, James M W, & Xia, P.-Q. (2000). Dynamic assessment of curved cable-stayed bridge by model updating. *Journal of Structural Engineering*, 126(2), 252–260.

BS 1881-209. (1990). *Testing Concrete. Part 209: Recommendations for the measurement of dynamic modulus of elasticity* (Vol. 3). London.

BS 1881. (1983). *Part 120: 1983--Testing Concrete. Method for Determination of Compressive Strength of Concrete Cores*, British Standards Institution.

BS 5400:Part 10-Code of practice for fatigue. (1980). *BS 5400:Part 10-Code of practice for fatigue*, British Standards Institution.

BS, 8110. (n.d.). *Structural use of concrete Part 1, Code of practice for design and construction*, British Standards Institution.

Caesar, B. (1986). Update and identification of dynamic mathematical models. In *International Modal Analysis Conference, 4 th, Los Angeles, CA* (pp. 394–401).

Caetano, E., & Cunha, A. (1993). Experimental identification of modal parameters on a full scale structure. *Transactions on Modelling and Simulation*, 5.

Cantieni, R, Deger, Y., & Pietrzko, S. (1994). Large structure investigation with dynamic methods: the bridge on the river Aare at Aarburg. In *Prestressed Concrete in Switzerland, Report of the Swiss FIP Group to the 12th FIP Congress*. Washington.

Cantieni, Reto. (2001). Assessing a dam's structural properties using forced vibration testing. In *Proc. IABSE International Conference on Safety, Risk and Reliability-Trends in Engineering*. Malta.

Cao, M. S., Sha, G. G., Gao, Y. F., & Ostachowicz, W. (2017). Structural damage identification using damping: a compendium of uses and features. *Smart Materials and structures*, 26(4), 043001.

Capraro, I., Pan, Y., Rollins, K., Gao, W., & Ventura, C. E. (2015). Ambient vibration testing of a 4-storey parking garage. In *Conference Proceedings of the Society for Experimental Mechanics Series, 2*, 31–38.

Carreira, M. R., Dias, A. A., & de Alcântara Segundinho, P. G. (2017). Nondestructive

Evaluation of Corymbia citriodora Logs by Means of the Free Transverse Vibration Test. *Journal of Nondestructive Evaluation*, *36*(2).

Carvelli, V., Pisani, M. A., & Poggi, C. (2010). Fatigue behaviour of concrete bridge deck slabs reinforced with GFRP bars. *Composites Part B: Engineering*, *41*(7), 560–567.

Cheng, L. (2011). Flexural fatigue analysis of a CFRP form reinforced concrete bridge deck. *Composite Structures*, *93*(11), 2895–2902.

Cho, K., Park, S. Y., Kim, S. T., Cho, J., & Kim, B. (2011). Fatigue Performance of Precast FRP-Concrete Composite Deck with Long Span. *Engineering*, 1115–1123.

Daniel J Inman. (2008). *Engineering Vibration* (Third Edit). Pearson Prentice Hall.

Dhawan, S. K., Bindal, A., Bhalla, S., & Bhattacharjee, B. (2019). Expected residual service life of reinforced concrete structures from current strength considerations. *Advances in Structural Engineering*, *22*(7), 1631–1643.

Ding, L., Hao, H., Xia, Y., & Deeks, A. J. (2012). Evaluation of Bridge Load Carrying Capacity Using Updated Finite Element Model and Nonlinear Analysis. *Advances in Structural Engineering*, *15*(10), 1739–1750.

Doebling, S. W., & Farrar, C. R. (1998). A summary review of vibration-based damage identification methods. *Shock and Vibration Digest*, 1–34.

Doebling, S. W., Farrar, C. R., Prime, M. B., & Shevitz, D. W. (1996). *Damage identification and health monitoring of structural and mechanical systems from changes in their vibration characteristics: a literature review* (No. LA-13070-MS). Los Alamos National Lab., NM (United States).

Ewins, D. J. (2000). *Modal Testing: Theory, Practice and application. Research Studies Press LTD*.

Fang, S.-E., Zhang, Q.-H., & Ren, W.-X. (2014). Parameter variability estimation using stochastic response surface model updating. *Mechanical Systems and Signal Processing*, *49*(1–2), 249–263.

Fang, S. E., Ren, W. X., & Perera, R. (2012). A stochastic model updating method for parameter variability quantification based on response surface models and Monte Carlo simulation. *Mechanical Systems and Signal Processing*, *33*, 83–96.

Farrar, C. R., & James, G. H. (1997). System Identification From Ambient Vibration Measurements on a Bridge. *Journal of Sound and Vibration*, *205*(1), 1–18.

Felber, A. J. (1994). *Development of a hybrid bridge evaluation system*. University of British Columbia.

Fernández, P., Reynolds, P., & Aenlle, M. L. (2011). Experimental evaluation of mass change approaches for scaling factors estimation. In *Dynamics of Civil Structures* (Vol. 4, pp. 109–118). Springer New York.

Foglar, M., & Göringer, J. (2015). Influence of Cyclic Loading on the Deflection Development of Concrete Specimens. *Stavební Obzor - Civil Engineering Journal*, *24*(4), 1–22.

Foti, D., Diaferio, M., Giannoccaro, N. I., & Mongelli, M. (2012). Ambient vibration testing, dynamic identification and model updating of a historic tower. *NDT & E International*, *47*, 88–95. https://doi.org/10.1016/j.ndteint.2011.11.009

Friswell, M., & Mottershead, J. E. (2013). *Finite element model updating in structural dynamics* (Vol. 38). Springer Science & Business Media.

Gardner-Morse, M. G., & Huston, D. R. (1993). Modal identification of cable-stayed pedestrian bridge. *Journal of Structural Engineering*, *119*(11), 3384–3404.

Guillaume, P., Verboven, P., Vanlanduit, S., Van Der Auweraer, H., & Peeters, B. (2003). A poly-reference implementation of the least-squares complex frequency-domain estimator. *Proceedings of IMAC*, *21*(2), 183-192.

Guo, Q. T., & Zhang, L. M. (2004). Finite element model updating based on response surface methodology. *Proc., IMAC-XXII: Conference and Exposition on Structural Dynamics , SEM, Dearborn, MI, USA;*, 1–8.

Hanson, J. M., Ballinger, C. A., & Linger, D. (1974). Considerations for design of concrete structures subjected to fatigue loading. *ACI Journal*, *71*(3), 97-120.

Hashim, H., Ibrahim, Z., & Razak, H. A. (2013). Dynamic characteristics and model updating of damaged slab from ambient vibration measurements. *Measurement*, *46*(4), 1371–1378.

Heylen, W., Lammens, S., Sas, P., & others. (1997). *Modal analysis theory and testing*. Katholieke Universiteit Leuven Leuven, Belgium.

Heylen, W., & Sas, P. (1987). Review of model optimization techniques. In *Proceedings of the International Modal Analysis conference IMAC 5* (pp. 1177–1183).

Hordijk, D. A. (1991). Local approach to fatigue of concrete, doctor dissertation. *Delft University of Technology*.

Hsu, T. T. C. (1981). Fatigue of Plain Concrete. *ACI Journal Proceedings*, *78*(4), 292–305.

Ibrahim, S. R. (1988). Correlation of analysis and test in modeling of structures: assessment and review. In *Structural Safety Evaluation Based on System Identification Approaches* (pp. 195–211). Springer.

Ibrahim, Z., & Reynolds, P. (2008). Modal testing of a cantilever grandstand. In *Proceedings of the International Conference on Construction and Building Technology (ICCBT'08)* (pp. 271–284).

Ivanovic, S. S., Trifunac, M. D., & Todorovska, M. I. (2000). Ambient vibration tests of structures-a review. *ISET Journal of Earthquake Technology*, *37*(4), 165–197.

Jacobsen, N.-J., Andersen, P., & Brincker, R. (2007). Using EFDD as a Robust Technique to Deterministic Excitation in Operational Modal Analysis. *Proceedings of the 2nd International Operational Modal Analysis Conference*, *1*, 193–200.

Jamali, S., Chan, T. H. T., Nguyen, A., & Thambiratnam, D. P. (2019). Reliability-based load-carrying capacity assessment of bridges using structural health monitoring and nonlinear analysis. *Structural Health Monitoring*, *18*(1), 20–34.

Kashif Ur Rehman, S., Ibrahim, Z., Memon, S. A., & Jameel, M. (2016). Nondestructive test methods for concrete bridges: A review. *Construction and Building Materials*.

Katakalos, K., & Papakonstantinou, C. G. (2009). Fatigue of Reinforced Concrete Beams Strengthened with Steel-Reinforced Inorganic Polymers. *Journal of Composites for Construction*, *13*(2), 103–112.

Ko, J. M., & Ni, Y. Q. (2003). Structural health monitoring and intelligent vibration control of cable-supported bridges: Research and application. *KSCE Journal of Civil Engineering*, *7*(6), 701–716.

Kong, X., Cai, C. S., & Hu, J. (2017). The state-of-the-art on framework of vibration-based structural damage identification for decision making. *Applied Sciences*, *7*(5), 497.

Kutanis, M., Boru, E. O., & Işık, E. (2017). Alternative instrumentation schemes for the structural identification of the reinforced concrete field test structure by ambient vibration measurements. *KSCE Journal of Civil Engineering*, *21*(5), 1793–1801.

Law, S. S., Ward, H. S., Shi, G. B., Chen, R. Z., Waldron, P., & Taylor, C. (1995a). Dynamic Assessment of Bridge Load-Carrying Capacities. I. *Journal of Structural Engineering*, *121*(3), 478–487.

Law, S. S., Ward, H. S., Shi, G. B., Chen, R. Z., Waldron, P., & Taylor, C. (1995b). Dynamic assessment of bridge load-carrying capacities. II. *Journal of Structural Engineering*, *121*(3), 488–495.

Lenschow, R. (1980). Long term random dynamic loading of concrete structures. *Materials and Structures*, *13*(3), 274–278.

Liu, Y., Fan, H., He, J., & Wu, D. (2012). Static and Fatigue Experimental Study on Flexural Behavior of Hybrid GFRP-Concrete Bridge Decks. In *The Third Asia-Pacific Conference on FRP in Structures (APFIS2012)* (p. 7).

Logan, D. L. (2011). *A first course in the finite element method* (5th ed.). Cengage Learning.

Maas, S., Zürbes, A., Waldmann, D., Waltering, M., Bungard, V., & Roeck, G. De. (2012). Damage assessment of concrete structures through dynamic testing methods . Part 1 – Laboratory tests, *34*, 351–362.

Mao, Q., Mazzotti, M., DeVitis, J., Braley, J., Young, C., Sjoblom, K., Bartoli, I. (2019). Structural condition assessment of a bridge pier: A case study using

experimental modal analysis and finite element model updating. *Structural Control and Health Monitoring*, *26*(1), e2273.

Mottershead, J. E., & Friswell, M. I. (1993). Model Updating In Structural Dynamics: A Survey. *Journal of Sound and Vibration*, *167*(2), 347–375.

Nanda, B., Maity, D., & Maiti, D. K. (2014). Modal parameter based inverse approach for structural joint damage assessment using unified particle swarm optimization. *Applied Mathematics and Computation*, *242*, 407–422.

Nanda, B., Majumdar, A., Maity, D., & Maiti, D. K. (2014). Performance comparison among vibration based indicators in damage identification of structures. In *Applied Mechanics and Materials*, 592, 2081–2085.

Nawy, E. (2005). *Reinforced concrete: A fundamental approach* (5th ed.). Pearson, Prentice Hall.

Neville, A. M. (2009). *Properties of Concrete* (4th ed.). Essex, England, UK: Addison Wesley Longman Ltd.

Nieto, A. J., Chicharro, J. M., & Pintado, P. (2006). An approximated methodology for fatigue tests and fatigue monitoring of concrete specimens. *International Journal of Fatigue*, *28*(8), 835–842.

Oh, H., Sim, J., & Meyer, C. (2005). Fatigue life of damaged bridge deck panels strengthened with carbon fiber sheets. *ACI Structural Journal*, *102*(1), 85–92.

Pavic, A, Williams, M. S., & Waldron, P. (1994). Dynamic FE model for post-tensioned concrete floors calibrated against field test results. In *Proceedings of the 2nd International Conference on Engineering Integrity Assessmentt* (pp. 11–12).

Pavic, A., Hartley, M. J., & Waldron, P. (1999). Updating of the analytical models of two footbridges based on modal testing of full-scale structures. In *Proceedings of the International Seminar on Modal Analysis* (Vol. 3, pp. 1111-1118). Katholike Universityteit Leuven.

Pavic, Aleksandar, Reynolds, P., Waldron, P., & Bennett, K. (2001). Dynamic modelling of post-tensioned concrete floors using finite element analysis. *Finite Elements in Analysis and Design*, *37*(4), 305–323.

Pavic, Aleksandar, Widjaja, T., & Reynolds, P. (2002). The use of modal testing and FE model updating to investigate vibration transmission between two nominally identical building floors. In *Proc., Int. Conf. on Structural Dynamics Modeling-Test, Analysis, Correlation and Validation* (pp. 347–355). Lisbon, Portugal: Instituto Superior Tecnico.

Peng, H., Zhang, J., Shang, S., Liu, Y., & Cai, C. S. (2016). Experimental study of flexural fatigue performance of reinforced concrete beams strengthened with prestressed CFRP plates. *Engineering Structures*, *127*, 62–72.

Pietrzko, S. J., Cantieni, R., & Deger, Y. (1996). Modal testing of a steel/concrete composite bridge with a servo-hydraulic shaker. In *Proceedings 14th International*

Modal Analysis Conference (pp. 91–98). Dearborn, Michigan.

Plachy, T., & Polak, M. (2007). Fatique Damage Identification on Concrete Structures Using Modal Analysis. In *3rd WSEAS International Conference on Applied and Theoretical Mechanics* (pp. 14–16). Spain.

Prasad, D. R., & Seshu, D. R. (2010). Study on change in modal parameters of RC beams due to fatigue type damage. *Asian Journal of Civil Engineering*, *11*(4), 521–532.

Razak, H. A., & Choi, F. C. (2001). The effect of corrosion on the natural frequency and modal damping of reinforced concrete beams. *Engineering Structures*, *23*(9), 1126–1133.

Ren, W.-X., & Chen, H.-B. (2010). Finite element model updating in structural dynamics by using the response surface method. *Engineering Structures*, *32*(8), 2455–2465.

Ren, W., & Chen, H. (2010). Finite element model updating in structural dynamics by using the response surface method, *32*, 2455–2465.

Ren, Wei X, Fang, S. E., & Deng, M. Y. (2011). Response surface – based finite-element-model updating using structural static responses. *J Eng Mech-ASCE*, *137*, 248–257.

Ren, Wei Xin, Zatar, W., & Harik, I. E. (2004). Ambient vibration-based seismic evaluation of a continuous girder bridge. *Engineering Structures*, *26*(5), 631–640.

Ren, W. X., & Zong, Z. H. (2004). Output-only modal parameter identification of civil engineering structures. *Structural Engineering and Mechanics*, *17*(3-4), 429-444.

Reynolds, P., Pavic, A., & Waldron, P. (1999). Modal testing, FE analysis and FE model correlation of a 600 tonne post-tensioned concrete floor. In *Proceedings of The International Seminar on Modal Analysis* (Vol. 3, pp. 1129–1136). Katholike Universityteit Leuven.

RILEM Committee. (1984). Long term random dynamic loading of concrete structures. *Mater. Constr.(Paris)*, *17*(9), 1-28.

Rodrigues, J., Brincker, R., & Andersen, P. (2004). Improvement of frequency domain output-only modal identification from the application of the random decrement technique. *Proc. 23rd Int. Modal Analysis ...*, 92–100. Retrieved from ftp://ftp.svibs.com/Download/Literature/Papers/2004/2004_4.pdf

Rytter, A. (1993). *Vibrational Based Inspection of Civil Engineering Structures*. Aalborg University, Denmark.

Salawu, O. S. (1997). Detection of structural damage through changes in frequency: a review. *Engineering Structures*, *19*(9), 718–723.

Sevim, B., Atamturktur, S., Altunişik, A. C., & Bayraktar, A. (2016). Ambient vibration testing and seismic behavior of historical arch bridges under near and far fault

ground motions. *Bulletin of Earthquake Engineering*, *14*(1), 241–259.

Shan, D., Li, Q., Khan, I., & Zhou, X. (2015). A novel finite element model updating method based on substructure and response surface model. *Engineering Structures*, *103*, 147–156.

Sidhu, J., & Ewins, D. J. (1984, February). Correlation of finite element and modal test studies of a practical structure. In *Proceedings of the 2nd international Modal Analysis Conference* (pp. 756-762). Union College Schenectady, New York.

Sohn, H., Farrar, C. R., Hemez, F. M., Shunk, D. D., Stinemates, D. W., Nadler, B. R., & Czarnecki, J. J. (2003). A review of structural health monitoring literature: 1996–2001. *Los Alamos National Laboratory, USA*, 1-7.

Somerville, G. (1997). Engineering design and service. In *Prediction of Concrete Durability: Proceedings of STATS 21st anniversary conference* (p. 58). CRC Press.

Stojković, N., Folić, R., & Pasternak, H. (2017). Mathematical model for the prediction of strength degradation of composites subjected to constant amplitude fatigue. *International Journal of Fatigue*, *103*, 478–487.

Suthiwarapirak, P., & Matsumoto, T. (2006). Fatigue Analysis of RC Slabs and Repaired RC Slabs Based on Crack Bridging Degradation Concept. *Journal of Structural Engineering*, *132*(June), 939–949.

Teughels, A., Maeck, J., & De Roeck, G. (2002). Damage assessment by FE model updating using damage functions. *Computers and Structures*, *80*(25), 1869–1879.

Van Overschee, P., De Moor, B., Overschee, P. Van, & Moor, B. De. (1996). Subspace Identification for Linear System: Theory - Implementation - Applications. *Conference Proceedings of the International Conference of IEEE Engineering in Medicine and Biology Society*, *2008*, 4427–4430.

Ventura, C. E., Lord, J.-F., & Simpson, R. D. (2002). Effective Use of Ambient Vibration Measurements for Modal Updating of a 48 Storey Building in Vancouver, Canada. *International Conference on Structural Dynamics Modeling– Test, Analysis, Correlation and Validation*, 1–10.

Walraven, J. C. (2009). Design for service life: How should it be implemented in future codes. In *Concrete Repair, Rehabilitation and Retrofitting II - Proceedings of the 2nd International Conference on Concrete Repair, Rehabilitation and Retrofitting, ICCRRR* (pp. 3–10).

Widjaja, T. R. (2004). *Vibration transmission between two nominally identical building floors*. The University of Sheffield.

Xia, P.-Q., & Brownjohn, J. (2004). Load-Carrying Capacity Evaluation of Damaged Reinforced Concrete Structures by Dynamic Testing and Finite-Element Model Updating, *32*(5), 1–7.

Xia, P. Q., & Brownjohn, J. M. (2004). Load-carrying capacity evaluation of damaged reinforced concrete structures by dynamic testing and finite-element model

updating. *Journal of Testing and Evaluation*, *32*(5), 366-372.

Yoon, M. K., Heider, D., Gillespie, J. W., Ratcliffe, C. P., & Crane, R. M. (2009). Local damage detection with the global fitting method using mode shape data in notched beams. *Journal of Nondestructive Evaluation*, *28*(2), 63–74.

Youn, S.-G., & Chang, S.-P. (1998). Behavior of composite bridge decks subjected to static and fatigue loading. *Structural Journal*, *95*(3), 249–258.

Zhai, X., Fei, C.-W., Choy, Y.-S., & Wang, J.-J. (2016). A stochastic model updating strategy-based improved response surface model and advanced Monte Carlo simulation. *Mechanical Systems and Signal Processing*, *82*, 323–338.

Zhang, L., Wang, T., & Tamura, Y. (2010). A frequency-spatial domain decomposition (FSDD) method for operational modal analysis. *Mechanical Systems and Signal Processing*, *24*(5), 1227–1239.

Zong, Z., Lin, X., & Niu, J. (2015). Finite element model validation of bridge based on structural health monitoring—Part I: Response surface-based finite element model updating. *Journal of Traffic and Transportation Engineering (English Edition)*, *2*(4), 258–278.

List of Publications and Papers Presented

List of publications:

1. Jamadin, A., Ibrahim, Z., Jumaat, M.Z., & Ab Wahab, E.S., (2019), Effect of High-cyclic Loads on Dynamic Response of Reinforced Concrete Slabs. *KSCE Journal of Civil Engineering*, 23(3), 1293-1301. ISI Q3 - Published.

2. Jamadin, A., Ibrahim, Z., Jumaat, M.Z., & Ab Wahab, E.S., (2020) Serviceability Assessment of Fatigue Concrete Structures using a Dynamic Response Technique. *Journal of Materials Research and Technology.* doi.org/10.1016/j.jmrt.2020.02.070 . – ISI Q2 - Published.

List of conferences:

1. Ibrahim, Z., Jamadin, A., Kamarudin, A.F., Ibrahim, A., Daud, M.E. and Madun, A. (2014, 20-21 October 2014). *Ambient Vibration Testing of Partially Damaged Reinforced Concrete Building Structure*. Innovation Trends in Multidisciplinary Academic Research (ITMAR2017), Istanbul, Turkey.

2. Jamadin, A., Ibrahim, Z., Jumaat, M.Z., and Wahab, E.S. (2015, 25-29 August 2015). *Vibration analysis of damaged reinforced concrete bridge deck slab due to static loading*. ASEM 15: The 2015 World Congress on Advances in Structural Engineering and Mechanics, Incheon, Korea.

3. Jamadin, A., Ibrahim, Z., Abu Bakar, A., and Jumaat, M.Z (2016, 31 May-1 June 2016). *Vibration analysis of damaged reinforced concrete bridge deck slab due to fatigue and static loading*. CONCET 2016, Shah Alam, Selangor.